NAGW-976

Clarkson University

# Center for Commercial Crystal Growth in Space

## Annual Report

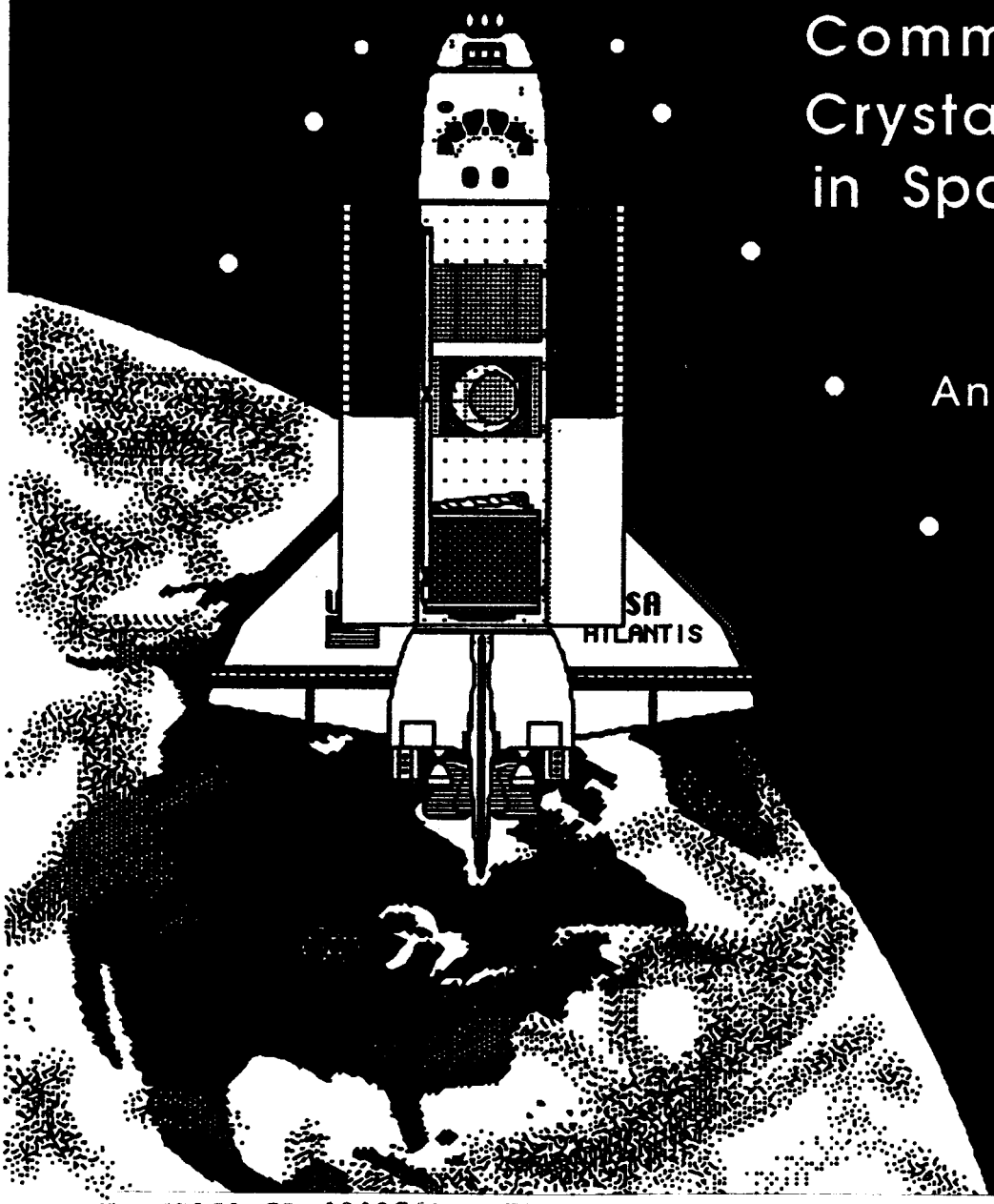


(NASA-CR-181356) CENTER FOR THE DEVELOPMENT OF COMMERCIAL CRYSTAL GROWTH IN SPACE Annual Report, 1 Sep. 1987 - 31 Aug. 1988 (Clarkson Univ.) 167 p

N89-15261

CSCL 22A

Unclas
G3/29 0183266

NAGW-976

# CENTER FOR THE DEVELOPMENT OF COMMERCIAL CRYSTAL GROWTH IN SPACE

## ANNUAL REPORT

September 1, 1987 to August 31, 1988


Director: William R. Wilcox
(315) 268-2336/6446

Deputy Director: Brian L. Hoekstra
(513) 372-0529

Administrative Assistant: Marcia F. Barnett
(315) 268-6662

CLARKSON UNIVERSITY
POTSDAM, NEW YORK 13676


Subcontractors:

Alabama A&M University
National Institute of Standards and Technology
Rensselaer Polytechnic Institute
University of Florida
Worcester Polytechnic Institute

# Center for the Development of Commercial Crystal Growth in Space

## Annual Report

Members:
II-VI Corp
Barnes Engineering
Boeing Aerospace Company
Dantec
E,G,&G Inc.
Grumman Research Corp.
Quantum Technology, Inc.
MetroLaser
Rockwell Int'l Science Center
SpaceHab
Spectron Development Labs
Teledyne Brown Engineering
TransTemp
Westinghouse R&D
Alabama A&M University
Clarkson University
Rensselaer Polytechnic Institute
University of Florida
Worcester Polytechnic Institute
National Institute of Standards
and Technology

Sponsors:
NASA Office of Commercial Programs
State of New York
State of Florida

Submitted by: **Center for Advanced Materials Processing**
**Clarkson University, Potsdam, NY 13676**

October 1,1987 - September 30,1987

William R Wilcox
Director, CCDS

Brian L Hoekstra
Deputy Director, CCDS

## SUMMARY

This report covers the second year of operation of the Center for Commercial Crystal Growth in Space. NASA funding for this second year was $1,000,000. Industrial funding in cash was $150,000, the States of Florida and New York contributed $289,000, the U.S. Department of Commerce supported $125,000 in research at the National Institute of Standards and Technology (NIST), universities contributed $185,000, and value-in-kind donations of $445,000 were received from industry in supplies, equipment usage and services.

This Center is a consortium of businesses, universities and national laboratories. The primary industrial members are Boeing Aerospace, EDO/Barnes Engineering, Grumman Research Corporation, the Rockwell Science Center, the Westinghouse R&D Center, and the II-VI Corporation. The principal university members are Alabama A&M University, Clarkson University, University of Florida, Rensselaer Polytechnic Institute and Worcester Polytechnic Institute. The principal national laboratory was NIST. Center meetings were held at Rockwell (Thousand Oaks, CA) in March and at Grumman (Bethpage, NY) in September.

The primary goal of the Center's research is the development of commercial crystal growth in space. A secondary goal is to develop scientific understanding and technology which will improve commercial crystal growth on earth. In order to achieve these goals the Center's research is organized into teams by growth technique; melt growth, solution growth, and vapor growth.

The melt growth team is working on solidification and characterization of bulk crystals of gallium arsenide and cadmium telluride. NIST workers characterized gallium arsenide and cadmium telluride wafers supplied by Rockwell and Grumman. They used high resolution X-ray topography performed at the National Synchrotron Light Source at Brookhaven National Laboratory. Streak-like features were found in the diffraction images of semi-insulating undoped LEC GaAs from Grumman and Rockwell. These were shown to be (110) antiphase boundaries, which have not been reported before but appear to be pervasive and responsible for features seen via less-sensitive characterization methods. The results on CdTe were not as definitive, but indicate that antiphase boundaries may also be responsible for the double peaks often seen in X-ray rocking curves of this material.

University of Florida researchers assembled a liquid encapsulated melt zone system for GaAs and developed techniques for casting feed rods. They found that scratching the inside of the quartz ampoules with silicon carbide abrasive minimized sticking of the GaAs to the quartz. Twelve floating zone experiments were done. An induction heating frequency of 2.5 MHz proved more useful than 450 kHz in forming and controlling a molten zone. Silicon dissolved in the boron oxide encapsulant, and from there was incorporated in the gallium arsenide, although at a lower level than in the absence of boron oxide. Boron was also incorporated in the GaAs. More Ga than As dissolved in the boron oxide. A flight experiment is planned using a lower temperature model substance in Rockwell's Fluid Experiment Apparatus.

Clarkson University workers made improvements in the computer model of the cadmium telluride Bridgman-Stockbarger apparatus. Radiant heat transfer was added and thermal stress in the crystal can now be calculated. Vibration experiments using water showed that the height of the liquid and the amplitide and frequency of the vibration all strongly influence the mixing pattern and intensity in the liquid. The contact angle and surface tension of molten CdTe on various surfaces were measured using the sessile drop technique. A Bridgman-Stockbarger apparatus was designed and assembled. Flight experiments are planned using either NASA's CGF apparatus or Grumman's B-S equipment.

Researchers at Alabama A&M University found that addition of L-alanine to triglycine sulfate crystals grown from aqueous solutions improved the infrared detector performance of devices fabricated from these crystals. The optical quality of L-alanine phosphate depended on the pH of the solution. A preliminary design was made for a Get Away Special apparatus to be flown in the Shuttle.

Worcester Polytechnic Institute workers were able to produce much larger zeolite Na -A crystals by adding triethanolamine (TEA) to the growth mixture. TEA was shown to reduce nucleation, probably by complexing with aluminum ions in the solution. TEA also stabilized zeolite synthesis gels at room temperature, which is necessary for storage prior to Shuttle flights. (Crystallization begins when the gels are heated.) Studies revealed that the zeolite synthesis mixture consists of three phases: a low viscosity solution, highly viscous aluminosilicate gel, and solid crystalline material. It was found that zeolites formed from the gel phase, which can be separated from the low viscosity solution. This allows more crystals to be formed in a lower volume. A Get Away Special experiment is ready for flight on the Shuttle, and an improved apparatus is being developed for the USML-1 mission.

Researchers at Rensselaer Polytechnic Institute are working on vapor transport growth of bulk mercury halide and cadmium telluride crystals. A laser doppler velocimetry system was developed which detected flows at velocities down to 150 micrometers per second during vapor transport growth. The influence of stoichiometry and contaminant gases on CdTe transport was elucidated; deviations from stoichiometry and the presence of CO both lower the growth rate. Better stoichiometry control was achieved by special synthesis and pretreatment procedures than reported in the literature for CdTe vapor growth. The dynamic microbalance system was modified to improve its performance, so that minute variations in CdTe growth rate could be detected. A flight experiment is planned using Boeing's transparent furnace (CVTE).

## CONTENTS

## MANAGEMENT SUMMARY

The Center for Commercial Crystal Growth in Space continued to focus on quality research on important crystal growth techniques (melt, solution, and vapor) through its excellent cadre of researchers. The challenge during this past year was to form this group of leading researchers into a more cohesive unit working toward common goals of space commercialization and self sustainment. To effectively accomplish these goals, we have formalized a strategic plan and have restructured the Center into research teams. The outline of our strategic plan is provided in this report. The new organization, which is designed to stimulate more interaction between industry and academia, is shown below:

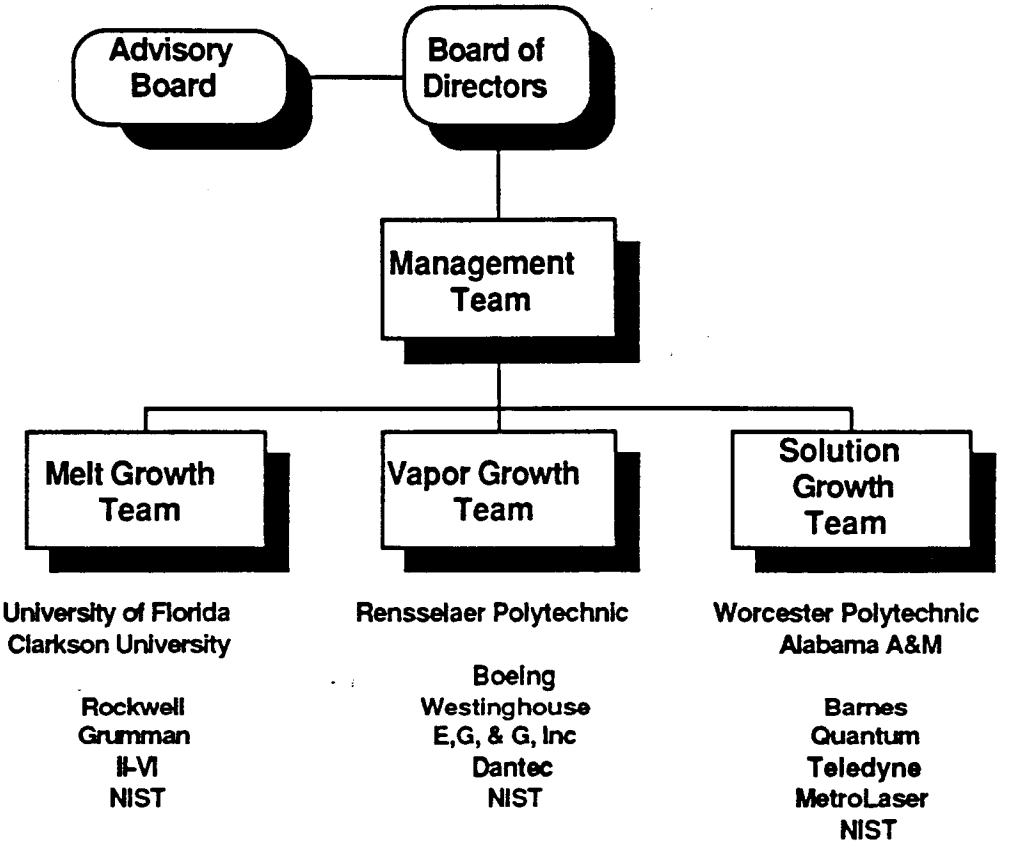


We are still in the process of restructuring the Center in the most efficient manner to promote commercialization. These research teams are further being divided into project elements including at least one university principal investigator and an industrial project manager assigned to oversee each project. At last count, we had eleven separate projects ongoing at six institutions. Each of these projects has been deemed to be of important commercial value by at least one of the Center industrial members. Following is the status of the current industrial membership.

## Industry Members

| Full Members | Associate Members | Small Businesses |
|---|---|---|
| **Boeing Aerospace** | **E,G,&G Inc** | **Trans Temp** |
| **Grumman Research** | **Spectron** | **Quantum Technology** |
| **Rockwell Science** | **Teledyne Brown** | **Spacehab** |
| **Westinghouse R&D** | **II-VI Corp** | **MetroLaser** |
| **Barnes Engineering** | **Dantec** | |

These pioneering members of the Center have provided significant contrubutions toward furthering the objectives of the Center. However, we still need to increase the industrial participation in the Center both by growing existing relationships and by recruiting new Center members. After two years of quality ground based research, we now feel that we have a tangible product to sell and have embarked upon a significant marketing effort. The Center management spent a considerable amount of time and effort in the last three months producing a quality brochure which is now ready for distribution. Our goal is to enlist at least two additional paying members per year for the next few years. These additional resources will be needed to carry out an aggressive flight experimentation plan as shown below:

## Current Flight Manifest for Clarkson CCDS

| Name of Experiment | P.I. (Org.) | Size (FEO's) | Wt. (kg) | Power (Peak) | Temp. (Peak) |
|---|---|---|---|---|---|
| LEMZ of Indium | Abbaschian (Florida) | .6 | 80 | 110W | 150 |
| Zeolite Crystallization | Sacco (WPI) | .5 | 90 | None | 150 |
| Zeolite Crystallization | Sacco(WPI) | .7 | 200 | 200W | 175 |
| CVTE of CdTe (Boeing) | Wiedemeier (RPI) | 1.7 | ~400 | 200W | 1000 |
| NLO/TGS Growth | Lal (AAMU) | 1.0 | 150 | 150W | 200 |
| DS of CdTe | White (Clarkson) | 1.0 | 200 | ~600W | 1100 |
| LEMZ of GaAs | Abbaschian (Florida) | 1.5 | ~300 | ~1.5 kW | 1300 |

| Continued... | Min. Time | Man Hrs. | G-Level | Other Rqts. | Target date |
|---|---|---|---|---|---|
| LEMZ of Indium | 2 days | 2 hrs | 10-3 | | 12/89 |
| Zeolite Crystallization | 4 days | 1 hr | 10-3 | Limited shelf life | Now |
| Zeolite Crystallization | 5 days | 10 hrs | 10-3 | Limited shelf life | 3/91 |
| CVTE of CdTe (Boeing) | 4 days | 10 hrs | 10-3 | | 12/91 |
| NLO/TGS Growth | 6 days | 4 hrs | 10-4 | | 6/92 |
| DS of CdTe | 8 days | 6 hrs | 10-4 | Active cooling | 12/91 |
| LEMZ of GaAs | 4 days | 8 hrs | 10-5 | Active cooling | 12/91 |

## YEAR IN BRIEF

**Project Starts**

- No new starts

**Marketing**

- Center brochure is nearing completion and will be sent out to numerous potential members in December
- Four potential new corporate members were visited
- Presentations were made at several commercial workshops
- Barnes Engineering joined as a full paying member

**Planning**

- Planning continues to key on flight experimention
- Added emphasis was placed on setting up mechanisms to make the Center self sustaining
- Formal Strategic Business plan was drafted (included in this report)

**Facilities and Equipment**

- Renewed emphasis on building CCDS flight hardware with at least part ownership or property rights to aid in structuring the Center to become self sustaining
- Center members continue to share facilities and equipment
- Unique capability is available at the National Synchrotron Light Source at Brookhaven National Laboratory

**Support of NASA Activities**

- Deputy Director attended numerous NASA sponsored meetings
- Active participation in first two Operational Management Council Workshops (Williamsburg, VA, Orlando, FL)
- Presented first one-on-one CCDS briefing to OCP staff (4/88)
- In general, more active interaction with NASA headquarters staff

# STRATEGIC BUSINESS PLAN OUTLINE

## 1.0 BACKGROUND

The purpose of the STRATEGIC BUSINESS PLAN is to identify:

1) the Center's goals - the direction it should be moving towards;
2) the Center's objectives - how best to address the goals;
3) the major plans and resources required to achieve the objectives;
4) the specific tasks required to develop and implement the plans.

Because of the dynamic nature of the field, this plan will be reviewed annually, and modified as necessary to reflect new scientific findings and the anticipated growth in the level of activity.

## 2.0 GOALS

1. To determine the potential for producing commercially an array of new crystal products in space.

2. To promote private sector investment in crystal growth in space by establishing new commercially oriented space ventures.

3. To become the leading center in the world for crystal-growth-in-space research and development.

4. To phase-out the need for seed-funds from NASA.

## 3.0 STRATEGY

The strategy for achieving the Center's goals is to pursue a focused R&D effort, directed by U.S. industrial and academic leaders in crystal growth, and funded by benefiting companies and government agencies, both state and federal. The major elements of the R&D and technology transfer program encompass:

1. High priority, high quality research
   - o space based activities
   - o supporting ground based activities.

2. Experiments in space as early as possible.

3. Communicating research results via publications, workshops and symposia.

4. Relying on the Center's industrial partners to identify potential business opportunities.

5. Working with the industrial and academic members to facilitate the commercial exploitation of the results from the Center-sponsored R&D.

**Key Objectives**

1. To induce U.S. companies at the forefront of crystal growth research to join the Center.

2. To develop interfaces with industry in related fields which will lead to expanded industrial support.

3. To establish a network of supporters from industry, federal agencies (other than NASA), and state agencies.

4. To demonstrate the advantages of growing crystals in micro-gravity by flying intelligent experiments in space as often as practical.

5. To develop the technology and capability necessary to grow crystals in space.

6. To continually foster collaborative research efforts between university, industry and government team members.

7. To serve as a user-friendly interface to NASA and the space community in order to facilitate the commercialization process especially for small, non-aerospace companies.

8. To serve as a conduit for technology transfer to U.S. industries in the crystal growth field.

9. To develop marketable patents that will lead to cash flow back into Center-sponsored research.

10. To develop other marketable products and services.

11. To develop and produce world-class space researchers.

## 4.0 RESEARCH PLAN

### 4.1 Project Selection Procedure

The research projects will be selected by a world-class peer review of proposals employing the following evaluation criteria:

1. must be industry driven,
2. must have the potential for a new JEA with NASA,
3. there must be a strong need for space experimentation,
4. there must be matching funds by a state agency and industrial partners,
5. the proposed research must be of highest quality.

### 4.2 Research Plans

## 5.0 SPACE EXPERIMENTATION PLANS

### 5.1 Payload Requirements

### 5.2 Flight Manifesting and Scheduling

### 5.3 Hardware Requirements

### 5.4 Strategy for Obtaining Necessary Hardware

## 6.0 GROUND-BASED RESEARCH FACILITIES

### 6.1 Current Facilities of the Members

### 6.2 Future Plans

### 6.3 Available Government Facilities

## 7.0 ASSESSING THE BUSINESS POTENTIAL FOR USE OF SPACE

## 8.0 INTELLECTUAL PROPERTY RIGHTS

### 8.1 Center Policy

### 8.2 Protection and Control Procedures

**9.0 FUNDING AND SUPPORT STRATEGY**

9.1 Funding and support goals (from industry)

9.2 Potential Sources

9.3 Techniques for Securing Funding

**10.0 MARKETING THE CENTER**

**11.0 Management**

11.1 Organization

11.2 Industrial Membership Categories

11.3 Directory of Current Industrial Members

11.4 Participating Academic Institutions

11.5 Contributions and Linkages to Other Agencies and Organizations

11.6 Advisory Board

11.7 Board of Directors

11.8 Collaboration Between Members

11.9 Reporting, Documenting, and Disseminating Results

**12.0 TASKS TO BE UNDERTAKEN**

## Center For Commercial Crystal Growth in Space

## MANAGEMENT EXPENDITURES

(October 1, 1987 through September 30, 1988)

| Category | Proposed | Actual | Overrun Due To |
|---|---|---|---|
| Director's Salary | $26,133 | $23,733 | |
| Deputy Director | 51,000 | 40,091 | |
| Admin. Asst. | 16,800 | 15,200 | |
| Fringe Benefits | 21,150 | 20,194 | |
| Office Equipment | 0 | 2,245 | Same as Sci. Equip. |
| Scientific Equip. | 8,891 | 0 | |
| Office Supplies | 3,000 | 4,609 | Needs larger than estimated |
| Duplicating | 0 | 290 | Annual Report |
| Postage | 680 | 1,135 | Annual Report |
| Publications | 4,000 | 3,000 | |
| Telephone | 2,374 | 4,035 | Needs larger than estimated |
| Travel | 18,500 | 16,092 | |
| Overhead | 73,604 | 20,489 | |
| Misc. & Other | 3,573 | 4,789 | Needs larger than estimated |
| TOTAL | $229,705 | $155,902 | |

## CCDS BUDGET RESOURCES

| Source | 1988 FY | 1989 FY |
|---|---|---|
| NASA (Cash) | $1,000,000 | $1,141,000 |
| States (Cash) (Florida, New York) | $289,000 | $300,000 |
| Other Govt (Cash) | $125,000 | $50,000 |
| Industry (Cash) | $150,000 | $175,000 |
| Value-in-Kind (From Industry) | $445,000 | $500,000 |
| Value-in-Kind (Others) | $185,000 | $200,000 |
| Total | $2,194,000 | $2,366,000 |

## 2. GROWTH OF LARGE ZEOLITE CRYSTALS IN SPACE

Gillian Scott, Julie L. D'Itri
Anthony G. Dixon, Albert Sacco, Robert W. Thompson

**WORCESTER POLYTECHNIC INSTITUTE**
Worcester, Massachussets 01609

## 1.0 INTRODUCTION

Zeolites are crystalline, hydrated aluminosilicates with 3-dimensional frameworks defined by repetitive units of small channels and larger cages. Many zeolites have high thermal and chemical stability making them useful materials for a wide range of important industrial processes including catalysis, separations, purifications and ion exchange. In many applications, particularly in petroleum and petrochemicals they totally dominate many established and most new processing.

Traditional synthesis methods produce crystals in the 1 to 10 μm size range. Many conventional applications in the detergent and petroleum industries, require only small crystals for optimum efficiency. However, many potential applications in the field of separation technology would become feasible with the availability of large crystals in significant quantities. Therefore new methods to provide crystal size enhancement are constantly being investigated.

Zeolites are crystallized under hydrothermal conditions in the presence of an amorphous aluminosilicate gel which acts as a source of nutrients. When the crystals reach a critical size, they fall to the bottom of the reactor, out of the nutrient pool, and stop growing. It is believed that under microgravity conditions they would be suspended in the nutrient rich gel and therefore grow larger than under normal gravity conditions. In order to successfully grow large crystals in space, a high level of understanding of the factors which affect nucleation and growth in a zeolite synthesis medium must be achieved.

## 2.0 EXPERIMENTAL APPROACH

The zeolite synthesis gels used in this study were prepared from high purity raw materials consisting of: fumed silica, Cab-O-Sil M5; aluminum wire, Aldrich (99.99%); sodium hydroxide pellets, Mallinckrodt (>98%); triethanolamine, Mallinckrodt (99%); other organics, Aldrich (>98%). Sodium aluminate solutions were obtained by dissolving aluminum wire in hot, aqueous sodium

hydroxide. These solutions were filtered through a membrane (0.2μm, Gelman) to remove any foreign particles and then mixed at room temperature with a slurry of fumed silica and water to produce a milky suspension. For syntheses including an organic amine, the amine was dissolved in water before addition to the silica water slurry.

Each reaction mixture was charged to six 10ml teflon autoclaves which then were sealed and heated in an oven under static conditions at 368±2K and autogenous pressure. Autoclaves were removed from the oven at regular intervals, the samples filtered (0.2μm, Gelman), washed with one liter of water, then dried at 333K for several hours.

**2.1 Characterization of Products**

Each sample was fully characterized using a variety of techniques. X-ray powder diffraction (Cu $K_\alpha$ G.E. XRD-Z80) was used for phase determination and degree of crystallinity. Optical microscopy (Olympus BH-2) and scanning electron microscopy (JSM-840 Scanning Microscope) were used to determine the crystal size and morphology of the products. Thermal gravimetric analysis, TGA (Mettler TC10A) was carried out (323-873K @ 10K $min^{-1}$) in order to determine the relative water content of hydrated (RH = 0.75, 298K, 24h) samples. Samples were analyzed before and after calcination (673K, 12h). Differential scanning calorimetry, DSC (Mettler DSC 20; 323-873K @10K $min^{-1}$) was used to determine the extent of occluded amine in each material.

Arc plasma emission spectroscopy (SMI, Spectraspan IV Emission Spectrometer) was used to determine the relative silicon and aluminum contents of the products. Particle size analyses were carried out using a Particle Data Inc, Electrozone Celloscope (Model 80X7) fitted with a 95μm orifice. Sample preparation involved placing a small amount of uncalcined material slurried in an aqueous solution of NaCl (0.1M), in an ultrasonic bath for 12h. Finally, carbon nuclear magnetic resonance spectra ($^{13}C$ NMR) were obtained on a Bruker ACE 200 nuclear magnetic resonance spectrometer (50.3 MHz).

## 2.2 Fluid Behavior

A study of the effect of raw materials on the nature of the precursor gel involved a modification in the synthesis technique described in Section 2.0. The silicon component of the synthesis gel was introduced as a clear sodium silicate solution rather than as a silica water slurry.

Phase separation studies were made using a variety of organic additives. These were added to a silica water slurry before the addition of sodium aluminate solution to form the zeolite reaction mixture. Materials produced in this way were characterized as described in Section 2.1. In addition, synthesis gels formed as precursors to the crystalline products were characterized using a Bohlin VOR Rheometer.

# 3.0 ACCOMPLISHMENTS

Several areas of interest are currently being pursued in order to reach the desired goal of growing large, perfect zeolite crystals, in high yield, in space. Both the physical and chemical properties of the chosen system have been studied. In terms of the chemistry of the system, nucleation control is one of the key areas in which significant progress has been made.

## 3.1 Nucleation Suppression

A substantial increase in crystal size was observed when triethanolamine (TEA) was added to zeolite Na-A synthesis gels.The relationship between the amount of TEA present and the maximum crystal size obtained is shown in Figure 1. There was a simultaneous increase in the crystallization time with increased concentration of the amine. Therefore, TEA was affecting the nucleation process, the growth process, or impacting both to some extent. Particle size analyses coupled with yield calculations revealed that TEA was indeed suppressing nucleation in the zeolite Na-A synthesis system.

Further experimentation was necessary in order to discover the mechanism through which TEA affects nucleation. Figure 2 shows

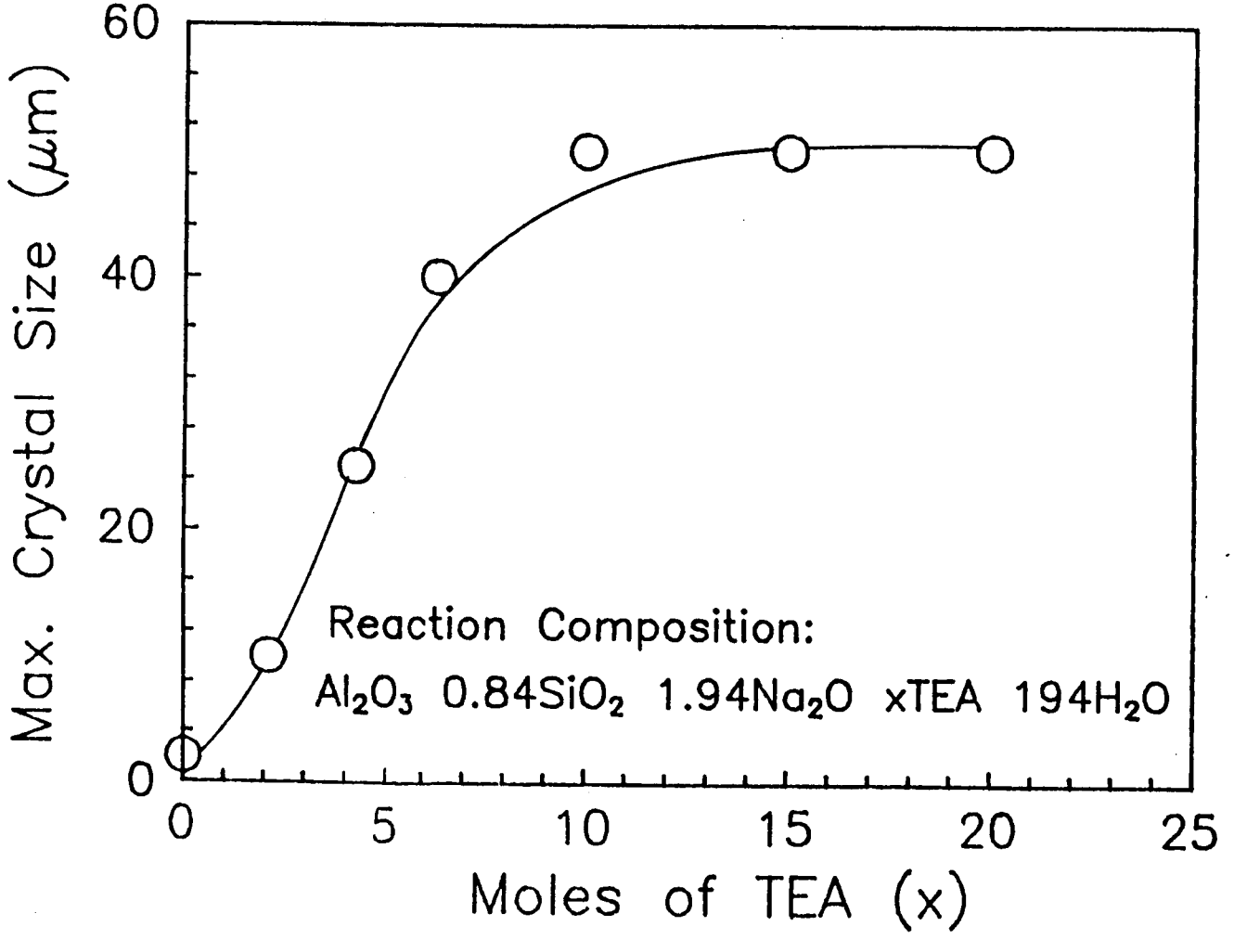


Fig. 1. Effect of TEA on Maximum Crystal Size of Zeolite Na-A Crystallized at 368K.

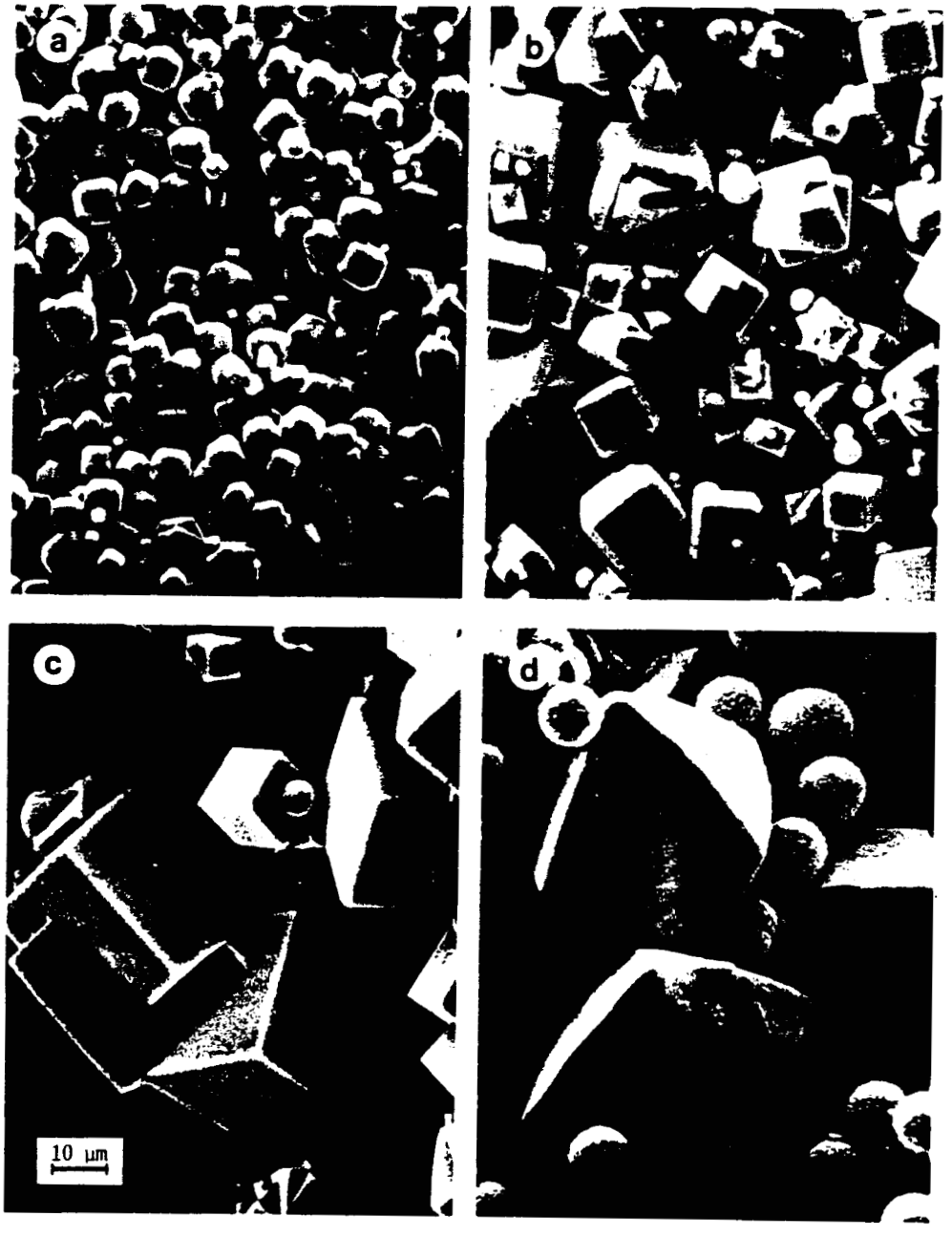


Fig. 2. Scanning Electron Micrographs of Crystals Obtained from Composition $Al_2O_3$ $0.84SiO_2$ $1.94Na_2O$ $194H_2O$ xTEA at 368K; x = (a) 2.12; (b) 4.23; (c) 6.34; (d) 30.0.

scanning electron micrographs of the products obtained in increasing amounts of TEA. These illustrate the size increase obtained in the presence of the amine. In addition, Figure 2d illustrates the occurrence of a different phase in high concentrations of TEA. The diamond shaped crystals are of zeolite Na-X which is normally formed from more siliceous gels than zeolite Na-A. This provided evidence that TEA may be complexing with the aluminum nutrient in the zeolite reaction mixture leading to a suppression of nucleation and ultimately a change in the zeolite phase obtained.

$^{13}C$ nuclear magnetic resonance spectroscopy provided further evidence of the existence of a TEA - aluminum complex in the reaction system. Carbon environments other than those representing unbound TEA were found to exist when the amine was in the presence of an aluminate solution. These additional peaks were attributed to aluminum - bound TEA. They were also present on analysis of TEA containing zeolite synthesis solutions.

Nucleation control is one of the major facets of microgravity processing. For example, it will be necessary to suppress nucleation in order to stabilize the zeolite gel against premature crystallization prior to launch. Shelf life experiments have shown that TEA is successful in stabilizing a zeolite synthesis gel against unwanted nucleation at room temperature. In the absence of TEA, a typical zeolite Na-A synthesis gel will begin to crystallize after 15 days at room temperature. Gels containing approximately 5% by weight TEA were found to be stable for up to 3 months after preparation.

During synthesis in orbit, nucleation control will be necessary to allow the growth of large crystals without depletion of nutrient due to excess nucleation. Studies have shown that TEA can provide this nucleation control and further work related to its mechanism of action may lead to the discovery of a more optimum material for the needs of the project.

### 3.2 Fluid Behavior

A thorough understanding of the fluid behavior of zeolite

reaction mixtures at various stages of the crystallization process is necessary for successful reactor design. Rheological studies were therefore carried out on the precursor reaction mixtures. Viscosity measurements made as a function of time in a constant shear environment, revealed unusual behavior. A viscosity versus time plot for a typical zeolite reaction mixture of composition $Al_2O_3$ $0.84SiO_2$ $1.94Na_2O$ $194H_2O$ after 45 minutes at reaction temperature is shown in Figure 3. This reveals oscillatory behavior which is a function of the non-homogeneity of the reaction mixture. It also shows that these reaction mixtures have a relatively high viscosity despite their high water content (>90%).

Further studies revealed that the zeolite synthesis mixture is a three phase system consisting of a low viscosity solution phase, a highly viscous aluminosilicate gel, and a solid crystalline material. This has important implications for space processing where secondary forces such as surface tension become primary in the absence of gravity. The phenomenon of phase separation may therefore present a problem in microgravity processing.

Several experiments were carried out in mixed solvent systems in order to try to eliminate the phase separation of gel and solution during zeolite crystallization. Addition of low molecular weight alcohols to the synthesis mixtures did not retard phase separation and led to the crystallization of hydroxysodalite, a dense zeolitic phase, which is of little interest commercially. The organic polymer, methyl cellulose, and surfactants, such as oleic acid, failed to stabilize the system with respect to phase separation. None of the above systems exhibited an advantage over the present aqueous solvent.

A second approach to the problem of phase separation was to intentionally separate the gel and solution phase by centrifugation prior to crystallization. A zeolite reaction mixture was prepared and separated into a clear solution phase and dense gel component. These were then reacted separately at 368K. The solution phase crystallization produced a small yield (<1%) of an unknown material. The dense gel component which represented a reaction gel which had been reduced from 95% to 25%

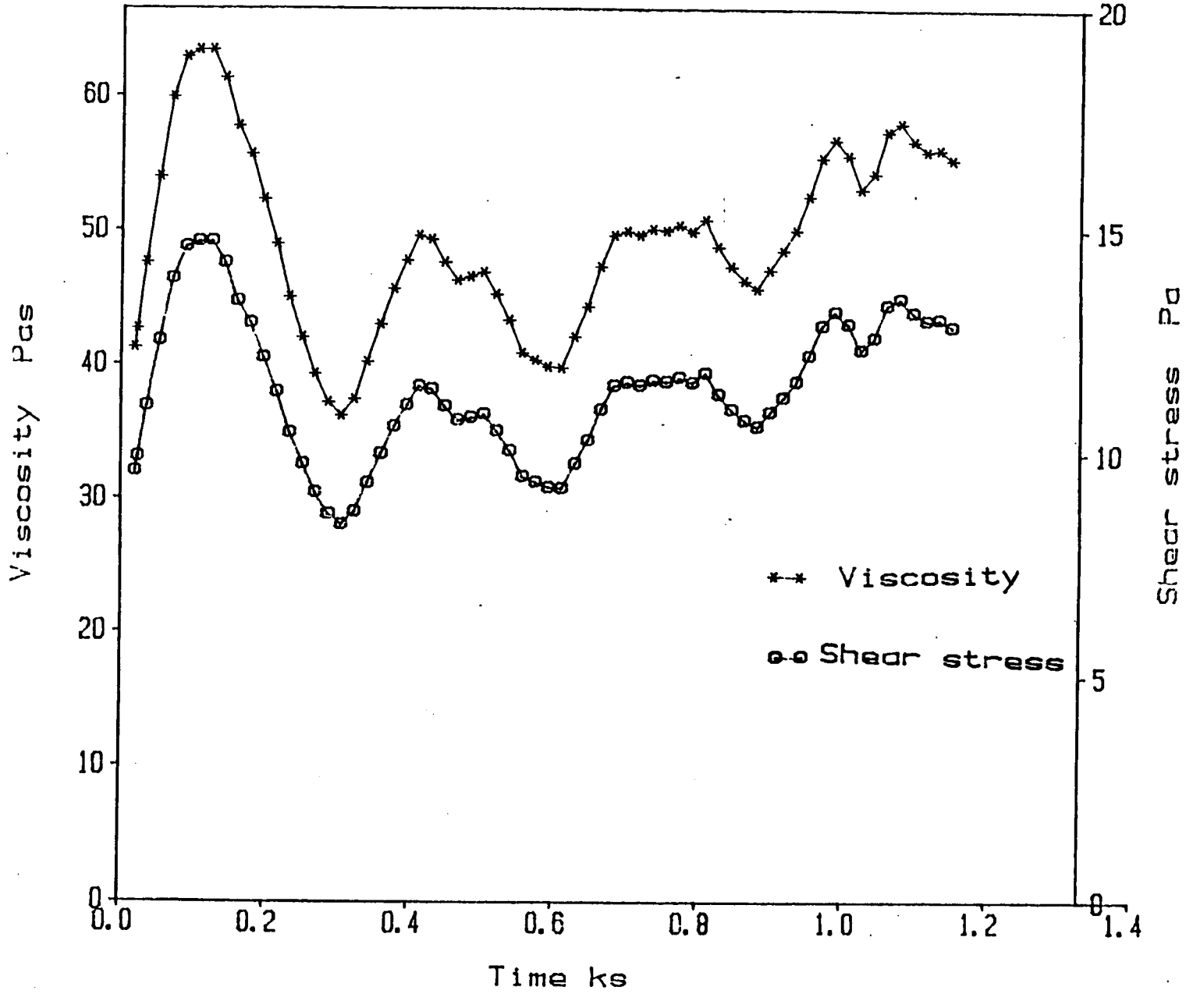


Fig. 3. Viscosity versus Time Relationship for a Zeolite Reaction Mixture of Composition $Al_2O_3$ $0.84SiO_2$ $1.94Na_2O$ $194H_2O$.

water, produced a high yield of zeolite Na-A which exhibited a slight size increase over the standard synthesis mixture.

There are several processing advantages directly linked to this discovery. The first is that phase separation will be reduced in the "reduced water" gel. In addition, the energy costs associated with crystallization from a gel containing 25% water are vastly reduced relative to a gel with 95% water producing similar quantities of zeolite. A reduced water synthesis will therefore be employed in shuttle experiments.

### 3.3 Design Considerations

The design work presently underway is divided into two areas. Initial experiments were aimed towards choosing an appropriate system to fly on NASA's Get Away Special (GAS) program. Design studies are now focused on producing flight ready hardware for NASA's MFL-1 mission.

NASA's Get Away Special (GAS) program provides a low cost method to fly self-contained experiments aboard the space shuttle. A "GAS CAN" was donated to WPI by the MITRE corporation in 1983. A flight-ready synthesis system has been developed which matches NASA safety requirements and is compatible with shuttle operating procedures.

The initial experiments in the "GAS CAN" will provide valuable information regarding zeolite processing in space. Results obtained will aid in the design of second generation hardware for the MFL-1 mission. The advanced reactor will include provision for in-flight mixing and sampling using astronaut participation.

## 4.0 Future Work

The main areas of study now being pursued include further evaluation of reagents for nucleation control and detailed modelling studies of zeolite synthesis gels. The nucleation control studies will be aimed at providing a better understanding of this phenomenon. Aluminum complexation has been established as one mechanism of nucleation control but other possible methods

will be sought.

Detailed modelling studies concerning heat and mass transfer in zeolite synthesis gels under microgravity conditions will be carried out. These will ensure optimum design of the second generation zeolite synthesis reactor for microgravity processing.

## 3. X-RAY DIFFRACTION IMAGING FOR CRYSTAL CHARACTERIZATION

Masao Kuriyama, Bruce Steiner, Ronald G. Dobbyn,
Raghuraman Balasubramanian, and Harold E. Burdette

**NATIONAL INSTITUTE OF STANDARDS AND TECHNOLOGY**
Gaithersburg, Maryland 20899

Our activity with the NASA Center this past year has focussed on four areas:

Development of a comprehensive model for the defect structure in undoped semi-insulating LEC gallium arsenide; this new model interprets satisfactorily for the first time all observations of the principal defect structures in this technically extremely important material (in collaboration with David Larson and Margaret Brown of Grumman Aerospace and Hidehiko Kuwamoto of Rockwell International Science Center).

Initial interpretation of high resolution diffraction images of the defect structure of cadmium telluride grown in a furance designed for space use (in collaboration with Gary Bostrup of Rockwell International Science Center).

Preparations for initial *in situ* diffraction imaging experiments with cadmium telluride (in collaboration with William Wilcox and Raghuraman Balasubramanian of Clarkson University).

Planning for the resumption of *ex situ* experiments on our unique high resolution X-ray diffraction imaging beam line at the National Synchrotron Light Source (NSLS) at Brookhaven National Laboratory (BNL).

## I) The Defect Structure of Undoped Semi-insulating LEC Gallium Arsenide (in collaboration with David Larson and Margaret Brown of Grumman Aerospace and Hidehiko Kuwamoto of Rockwell International Science Center)

We have observed and interpreted pervasive streak-like features in diffraction images of transverse-cut wafers of undoped semi-insulating liquid-encapsulated-Czochralski (LEC) <100>-grown gallium arsenide. These features with the distinctive characteristics had not previously been found in images of semiconductors by any technique. These new features have been shown to be cross sectional images of {110} antiphase boundaries and otherwise characterized by: 1) coherence across the boundary and 2) a phase (atomic) shift at the boundary. This observation of antiphase boundaries also provides the first unified perspective on other prominent crystal imperfections and associated electronic anomalies in III-V materials, which previously appeared to be unrelated or irreconcilable. Furthermore, the new model provides fundamental insight into the increased difficulty in growing III-V materials, such as gallium arsenide over that in growing silicon, and indeed sheds light on the still greater difficulty in growing II-VI materials, such as cadmium telluride. Finally, the new model provides the first simple basis for understanding the role of isoelectronic doping in the reduction of defect density in both III-V and II-VI materials.

Two principal types of defect had previously been observed in such materials and are characteristic of the current observations as well. The first of these is an irregular cellular array of tangled defects for which Burgers vectors cannot be determined. The density of individual defects associated with these cells varies radially in a "W" pattern and azimuthally exhibiting <110> symmetry. The second defect type is a set of linear, very low angle subgrain boundaries normal to the <110> directions lying in the wafer (100) plane, forming a pinwheel pattern. These two types of defect are visible in all high quality wafers to a number of workers using a wide variety of analytic techniques: chemical etching, infrared microscopy, fluorescence, electron microscopy, and x-ray topography. However neither defect could be satisfactorily be explained by a simple model that explained all aspects of the observations; moreover, these two types of defect had not previously been viewed as fundamentally related to one another.

One major school of interpretation has ascribed the individual defects constituting the cells to dislocations, because of the similarity of the defect patterns observed by these various techniques. The genesis of these dislocations had been calculated to be the development of critically resolved shear stress during the rapid cooling intrinsic to LEC growth. However, the interpretation in terms of dislocations had been made without a single piece of firm, specific evidence for dislocations and indeed in spite of the universal failure to determine Burgers vectors for a single cellular defect. Very recently, however, electron diffraction has provided evidence for dislocations in a thinned sample.

In contrast to this school, a second school of interpretation, noting the previous inability to determine Burgers vectors for any of the elements of the cells by any technique and also the similarity of the cell patterns to those associated with constitutional supercooling, has ascribed the cellular structure to dendritic solidification chemistry rather than to dislocations. Both interpretations are based on modeling in conjunction with circumstantial evidence; however the two interpretations are in conflict with one another.

The opportunity provided for us to observe several high quality NASA Center wafers of undoped semi-insulating LEC gallium arsenide with the unique sub arc-second, one micrometer resolution monochromatic synchrotron radiation diffraction imaging capability developed on our NIST beam line at NSLS has enabled us to take a fresh look at the question of the defect structure in such materials, a look independent of the interpretative assumptions that had previously been required.

We observe streak-like features whose visibility is a strong function of the direction of diffraction, a delta function: only that subset of these features that is precisely aligned with the diffraction vector is visible in a given image. and different subsets appear in conjunction with different diffraction vectors. Such visibility behavior is inconsistent with previously accepted classical scattering theory, and required an extension of fundamental theory, which we have carried out and which is now in press[1]

We have obtained the new visibility laws and we have shown that they are required when internal interfaces are present and obey the coherence/phase shift criteria noted above. Of the various possible defect structures, only antiphase boundaries are consistent with the observed restriction of the coherent, phase shifted {110} boundaries. These boundaries are expected to display a lattice tilt because the lengths of the homopolar bonds across the antiphase boundary differs for the bonds characteristic of a single phase. This tilt is actually observed in both types of feature previously observed: the cellular boundaries and the linear, very low angle subgrain boundaries. The distinction arises from the two possible orientations available for propagation of such a tilt. Association of the features observed with antiphase boundaries is confirmed by observation of an anomalous spread in the width of <444> diffractions, derived from the differing lengths of antiphase boundary homopolar and matrix heteropolar bonds, both of which are oriented in <111> directions. A paper has been submitted for publication to describe this unified view of the genesis of the observed defects.

## II) Initial Interpretation of High Resolution Diffraction Images of the Defect Structure of Cadmium Telluride Grown in a Furnace Designed for Space Use (in collaboration with Gary Bostrup of Rockwell International Science Center)

A high resolution symmetric diffraction image of a <111>-slice of cadmium telluride <111>-grown in a furnace designed for space flight and a video tape of this diffraction in the vicinity of the Bragg peak had been obtained in Bragg geometry before the upgrade of the ring was initiated. Detailed analysis of these images has shown several highly interesting aspects of this crystal.

First, no major grain or subgrain boundaries were observed to divide the crystal into two distinct regions; such a division had been postulated to explain the occurrence of two, barely resolved peaks in the diffraction rocking

---

[1] Kuriyama, M., Steiner, B., Dobbyn, R. C., Laor, U. Streaking Images that Appear Only in the Plane of Diffraction in Undoped GaAs Single Crystals: Diffraction Imaging (Topography) by Monochromatic Synchrotron Radiation J. Physical Review B (in press, to be published Dec. 15, 1988).

curve. The current analysis of the images has shown that this aspect of the rocking curve was due either to pitched-roof-like warping of the crystal in the middle or to a relatively sudden change in the lattice parameter along a central stripe in the wafer. Second, unresolved micrometer-sized features are arranged in <110> directions; these features diffract more intensely than the surrounding areas. Third, roughly circular regions several hundred micrometers in diameter are relatively free of these highly diffracting micrometer-sized features.

These aspects of the growth of this cadmium telluride wafer are reminiscent of the defect structure observed in high resolution images of gallium arsenide in Bragg (surface reflection) geometry. Unfortunately, observations of this cadmium telluride wafer could not be made in Laue (transmission) geometry, an approach that had proved crucial to the development of satisfactory insight into the defect structure of gallium arsenide and other semiconductors. However, the similarity of the features observed in cadmium telluride and in gallium arsenide suggest that the initiation and propagation of antiphase boundaries may play a crucial role in the growth of cadmium telluride, as has been shown to be the case for gallium arsenide.

The consequences of antiphase boundaries, if any, in cadmium telluride will be far more severe than in gallium arsenide because of the substantially greater disparity between the length of homopolar Cd-Cd and Te-Te antiphase boundary bonds and the length of heteropolar Cd-Te single phase bonds, in comparison with the smaller disparity between the homopolar Ga-Ga and As-As antiphase boundary bonds and the heteropolar Ga-As single phase bonds. Observations in Laue geometry thus assume a high priority for Center work in the immediate future.

**III) Preparations for Initial <u>In Situ</u> Diffraction Imaging Experiments with Cadmium Telluride (in collaboration with William Wilcox and Raghuraman Balasubramanian of Clarkson University)**

Our ultimate goal in this phase of the activity is to observe in monochromatic synchrotron radiation the evolution of defects during crystallization of cadmium telluride. Several recrystallization experiments have been carried out elsewhere with white radiation. However, the much higher resolution inherent in monochromatic synchrotron radiation should permit much more detailed analysis than that previously possible with white beams.

We have laid plans to carry out this work in three stages. First we will observe the defect behavior of a cadmium telluride sample while it is pulled and heated. This phase will be carried out from room temperature to about 400° C, which can be accomplished in air. In the second stage, we plan to follow defect behavior as the temperature is increased to the vicinity of the melting point. This will require the isolation of the experiment from the surrounding atmosphere. In the third stage, defect behavior will be monitored as part of the sample is melted and recrystallized.

We are currently in the middle of phase one. The experiment for work to 400° C has been designed and is being constructed. Special samples are being manufactured by II-VI Corporation. Essential to this phase of the work has been the familiarization of the student, who has been in residence in Gaithersburg for

six months, with the requirements imposed by monochromatic diffraction imaging and the care required in holding the sample.

IV) **Planning for the Resumption of Ex Situ Experiments on Our Unique High Resolution X-ray Diffraction Imaging Beam Line at the National Synchrotron Light Source (NSLS) at Brookhaven National Laboratory (BNL); (in collaboration with William Wilcox of Clarkson University, Ravi Lal of the University of Alabama, H. Wiedemeier of Rensselaer Polytechnic Institute, Ronald Paulson of Barnes Engineering, Margaret Brown of Grumman Aerospace Corporation, John Viola of the Rockwell International Science Center, and Richard Hopkins of the Westinghouse Research Center).**

The x-ray storage ring at NSLS has recently been recommissioned after a series of modifications. Operation is now far more steady than before the changes. Beam current is being increased gradually and has now reached 130 ma. There is now great interest in the Center not only in continuing the previous set of collaborations but in expanding the set of groups with whom we are collaborating directly.

Unfortunately this desire for broadening our interactions with a wider circle of Center members has come simultaneously with a change in emphasis in the Center in the direction of flight experiments themselves. The establishment of the scientific base that is necessary to provide for the most sophisticated control of the experiments in space has now assumed a lower priority.

We must therefore select with unusual care the samples that we can observe with our unique high resolution diffraction imaging capability. We have had a series of extended discussions on these priorities with Center members, the provisional result of which is to establish priorities for the work that we can carry out under Center sponsorship. We plan to split our work evenly between the in situ and ex situ activity. The in situ work has just been described. The current ex situ priorities are as follows: two organic solution-grown crystals, one each of carefully selected TGS and LAP; a second cadmium telluride sample grown by Rockwell in the Huntsville furnace designed for space flight; a low defect density gallium arsenide sample obtained by Grumman; and a second sample supplied by Rockwell.

## FY 1988 Published Articles


1. Kuriyama, M. Trans. Tech. Publ. Materials Science Forum "Advanced Techniques for Microstructure Characterization" ed. by T. R. Anatharaman and R. Krishnan (1988) Aedermannsdorf, Switzerland.

2. Steiner, B., Kuriyama, M., Dobbyn, R. C., Laor, U. "Diffraction Imaging (Topography) with Monochromatic Synchrotron Radiation," NIST Journal of Research, (Sep/Oct 1988).

3. Kuriyama, M., Steiner, B., Dobbyn, R. C., Laor, U. "Streaking Images that Appear Only in the Plane of Diffraction in Undoped GaAs Single Crystals: Diffraction Imaging (Topography) by Monochromatic Synchrotron Radiation" J. Physical Review B, in press, to be published Dec 15, 1988.

4. Steiner, B., Kuriyama, M., Dobbyn, R. C., Laor, D., Brown, M. "Structural Anomalies in Undoped Gallium Arsenide Indicated in High Resolution Diffraction Imaging with Monochromatic Synchrotron Radiation" submitted to Journal of Applied Physics.

## Figures

Fig. 1. Enlarged image of $(0\hat{4}0)$ H-diffraction in Laue geometry from sample GaAs4 at 8 keV showing streak-like antiphase boundaries forming cell-like walls and the cell center defects.

Fig. 2. Enlarged image of $(\bar{4}44)$ diffraction in Bragg geometry from sample GaAs4.

Fig. 3. Image of (444) diffraction in Bragg geometry from sample CdTe36 at 8 keV. This sample was grown in a furnace designed for use in microgravity.

Fig. 4. Enlarged portion of Figure 3. Note similarity of structure in this cadmium telluride sample to that of gallium arsenide in Figure 2.


FIGURE 1.

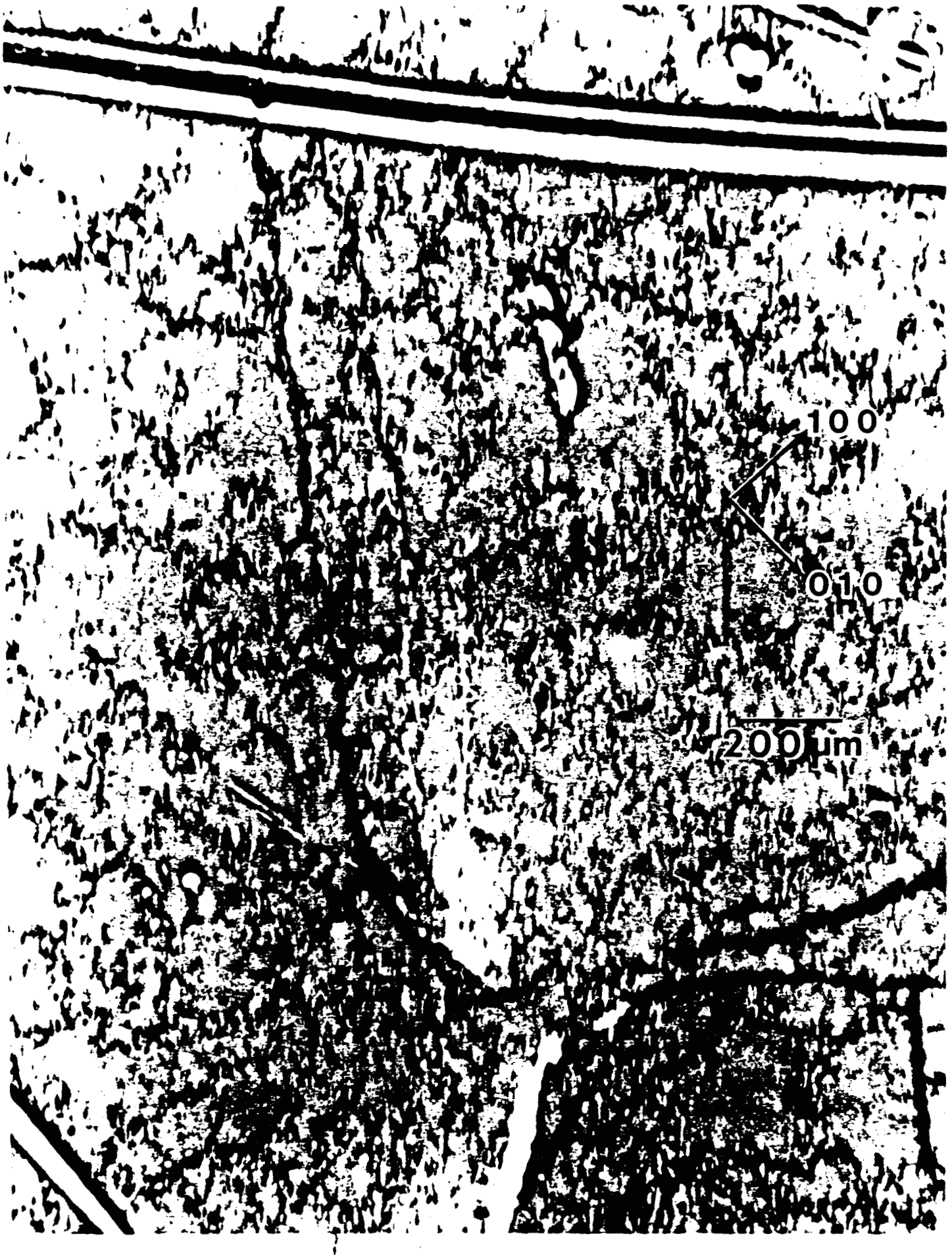


FIGURE 2.




FIGURE 3.


FIGURE 4.

# 4. LIQUID ENCAPSULATED MELT ZONE GROWTH OF GALLIUM ARSENIDE

G.J. Abbaschian, T.J. Anderson, P.H. Holloway, R. Narayanan, W.H. Harter, H.D. Lee, and J.A. Vandezande

**UNIVERSITY OF FLORIDA**
Gainesville, Florida 32605

| | |
|---|---|
| PROJECT TITLE: | Liquid Encapsulated Melt Zone Growth of Gallium Arsenide |
| PRINCIPAL INVESTIGATOR: | G. J. Abbaschian<br>University of Florida |
| CO-PRINCIPAL INVESTIGATORS: | T. J. Anderson<br>P. H. Holloway<br>R. Narayanan |
| ADDITIONAL PROJECT PERSONNEL: | W. H. Harter<br>H. D. Lee<br>J. A. Vandezande |

SUMMARY

The objective of this project is to design, build and test a Liquid Encapsulated Melt Zone (LEMZ) system capable of growing GaAs single crystals. This year, the LEMZ system was assembled, a process for growing GaAs feed stock was developed, and several LEMZ experiments were completed. A number of potential mixed oxide encapsulants have been tested for chemical compatibility with molten GaAs, using ICP and spark source mass spectrometry respectively for quantitative analysis of the major and minor impurities and dopants. Mathematical modelling of the LEMZ process continued; the flow pattern due to forced convection appears to be unicellular, based on analysis using approximate values for thermophysical properties. Apparatus for measuring high temperature properties (viscosity, surface tension) has been received and is being assembled. A simulated LEMZ experiment onboard the NASA space shuttle has been planned for 1990, which will utilize Rockwell's FEA apparatus.

## INTRODUCTION

The objective of this project is to design, build and test a Liquid Encapsulated Melt Zone (LEMZ) system capable of growing GaAs single crystals. This process appears suitable for the microgravity environment, by minimizing buoyancy driven convection during growth and deleterious container effects, thus reducing the associated crystal defects. The long range goal of the project is pilot-scale demonstration of the LEMZ process aboard the NASA space shuttle. This report describes accomplishments for the period October 1987 - September 1988. It is organized into three major sections, 1) Process development and crystal growth, 2) Encapsulant design and product analysis, and 3) Process modelling.

## PROCESS DEVELOPMENT AND CRYSTAL GROWTH

Perhaps the major accomplishment of the current year was assembly and testing of the LEMZ system. Figure 1 is a schematic of the LEMZ furnace and sample assemblies. Based upon the U.F. design described in the previous annual report, the LEMZ frame, preheat and anneal furnaces and power supplies, translators and rotator were built by the Mellen Corporation. These components were assembled at U.F., and coupled to a Lepel R.F. power source and a Zenith computer control system. Initially, problems with the computer control system caused a delay in using the system. These were corrected by modifying the communications system.

A procedure for growing polycrystalline feed-stock rods in the LEMZ furnace using the vertical Bridgeman technique and quartz containment crucibles was developed. As in previous investigations by others, cracking of the quartz crucible and resulting oxidation of the gallium arsenide during growth was initially a serious problem. This was solved by 1) minimizing the superheat of

the molten GaAs, 2) scratching the inner surface of the quartz crucible with 400 grit SiC to minimize wetting, 3) special attention to cleanliness of the crucible and GaAs, involving etching with aqua regia and extensive rinsing with high purity water, and 4) optimizing the temperature gradient in the solidification zone. Using this procedure, a total of 13 polycrystalline GaAs rods, each approximately 10 mm diameter by 100 mm length, were produced from "grade B" GaAs obtained from the Morgan Semiconductor Co. With the optimized procedure, the yield of feedstock production from raw GaAs now approaches 100%.

Initial floating-zone experiments indicated precise control of the molten zone temperature is crucial. Toward this end, a two-color optical pyrometer was purchased from Capintech, Inc. The pyrometer was tested and calibrated using the LEMZ furnace in the float-zone configuration, and a type R thermocouple probe. In general, because of convective cooling of the thermocouple tip by the water-cooled induction coil and/or reflection to the pyrometer from high-temperature areas of the furnace, the "pyrometer temperature" fell between the furnace setpoint (highest) and the "thermocouple probe temperature" (lowest). However, in every case the pyrometer signal was found to be very steady (more so, in fact, than either the control or probe thermocouples). Based on the above, the pyrometer output was used as the control signal for the float-zone experiments described below.

A total of 12 float zone experiments have been performed to date, 10 in the current configuration of the LEMZ system. Experiments 1-5 were preliminary and were intended to provide design parameters for the LEMZ furnace and to develop experimental technique. Experiments 6-10 were performed to investigate coupling of 450 kHz R.F. power with the feedstock. It was found that the 450 kHz power does not couple directly to the GaAs at temperatures below the melting point with adequate efficiency to form a molten zone. For this reason, conductive

susceptors, using graphite or platinum wire, were positioned around the GaAs rods to initiate the molten zone. With the graphite susceptor, it was possible to initiate a "hot zone" at a temperature of up to 200°C above that of the preheat temperature and pass it along the length of the sample, for preheat temperatures above about 900°C. However, because of the large size of the zone, it was not possible to produce a stable molten zone regardless of the preheat temperature. When a thin platinum wire susceptor was used, a groove was cut in the GaAs rod, inside which the susceptor was placed. The platinum susceptor easily coupled to the R.F., forming a small molten zone. With this arrangement, it was possible to establish a 1250°C surface temperature melt zone, and pass it along the length of the sample. After growth, the diameter of the sample was found to be fairly uniform, but the platinum susceptor appeared to have reacted with the sample.

For the most recent three experiments, the frequency of the R.F. generator was changed from 450 kHz to 2.5 Mhz. With the higher frequency, it is possible to couple directly to the GaAs, for preheat temperatures of 900°C and above. However, shortly after the MHz R.F. power is applied, the computer control system for the LEMZ furnace invariably "freezes", and cuts off power to the resistance furnaces. For the last experiment, the computer was disconnected from the resistance power supplies prior to application of R.F. power, and it was possible to establish and traverse a molten zone in the sample. However, this procedure requires manual control of the resistance furnaces without the computer, making it difficult to monitor the preheat and anneal temperatures. To eliminate this problem, a new R.F. power supply has been purchased, which will be connected directly to the pyrometer for control of the power input to the coil. In addition, plans are underway to shield the computer from the R.F. signals.

ENCAPSULANT DESIGN AND PRODUCT ANALYSIS

In the LEMZ process, the ideal encapsulant would serve several useful purposes, specifically, 1) prevention of As loss from the crystal by evaporation, 2) minimization of mechanical stress due to containment during solidification (low melting point), 3) minimization of surface energy driven convection (matching surface energy), and 4) reduction of buoyancy driven convection in the molten zone (high viscosity). In addition, the ideal encapsulant would be non-reactive with the GaAs crystal and the crucible, and would have a low vapor pressure at the processing temperature. In spite of the important role played by the encapsulant in GaAs crystal growth, there has yet to be a complete study taking into account the effect of $B_2O_3$ on the crystal growth or an attempt to find any other material to replace $B_2O_3$.

This year, an experimental method was developed which allows impurity transport between the crystal, encapsulant, and crucible to be studied. This method involves vertical gradient (Bridgeman) solidification, using a two-zone resistance heated furnace and GaAs and encapsulant sealed in quartz crucibles (Figure 2). As in the feedstock and crystal growth experiments, cracking of the crucible during solidification was initially a problem, and was solved using a similar procedure. With the new procedure, and a temperature gradient of 0.2°C/mm, solid GaAs can be grown at a translation speed of 90 mm/h, which is very high compared to the usual speed for single crystal growth.

GaAs samples were grown using $B_2O_3$ and several mixed oxide encapsulants. As reported previously, mixed oxides consisting of (98% $B_2O_3$, 2% $Al_2O_3$), (99% $B_2O_3$, 1% $Nb_2O_3$), and (99.5% $B_2O_3$, 0.5% $La_2O_3$) appeared promising based on consideration of equilibrium phase diagrams and, where available, temperature dependent thermophysical properties. Small ingots of GaAs were produced from each of these encapsulants with no gross damage to the silica crucible or surface

defects in the sample. Other apparently promising mixed oxide encapsulants ($B_2O_3$ + $Bi_2O_3$ or $V_2O_5$) were also tested, but these did cause obvious reactions with the GaAs melt, leading to a very irregular ingot surface.

After growth ampoules containing encapsulant layers and GaAs were cut and polished for optical microscopy, EDS, and microprobe analysis. Optical microscopy indicated reaction between the $SiO_2$ and encapsulant, based on alteration of color and morphology. This was confirmed by EDS, which showed that Si was dissolved into all encapsulants evaluated. Microprobe analysis revealed that in all cases the GaAs also contained dissolved Si, and a small amount of dissolved B. Apparently, $B_2O_3$ dissolves $SiO_2$, and the Si dissolved in the $B_2O_3$ is transported to the GaAs. Also, $B_2O_3$ appears to react with the GaAs melt, leading to incorporation of B in the GaAs.

For quantitative analysis, ICP (Inductively Coupled Plasma spectroscopy) was used to determine the concentrations of Si, Ga, and As in the encapsulants (Table I). As expected, the concentrations of Si were very high, ranging from $6x10^4$ to $10x10^4$ ppmw. The concentrations of Ga ranged from $4.1x10^3$ to $8.4x10^3$ ppmw, and that of As ranged from $1.2x10^2$ to $6.6x10^2$ ppmw. In all cases, the concentration of Ga is higher than that of As by about an order of magnitude, meaning that Ga was removed preferentially from the GaAs melt, and the grown GaAs samples are likely As rich. Spark source mass spectrometry, performed by Northern Analytical Laboratory in Amherst, New Hampshire, was used for analysis of trace elements in the GaAs samples (Table II). The values for boron content are being re-checked, as two samples seem to have been misidentified. Encapsulation appears to have been effective in reducing pickup of Si during growth; the concentration of dissolved Si in the GaAs was reduced from 30 ppma to 1-3 ppma relative to a sample grown without encapsulant. Compared to the initial GaAs used for these experiments, the concentrations of Mg, Al, Ca, and

TABLE I

ICP ANALYSIS OF ENCAPSULANTS
(Samples were grown for 24 h at 1250°C)

| Sample No. | Sample Identification | Concentration (ppmw) Ga (x103) | As (x102) | Si (x104) |
|---|---|---|---|---|
| 1 | B2O3/SiO2 | 0 | 0 | 7.61 |
| 2 | B2O3,Nb2O3/SiO2 | 0 | 0 | 6.94 |
| 3 | B2O3,Al2O3/SiO2 | 0 | 0 | 7.14 |
| 4 | B2O3,La2O3/SiO2 | 0 | 0 | 5.94 |
| 5 | GaAs/B2O3/SiO2 | 4.1 | 1.2 | 8.96 |
| 6 | GaAs/B2O3,Nb2O5/SiO2 | 5.6 | 3.0 | 10.14 |
| 7 | GaAs/B2O3,Al2O3/SiO2 | 3.5 | 6.6 | 9.55 |
| 8 | GaAs/B2O3,La2O3 | 8.4 | 1.9 | 9.84 |

* Samples 1-4 grown without GaAs, Samples 5-8 grown with GaAs

TABLE II

Spark Source Mass Spectrometry Analysis of GaAs

Concentration (ppma)

| El | Raw GaAs | Only GaAs | GaAs with B2O3 | GaAs with B2O3+Al2O3 | GaAs with B2O3+La2O3 | GaAs with B2O3+Nb2O5 |
|---|---|---|---|---|---|---|
| Mg | 0.02 | 0.05 | <0.01 | 0.07 | 0.05 | 0.03 |
| Al | 0.07 | 0.1 | 0.05 | 2 | 0.02 | 0.02 |
| Si | <1.0 | 30 | <1.0 | 3 | 2 | 2 |
| S | <0.2 | 0.5 | <0.2 | 0.7 | 0.5 | 0.5 |
| Cl | 0.03 | 0.2 | 0.08 | 0.2 | 0.1 | 0.2 |
| K | 0.01 | 0.01 | <0.01 | 0.01 | 0.02 | 0.01 |
| Ca | 0.03 | 0.05 | 0.02 | 0.2 | 0.05 | 0.05 |
| Cr | 0.02 | 0.02 | 0.02 | 0.02 | 0.02 | 0.02 |
| Fe | 0.03 | 0.03 | 0.02 | 0.02 | 0.02 | 0.02 |
| Ni | <0.01 | <0.02 | 0.05 | <0.02 | <0.02 | <0.02 |
| Cu | <0.01 | <0.01 | <0.01 | 0.1 | <0.01 | <0.02 |
| Nb | | | | | | 30 |
| La | | | | | 0.5 | |

Fe were reduced by small amounts, and the concentration of Cl and Ni were increased by small amounts.

## PROCESS MODELING

Space-based crystal growth experiments are expensive, and cannot be duplicated on Earth. Therefore, a mathematical model of the LEMZ process will be used to help design the microgravity experiments. As described in the project proposal, the modeling effort has been broken into four parts, specifically 1) the limiting case of zero gravity and negligible Marangoni effect, 2) inclusion of Marangoni effect, i.e., the deflection of interfaces, 3) the effect of low gravity on the above, and 4) the continuation into a high gravity field. The advantage of following this order of analysis is that the first three cases lead to elegant analytical solutions against which the numerical solutions can be compared.

The solution for the first part of the problem has been found, and an abstract of a paper based on this work was recently approved for publication. The technique used is a novel "analytical" one, in which the natural eigenfunctions relevant to the system are used to arrive at a series solution to the velocity profiles. Some numerical calculations are needed, however, to evaluate coefficients of the series such that the boundary conditions are satisfied. This led to consideration of special techniques for solving large order matrices. In particular, rapid convergence techniques based on Pade approximations were considered. These have proven successful, and convergent solutions were found to all matrices involved in the analysis of forced convective fluid flow in the LEMZ. Using estimated values for thermophysical properties, the results indicate unicellular flow of fairly small magnitude for typical LEMZ processing conditions. Due to the small magnitude of the flow, it

may be possible to decouple the forced fluid flow from the heat transfer equations, simplifying the description of both.

Despite the inherent efficiency of this technique, solution of the large matrices involved in this analysis required several hours on a small personal computer. Recently, an Apollo work-station computer was purchased and installed at U.F., and the computation time has been reduced from hours to minutes. A commercial software package, PHOENIX, is currently being evaluated for solution of the gravity driven convection.

## University of Florida - LEMZ Growth of GaAs

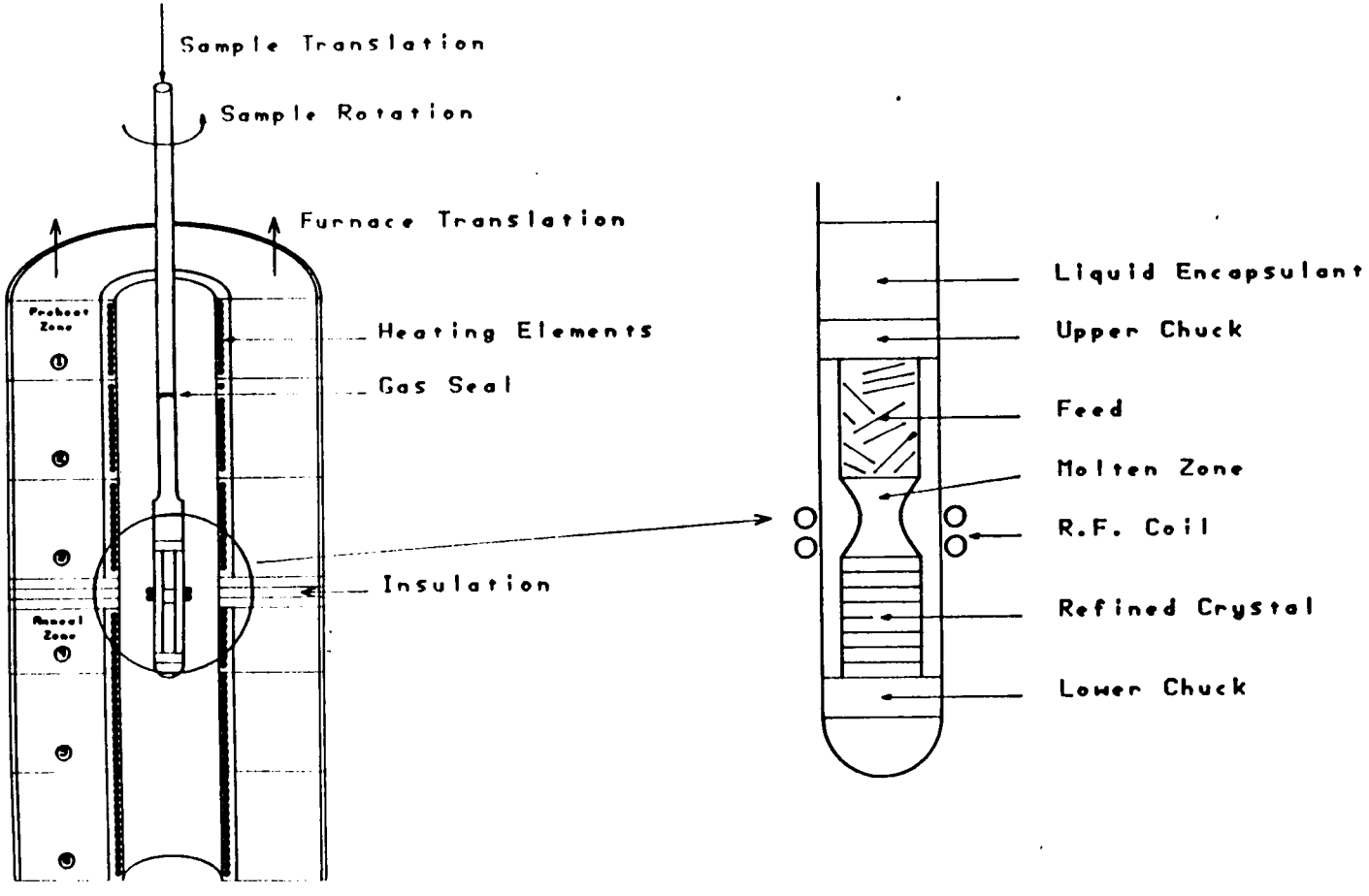


Figure 1: Furnace and Sample Assemblies

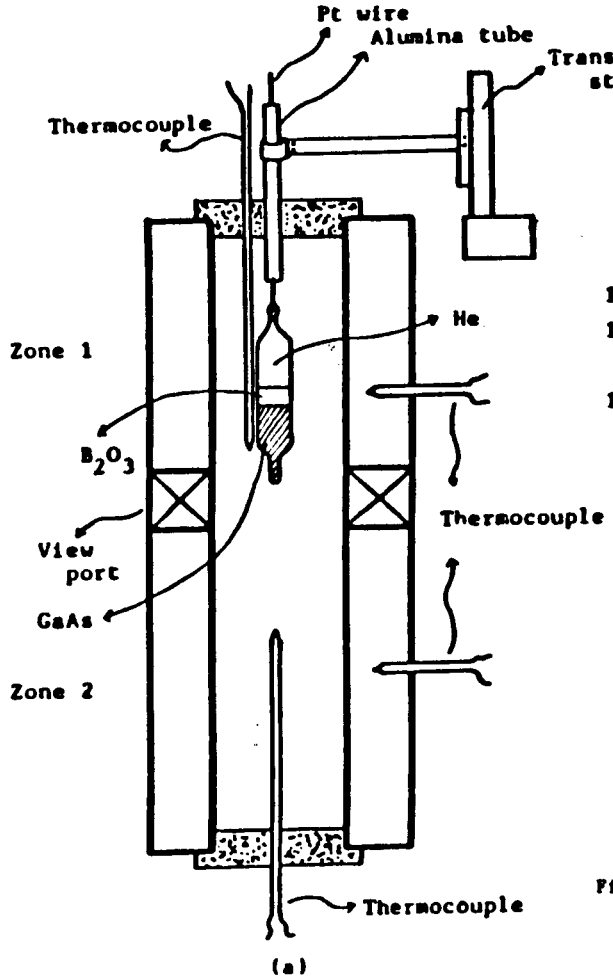


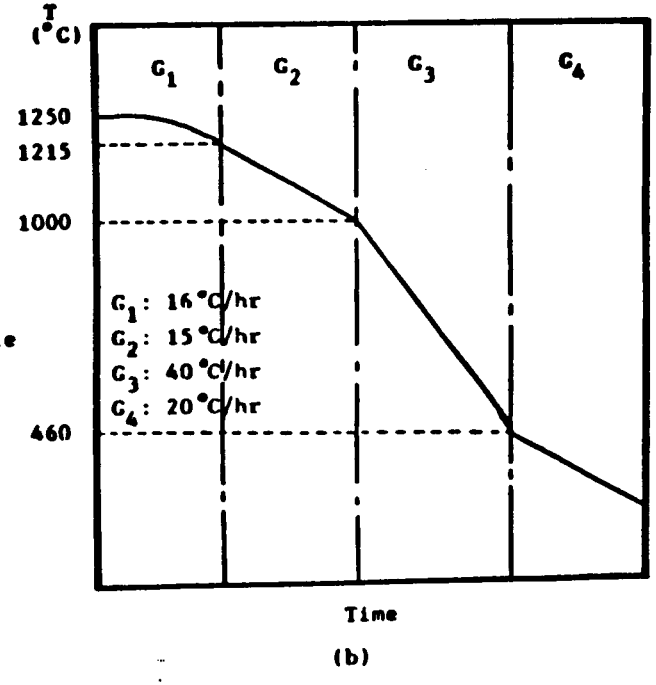


Figure 2. (a) Schematic of Vertical Gradient Freeze Growth
(b) Cooling Schedule for Vertical Gradient Freeze Growth

ORIGINAL PAGE IS
OF POOR QUALITY

University of Florida - LEMZ Growth of GaAs

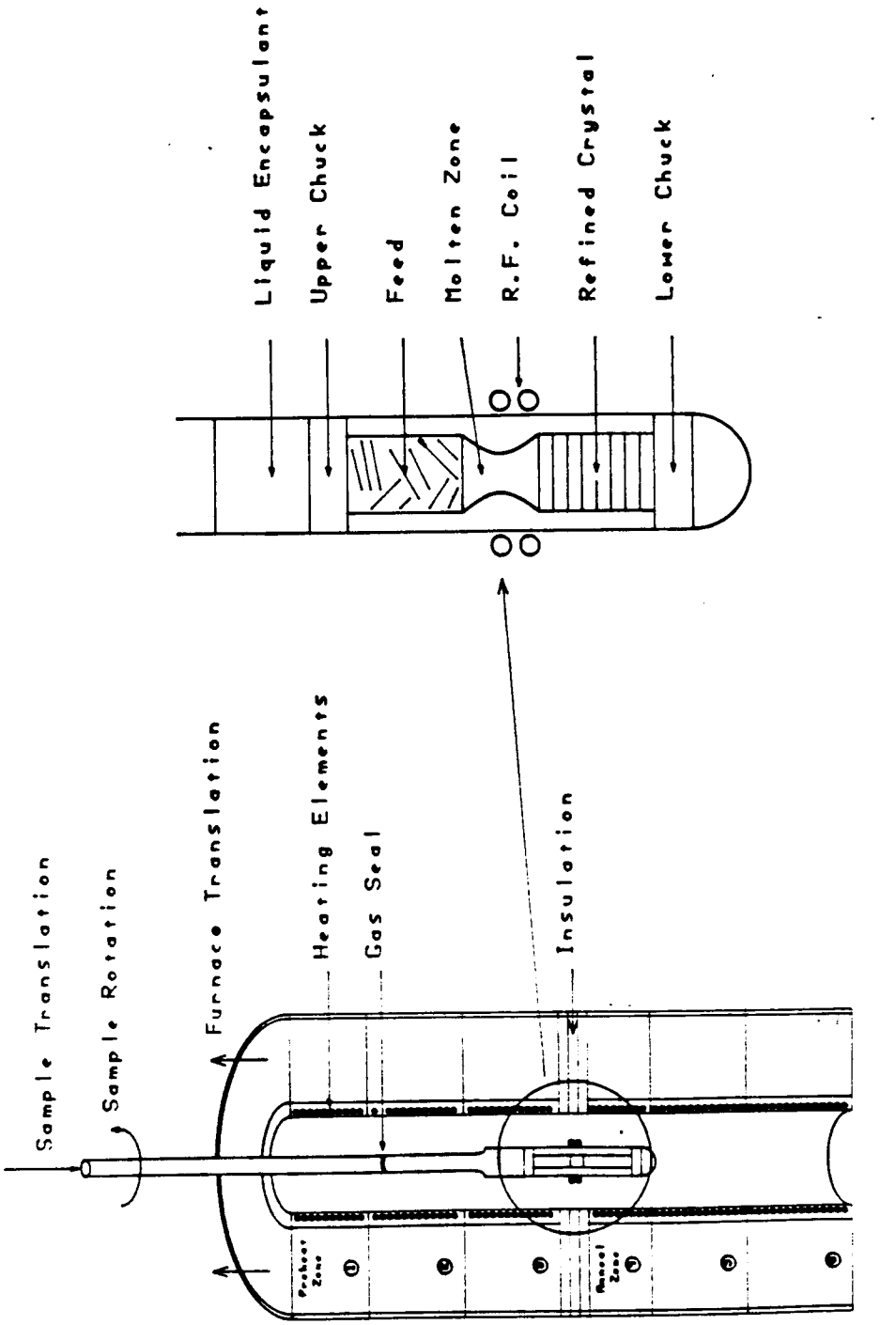


Figure 1: Furnace and Sample Assemblies

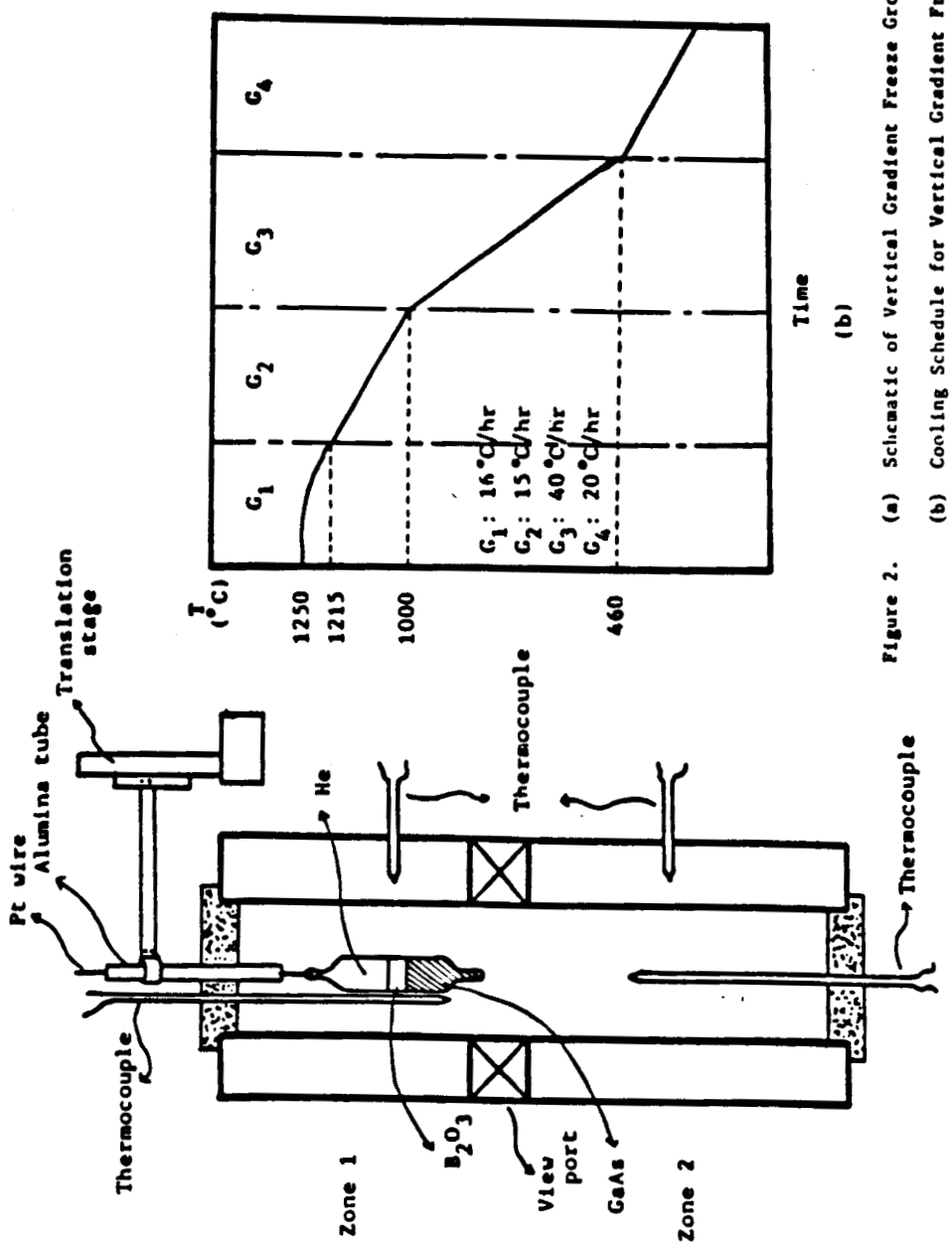


Figure 2. (a) Schematic of Vertical Gradient Freeze Growth
(b) Cooling Schedule for Vertical Gradient Freeze Growth

# 5. EFFECT OF THERMAL AND ACCELERATIONAL PERTURBATION ON FLUID FLOW AND CRYSTAL MORPHOLOGY IN VAPOR PHASE CRYSTAL GROWTH

M.E. Glicksman and Owen Jones

**RENSSELAER POLYTECHNIC INSTITUTE**
Troy, New York 12180

**RENSSELAER POLYTECHNIC INSTITUTE**
**CENTER FOR MULTIPHASE RESEARCH**

# "Effect of Thermal and Accelerational Perturbation on Fluid Flow and Crystal Morphology in Vapor Phase Crystal Growth"

**October 1988**
**CCDS Annual Report**


**Co-Principal Investigators:**

Dr. M.E. Glicksman
Materials Engineering Department
Rensselaer Polytechnic Institute
Troy, NY 12180

and

Dr. Owen Jones
Nuclear Engineering Department
Rensselaer Polytechnic Institute
Troy, NY 12180

**BACKGROUND**

A wide class of photonic materials can be grown by vapor-phase processes into single crystal forms of considerable chemical and physical perfection. Vapor phase crystal growth is relatively slow compared to melt growth techniques, but the method nonetheless provides certain advantages in the specific case of the mercurous and mercuric halides. In the case of $Hg_2Cl_2$ , the melt phase decomposes into two immiscible phases--one a mercury-rich metallic phase, the other a phase rich in mercuric chloride--making useful crystal growth from the melt impossible. This type of undesirable disproportionation is avoidable during vapor-phase crystal growth, provided that the temperature of crystal growth is kept sufficiently low to avoid formation of liquid phases. Fortunately, in the case of $Hg_2Cl_2$ , the vapor pressure of the solid is sufficient in the range 200-300C to allow reasonably rapid transport rates at these temperatures, which are well below the liquidus. Prior work at the Westinghouse R&D Center, by Singh et al., has shown that large, relatively high quality crystals of mercurous chloride can be grown by physical vapor transport in closed ampoules. The commercial potential for such acousto-optical materials have been described by Singh et al.

The quality of a mercurous chloride crystal depends on a number of technical factors associated with its growth. The material purity, for example, has a strong influence, as does the growth rate, crystallographic orientation, spatial orientation, and temperature gradient. Since physical vapor transport of $Hg_2Cl_2$ involves a fluid phase (the vapor) which has a low density compared to that of the solid, the process requires considerable advective flows within the ampoule. The presence of a temperature gradient also suggests that buoyancy effects will also be present during crystal growth. Indeed, prior work at Westinghouse R&D has shown that if mercurous chloride is doped with impurities, then striations appear along the length of the crystal, suggesting that fluctuations occurred in the growth rate, which, in turn, altered the incorporation of the impurities. Such effects are well known in melt growth, where the influences of convection on the temperature and the impurity distribution are well documented.

The research being pursued at Rensselaer on the vapor phase growth of mercurous chloride is directed primarily at exposing the influence of internal convection on the crystal behavior. Specifically we are attempting to measure by non-intrusive

techniques the internal velocity fields during crystal growth. Conditions for growth are selected to be as close as possible to the actual practice of the industrial partner's laboratory. Laser doppler velocimetry (LDV) was selected as the method of choice for measuring these flows. The technique is almost completely non-intrusive, and is capable of high spatial resolution. The major technical problems with which the Rensselaer team was challenged involved: 1) detecting the extremely slow flows characteristic of vapor-phase growth of mercurous chloride, and 2) providing suitable light scattering centers that would be compatible with the crystal growth process. Both areas were addressed during 1988.

Specifically, work over the past year has been directed toward modifying a Spectron industrial laser particle detecting system to permit flow detection down to 50 $\mu$/sec flow velocities. Described below are some of the accomplishments in achieving operation of this system using an unique Bragg cell heterodyne system to electronically frequency shift one laser beam to permit slow flow detection. The first successful measurements of flows in a mercurous chloride growth reactor, as small as 150-200$\mu$/sec along the crystal growth axis, were achieved at Rensselaer early in the fall of 1988. By employing relatively impure mercurous chloride for the crystal growth, the required light scattering was achieved by naturally occurring motes, which are dispersed in the vapor space during crystal growth. These motes are believed to be small (0.1$\mu$ diameter) pinchite crystals, which is a commonly occurring oxychloride of mercury often observed in slightly moist $Hg_2Cl_2$ .

As described below in detail, the Spectron system is continuing to be improved to permit better computerized data acquisition and analysis. The crystal growth furnace is also currently being modified by Westinghouse to allow more measurements to taken, especially away from the ampoule axis. These measurements should begin during the early part of 1989.

**Overall Program Status Report**

A brief overall program status report is given with details presented subsequently.

* A new laboratory in the R.P.I. Materials Research Center. Electrical and plumbing modifications, required for laser operation, were completed.

* Special direct memory access software required to transfer data from the Spectron system to a Compac 386 microcomputer was developed.

* The crystal growth furnace was returned to Westinghouse for modifications.

* A laser traversing system has been designed. Specification and purchase of essential parts is in progress.

**SUMMARY OF RESULTS AND ACHIEVEMENTS**

The main objective of this year's research was to determine if it is possible to use Laser Doppler Velocimetry (LDV) to study flow fields during physical vapor transport. Preliminary results indicate that LDV can indeed provide us with data on velocity distribution inside the closed crystal growth ampoule. We have been able to determine the velocity vector at a single point inside the ampoule and plans are underway to measure the complete radial and axial vapor phase velocity distributions as a function of the crystal growth operating parameters.

During the early stages of this research, our effort was directed at solving the problem of "seeding" the flow with sub-micron particles which could provide scattering sites for the LDV system. It was also necessary to know how long the seed particles would remain in the flow once they were introduced. Typical vapor phase crystal growth takes approximately two days to complete and it is possible that new seeds would have to be introduced to study the complete transient velocity profile. We used incense smoke to initially examine this question. Incense smoke typically has a most probable diameter on the order of 0.5 microns. We found that it took the incense particles four to six hours to settle down in stagnant air. The time it took these particles to settle down in a closed system with convection was again four to six hours. We then concluded that it would be necessary to introduce new particles if we were to observe flows for the entire duration of vapor phase crystal growth. Next we performed tests with highly pure, distilled and zone refined camphene. Scattering particles were not observed at under any conditions of vapor pressure in the highly-purified camphene. All this led us to believe that seeding could possibly turn out to be a serious problem.

After several discussions with co-investigators at Westinghouse, it was decided to use stock material for this study which is a somewhat impure form of, mercurous chloride. Visual observation of the mercurous chloride ampoule provided by Westinghouse revealed the presence of small contaminant

particles. We decided to test the material at this level of purity to see if these particles could be used as seed particles thereby eliminating the need to introduce the seeds separately.

Initial tests of the above mercurous system were performed. We were able to observe scattering centers passing through the laser beams at typical operating temperatures and to record the velocity data with the LDV system. Figures 1 and 2 show the actual temperature distribution in the furnace. The arrow shows the position where the laser beams crossed and thus the position where the vapor velocity was measured. Approximately 5 to 10 particles crossed the path of the laser beams every second (on an intermittent basis) and we measured a large distribution of particle velocities ranging from -200 microns/sec to +260 microns/sec. This velocity distribution is shown in Fig. 2 where the average and most probable velocity are indicated. We found the typical values for average velocity to be around 70 microns/sec and the most probable velocity to be around 150 microns/sec. These values seem to be quite reasonable under the conditions we are operating. However, they pose a number of interesting questions. For example, why do we observe negative velocities? Are some of the particles so big that they are settling down? Are there any convection cells or flow reversals in the ampoule?

To answer these questions, we need to modify the LDV system so that it can give us simultaneous data and particle size and particle velocity. We also would like to take a radial and an axial scan of the velocity profile in the ampoule. This would require that the furnace be re-wired with the heating coils wrapped around at sufficient distances to permit the laser beam from entering the ampoule without hitting the coils. Plans to do these are underway. The furnace has been sent to Westinghouse for rewiring. New software is being written to ease data acquisition and analysis. Some of the details of this software development are given below.

**Software Development**

Software Development is required before proceeding with further measurement. The method used for previous measurements provided the period, with a shift caused by the Bragg Cell, in hexadecimal form. To perform the required data conversion for the number of measurements required for the velocity distribution would slow the process of data collection. The software currently being developed allows the data to be collected by a Compaq 386 microcomputer with

output of velocity in cm/sec and of a graph of velocity histogram.

The Spectron analyzer provides two types of information; front panel information and experimental data. Front panel data consists of various experimental parameters such as laser beam spacing, photomultiplier voltage and fringe spacing which remain constant during the reading of data. Experimental data consists of two measured quantities, period and visibility, for each scattering center which passes through the measuring volume. The velocity of the scattering center can be calculated from the period data which is provided as unsigned binary. Visibility data can be used to calculate scattering particle size in the standard Spectron system . With addition of the Bragg cell, the visibility data is unreliable and is not used.

A Metrabyte PDMA-16 high speed digital interface board captures the data via the Compaq 386 direct memory access controllers directly from a Spectron signal processor. The data is placed in an array in RAM where it can be accessed by a computer program which will convert the data to velocity and output the velocity in a useable form. Since all of the data is sent via the same PDMA-16 I/O address, it is collected together in the same memory location and must be separated before the period can be processed into velocity. Additionally, the period is frequency shifted due to the Bragg cell and must be corrected before velocity is calculated. The software that captures the information into an array has been written; further effort is needed on the conversion of the raw data to useable form.

## ADMINISTRATION AND PERSONNEL

Several significant changes in project management, location, and personnel occurred near the end of FY 1987-1988.

- The project manager and co-PI, Professor Owen C. Jones, Nuclear Engineering Department, left the US on a one-year sabbatical leave. Professor Jones will not manage the current research program until his return to Rensselaer late in 1989. Professor M.E. Glicksman, Materials Engineering Department, will, to the extent possible, assume those managerial and technical duties normally provided by Professor Jones during this period.

- Dr. Edward Kurz, the post-doctoral associate assigned to this research program left Rensselaer for other employment in October, 1988. Dr. Kurz was primarily responsible for developing the low-velocity LDV system. His presence on the program will be

missed. We have assigned Mr. Christopher Paradies and Dr. Shakeel Tirmizi to the program. Mr. Paradies is a graduate student in Materials Engineering, and Dr. Tirmizi is a post-doctoral research associate. Dr. Tirmizi's assignment is part time. Mr. Paradies is currently concentrating on completing the software development phase to permit more convenient use of the LDV system with the associated microcomputers. Dr. Tirmizi, a Ph.D. in chemical engineering, will assist in the analysis of data and provide some of the day-to-day technical supervision.

• The laboratory housing the research program was changed in September 1988. The original location was a high-quality, air conditioned space in Rensselaer's Center for Industrial Innovation, an ultra-modern laboratory and office complex. Unfortunately, that laboratory space, which was on loan to this project, was needed urgently for other purposes. The project equipment was moved to a laboratory in the Materials Research Center, which, unfortunately, lacks such amenities as a chemical fume hood and temperature control. The basic LDV system is again operational, but experiments with mercurous chloride have been halted pending installation of a suitable fume duct.

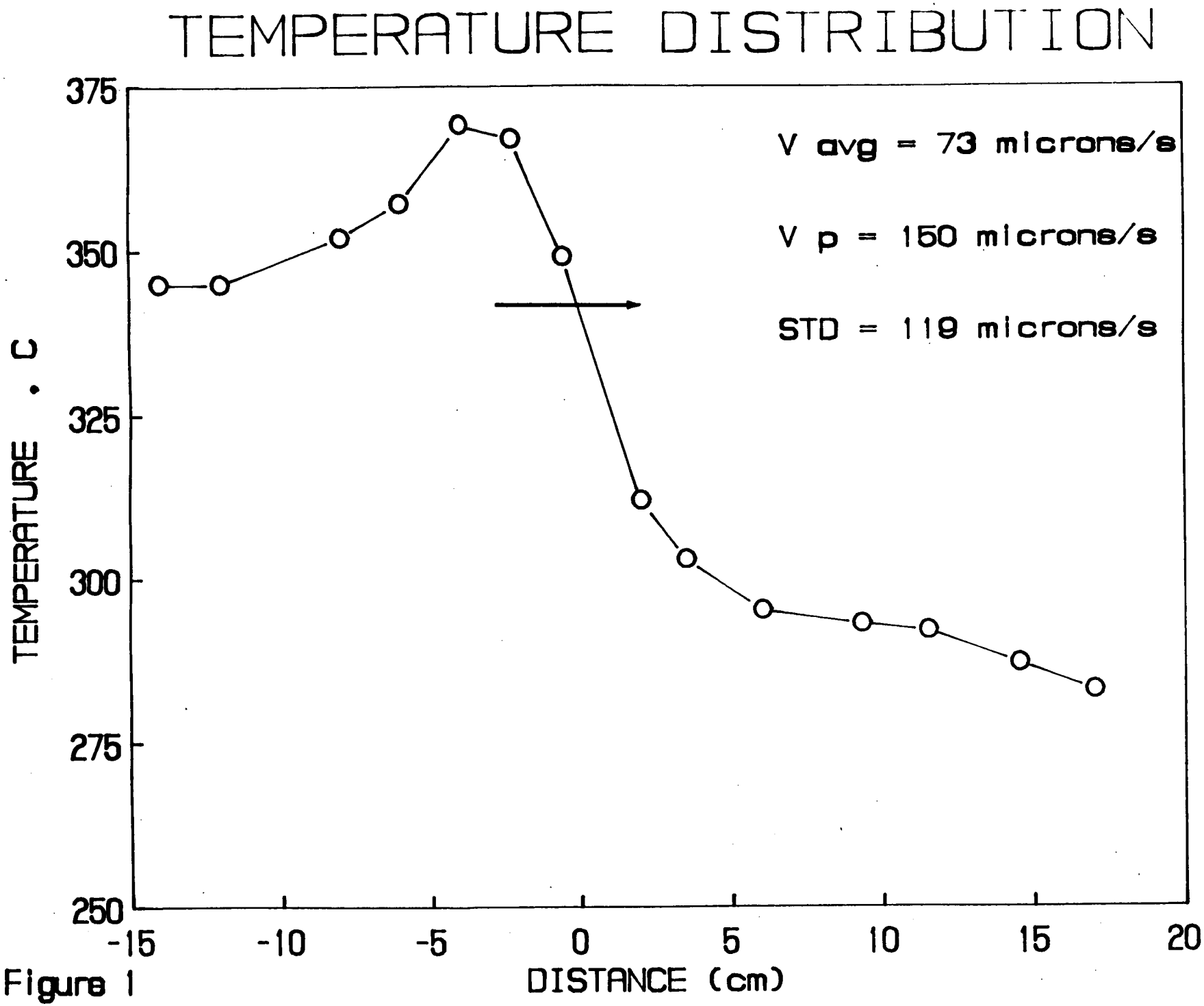
TEMPERATURE DISTRIBUTION
V avg = 73 microns/s
V p = 150 microns/s
STD = 119 microns/s
TEMPERATURE • C
375
350
325
300
275
250
-15
-10
-5
0
5
10
15
20
DISTANCE (cm)

Figure 1

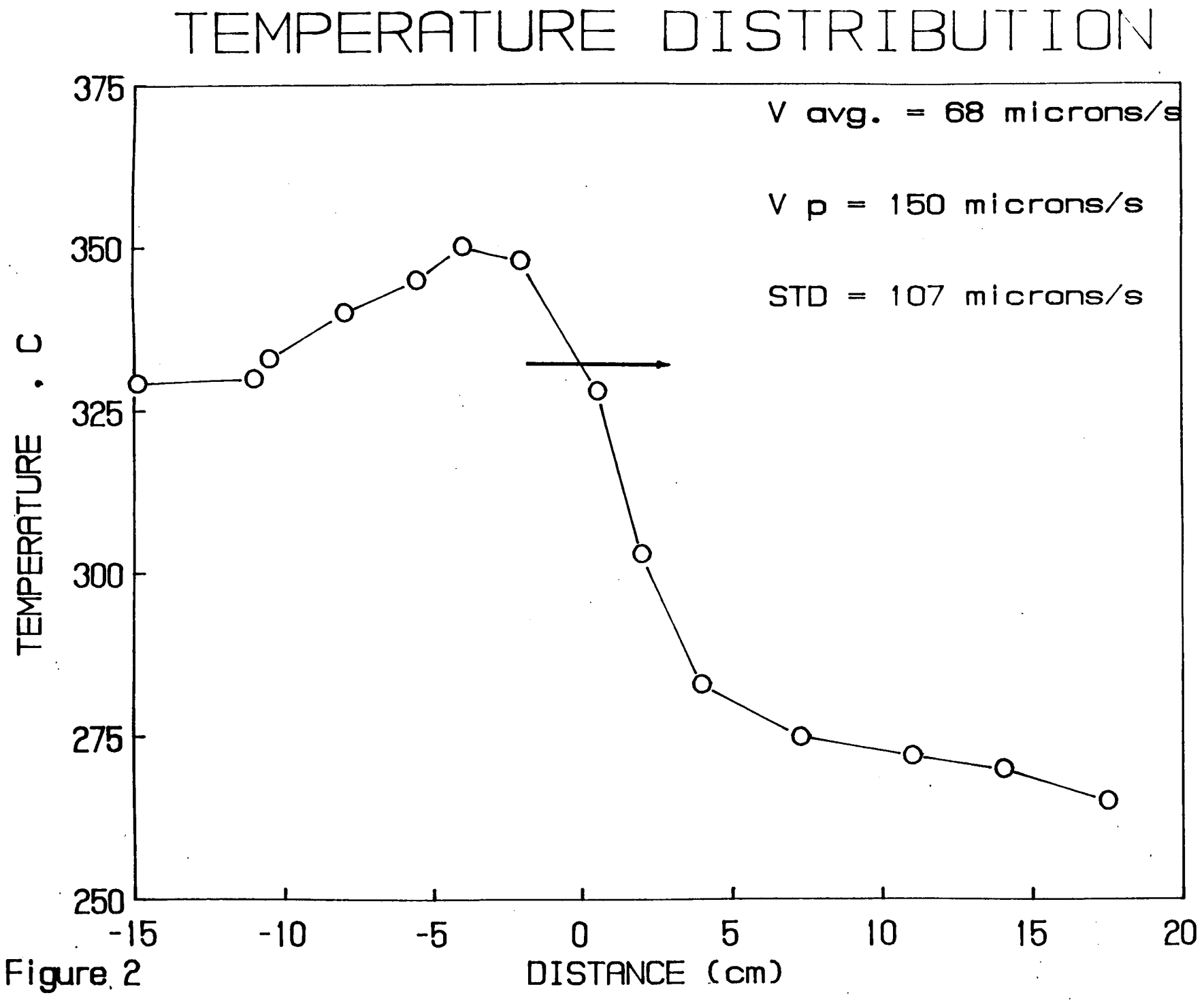
TEMPERATURE DISTRIBUTION
V avg. = 68 microns/s
V p = 150 microns/s
STD = 107 microns/s
TEMPERATURE . C
375
350
325
300
275
250
-15
-10
-5
0
5
10
15
20
DISTANCE (cm)

Figure 2

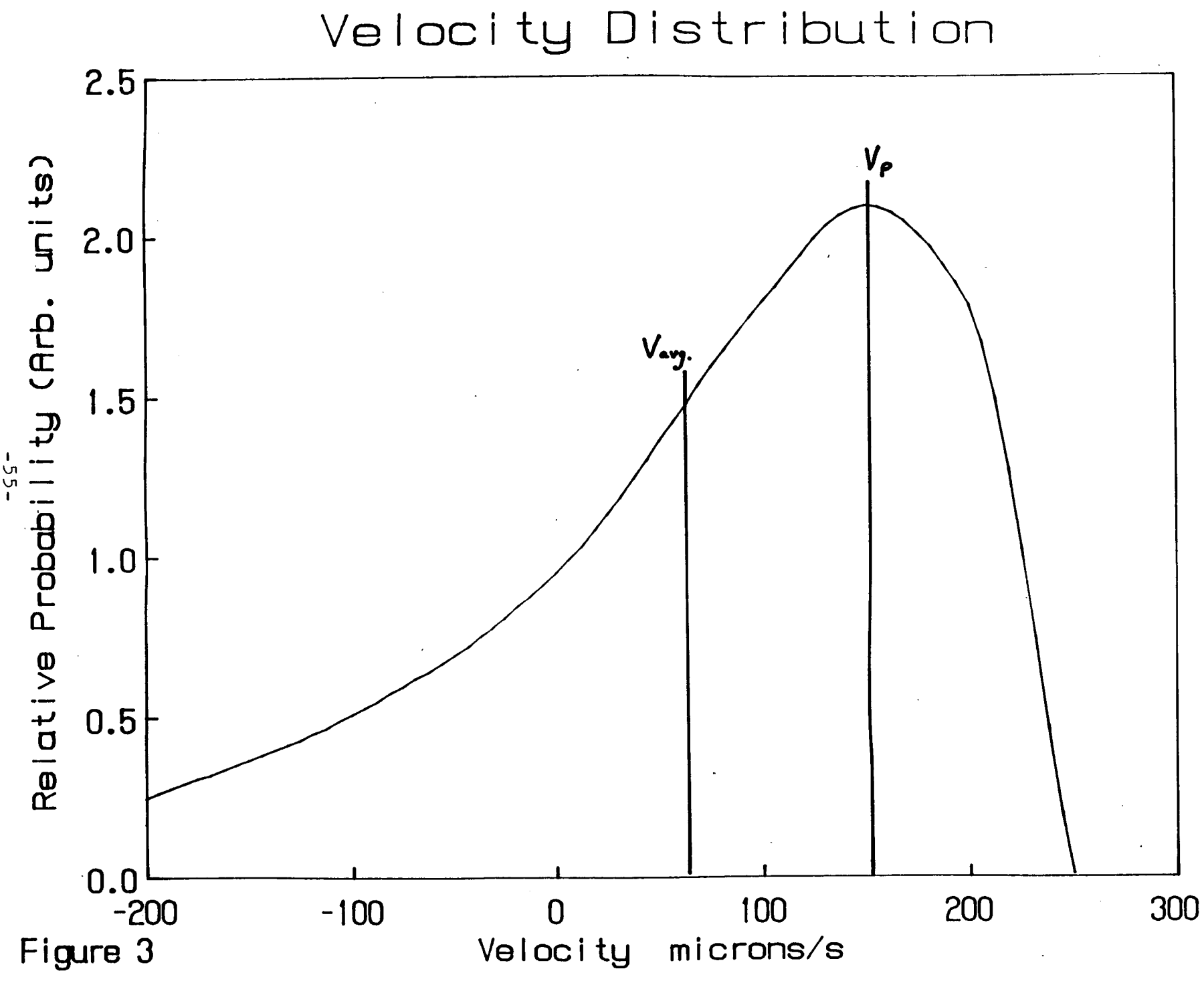
Velocity Distribution
2.5
2.0
1.5
1.0
0.5
0.0
Relative Probability (Arb. units)
$V_p$
$V_{avg.}$
-200
-100
0
100
200
300
Velocity microns/s

Figure 3

# 6. GROWTH OF CRYSTALS FOR ROOM TEMPERATURE INTRARED DETECTORS AND NON-LINEAR OPTICAL DEVICES

R.B. Lal and A.K. Batra

**ALABAMA A&M UNIVERSITY**
Normal, Alabama 35762

## Personnel

| | |
|---|---|
| Principal Investigator: | R. B. Lal<br>Professor of Physics<br>Alabama A and University<br>P.O. Box 71<br>Huntsville, AL 35762 |
| Other Personnel: | Dr. A. K. Batra<br>Research Assistant Professor<br><br>2 Graduate Students |
| Industrial Partners Sponsoring this Work: | EDO/Barnes Engineering Division<br>Teledyne Brown Engineering<br>Quantum Technology<br>Metro Laser<br>Spectron Development Lab |

# GROWTH OF CRYSTALS FOR ROOM TEMPERATURE I.R. DETECTORS AND NON-LINEAR OPTICAL DEVICES

## I. INTRODUCTION

The major tasks for research at Alabama A and M University deals with the following two areas.

1. Growth and characterization of crystals required for room temperature infrared detectors.

2. Growth and characterization of organic and inorganic non-linear optical crystals for second harmonic generation.

The crystals for both I.R. detectors and for non-linear devices are grown by low temperature solution crystal growth technique. During this period the main emphasis is placed towards the growth of doped - Triglycine Sulfate (TGS) crystals for I.R. detectors and L-Arginine Phosphate (LAP) crystals for frequency doubling of Nd-YAG laser.

Also initial plans were made including a concept towards designing a simpler solution growth hardware capable for either GAS experiment or mid-deck experiments. Preliminary design for GAS experiments were made including a concept of a simple optical system.

TGS crystals doped with 8000 ppm L-alanine in solution grown in small crystallizer (1 liter) gave much improved I.R. detector characteristics. Later, the same experiment was repeated in a larger crystallizer (5 liter) to produce larger crytals ( 3 cm size). The crystals are now with EDO/BEO for fabrication of I.R. detectors. It is significant to note that five detector cells made on one single crystal slice gave uniform and improved detector characteristics (see table for detector characteristics).

During this year an optimum value of the pH for LAP solution has been determined, which produced optical quality LAP single crystals. This study is no way complete and further pH ranges will be studied to produce better crystals. Also, other growth rate studies are underway to determine optimum conditions for growing optical quality larger crystals.

# INVESTIGATION AND GROWTH OF MATERIALS FOR ROOM TEMPERATURE I. R. DETECTORS

R. B. LAL (AAMU) AND R. F. PAULSON (EDO/BED)

## ● LONG TERM GOALS AND OBJECTIVES:

1. TO INVESTIGATE THE GROWTH OF CRYSTALS REQUIRED FOR ROOM TEMPERATURE I. R. DETECTORS.
2. TO INVESTIGATE/CHARACTERIZE MATERIALS FOR DETECTORS AND TO IMPROVE THEIR DEVICE CHARACTERISTICS.
3. INVESTIGATE MATERIALS WITH HIGHER D* VALUES AND HIGHER $T_c$
4. TO FABRICATE I. R. DETECTORS AT BARNES ENGINEERING
5. INVESTIGATE MATERIALS FOR LARGE-FORMAT ARRAYS. (EDO/BEC)
6. PLAN AND DESIGN FLIGHT EXPERIMENT



## ● SHORT TERM GOALS AND OBJECTIVES:

1. TO INVESTIGATE OTHER DERIVATIVES OF TRIGLYCINE SULFATE (DOPING WITH INORGANIC AND ORGANIC IMPURITIES) FOR HIGHER D* VALUE AND HIGHER $T_c$
2. TO GROW CRYSTALS AND STUDY GROWTH KINETICS.
3. MEASURE ELECTRICAL PROPERTIES OF GROWN CRYSTALS.
4. TO FABRICATE DETECTORS AT EDO/BEC
5. PLAN AND DESIGN "GAS" CAN EXPERIMENT IN COLLABORATION WITH TBE.

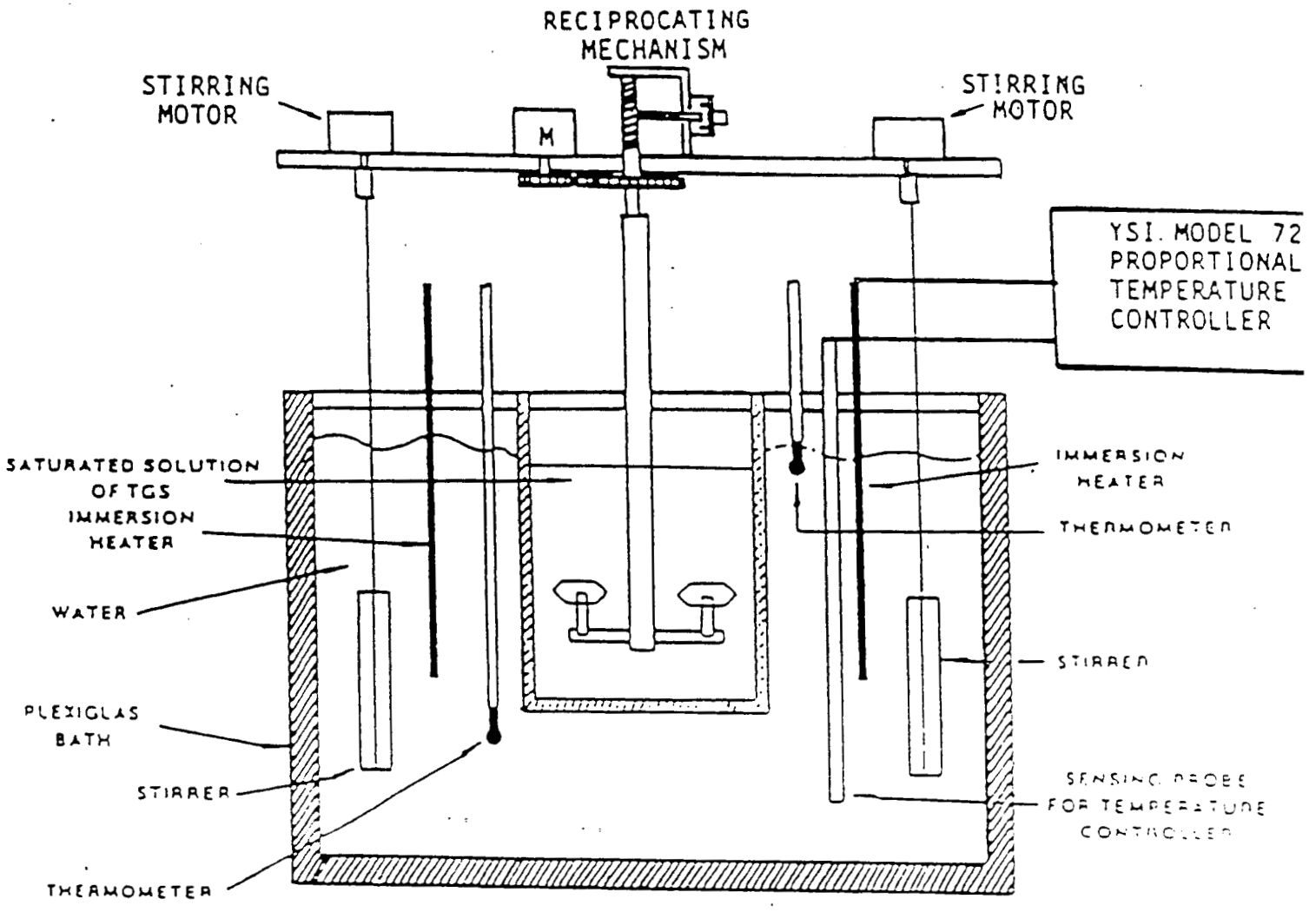


Fig. 1: . Schematic Diagram of Solution Crystal Growth Set-up

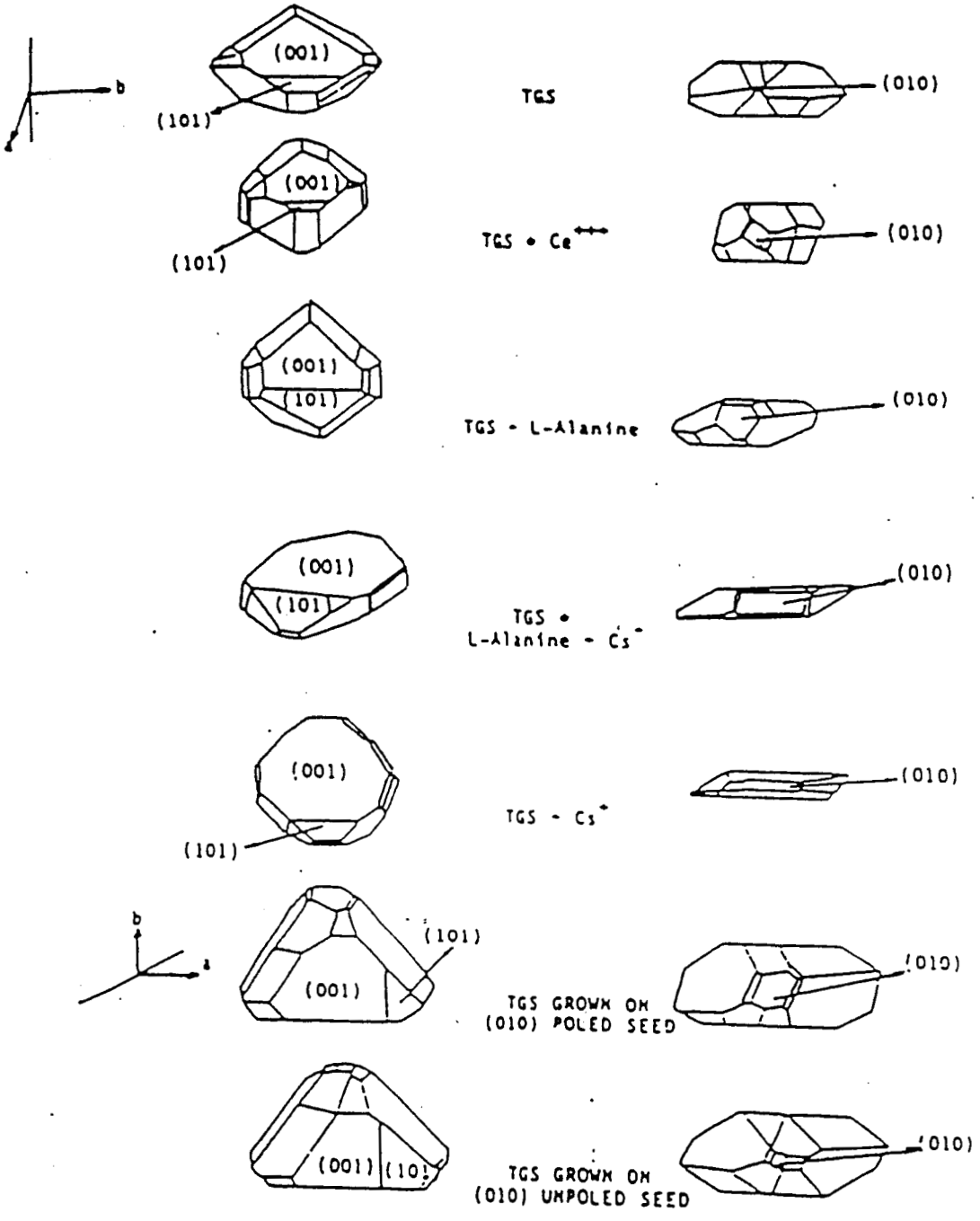




Fig. 2. Morphological Description of Various TGS Crystals

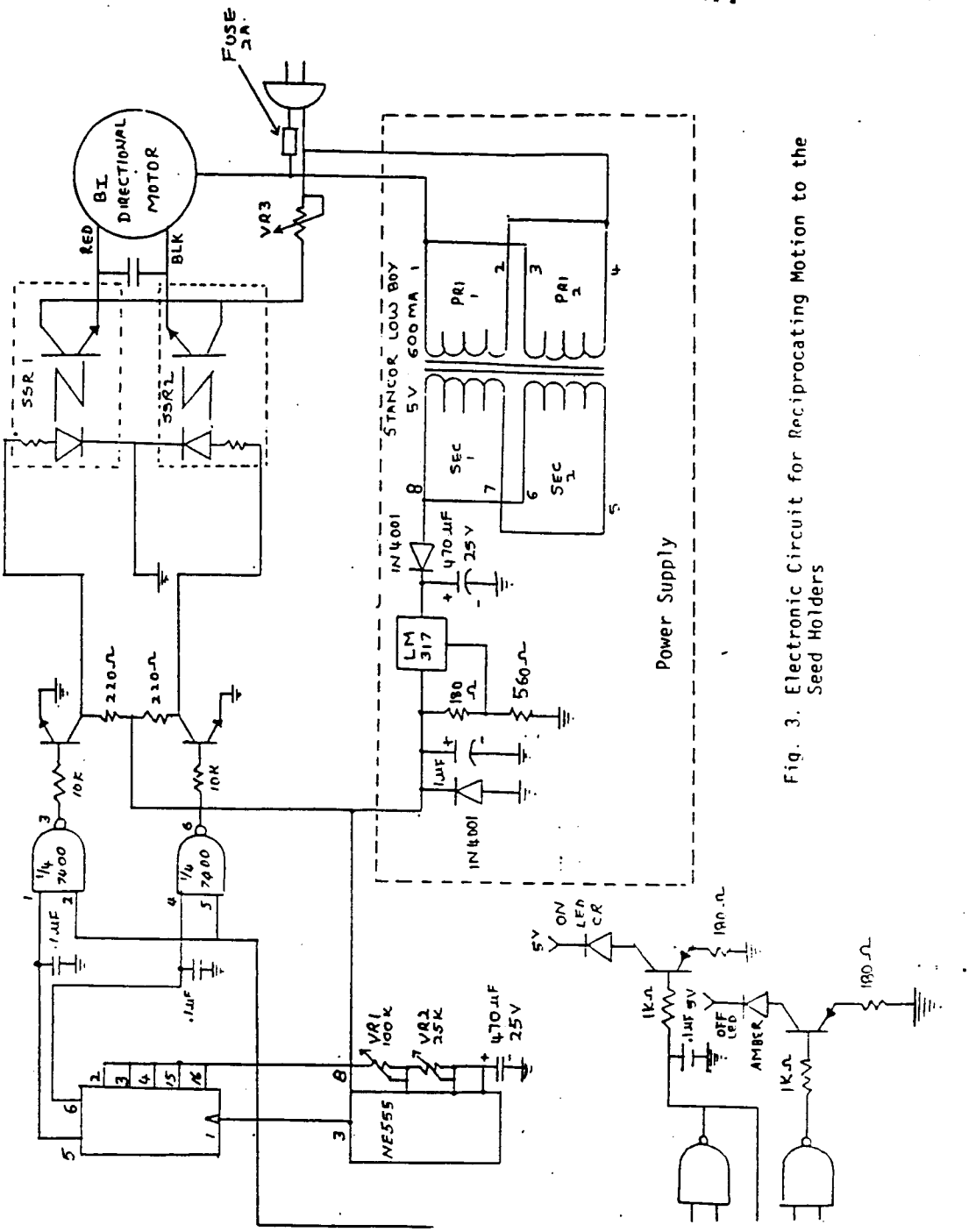


Fig. 3. Electronic Circuit for Reciprocating Motion to the Seed Holders

# MATERIAL PARAMETERS OF TGS CRYSTALS

| CRYSTAL / TEMP°C | PYROELECTRIC COEFFICIENT, p ($nC/cm^2°C$) | | | | DIELECTRIC CONSTANT $\epsilon'$ | | | | FIGURE OF MERIT $p/\epsilon'$ ($nC/cm^2°C$) | | | |
|---|---|---|---|---|---|---|---|---|---|---|---|---|
| | 30 | 35 | 40 | 45 | 30 | 35 | 40 | 45 | 30 | 35 | 40 | 45 |
| TGS | 53 | 70 | 98 | 170 | 48 | 64 | 106 | 250 | 1.1 | 1.09 | 0.92 | 0.68 |
| TGS + LA6 | 68 | 85 | 115 | 215 | 65 | 125 | 280 | 710 | 1.04 | 0.68 | 0.41 | 0.30 |
| TGS + Cs | 43 | 64 | 85 | 155 | 67 | 84 | 120 | 300 | 0.64 | 0.76 | 0.70 | 0.52 |
| TGS + LA | 38 | 44 | 80 | 172 | 30 | 37 | 48 | 62 | 1.2 | 1.48 | 1.6 | 2.7 |
| TGS + Cs + LA | 55 | 134 | 200 | 315 | 38 | 41 | 54 | 69 | 1.44 | 3.26 | 3.7 | 4.5 |

# FABRICATION OF I. R. DETECTORS

- SAMPLE NO. 1 (PURE TGS)
  SAMPLE NO. 2 (TGS-DOPED WITH L-ALANINE)
  SAMPLE NO. 3 (TGS-DOPED WITH Cs + L-ALANINE)

- ALL SAMPLES WERE POLISHED, LAPPED, WATER ETCHED AND ELECTRODED WITH TRANSPARENT GOLD

- CELL SIZE 2mm x 2mm x 50m

- CELL MOUNTED BEC PYROELECTRIC HEADERS WITH 5 x 10" OHMS LOAD RESISTER

- WINDOW USED KRS-5

- NOISE BANDWIDTH $\sim$ 6Hz

- SYSTEM GAIN FOR SET-UP $\sim$ 500

- RMS POWER DENSITY $\sim$ $3.54 \times 10^{-4}$ WATT/$Cm^2$ AT THE DETECTOR

# DETECTOR CHARACTERISTICS

| SAMPLE | CELL NO. | RESPONSIVITY (V/W) 1000 K / BLACKBODY | | NOISE(nV/Hz ) | | D* (1000K,f,1)x$10^8$ | |
|---|---|---|---|---|---|---|---|
| | | 15 Hz | 90 Hz | 15 Hz | 90 Hz | 15 Hz | 90 Hz |
| NO. 1 (TGS) | 20930 | 1 x $10^3$ | 160 | 260 | 80 | 7.7 | 4.0 |
| | 20944 | 1 x $10^3$ | 160 | 170.5 | 56 | 12.0 | 5.5 |
| NO. 2 (TGS+ L-ALANINE) | 20752 | 1 x $10^3$ | 160 | 190 | 65 | 11.0 | 5.0 |
| | 20885 | 1 x $10^3$ | 160 | 167 | 60 | 11.8 | 5.3 |
| | 20963 | 950 | 160 | 190 | 66 | 12.0 | 5.2 |
| | 20803 | 1 x$10^3$ | 160 | 175 | 60 | 13.5 | 5.6 |
| | 20941 | 1 x $10^3$ | 160 | 167 | 54 | 12.3 | 5.7 |
| NO. 3 (TGS+ Cs+ L-ALANINE) | 20986 | 1 x$10^3$ | 150 | 560 | 140 | 3.35 | 2.05 |
| | 20924 | 850 | 130 | 280 | 92.5 | 6.25 | 3.0 |
| | 20980 | 890 | 140 | 760 | 170.5 | 2.20 | 1.6 |

# RUTHERFORD BACKSCATTERING CHARACTERIZATION OF

# TGS CRYSTALS

---

- TGS-Fe-Cs
- TGS-LA-Cs *

---

* THE DISTRIBUTION OF THE CONSTITUENTS WERE MEASURED AT SIX POINTS ON THE SURFACE OF THE CRYSTAL.

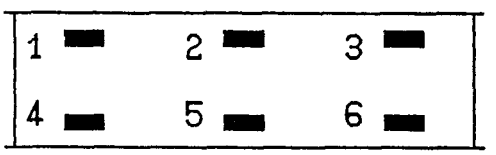


TGS-LA-Cs

ATOMIC RATIO OF THE ELEMENTS TO CARBON
BY RBS

| | HOi | Zi | Mi | $N_1/N_2$ | | |
|---|---|---|---|---|---|---|
| C | 2560 | 6 | 12 | 97±7 | TGS-LA-Cs | 6 |
| S | 190 | 16 | 32.066 | | | |
| C | 2560 | 6 | 12 | 2.34±0.06 | TGS-LA-Cs | 6 |
| N | 1492 | 7 | 14 | | | |
| C | 2592 | 6 | 12 | 107. ±8 | TGS-LA-Cs | 5 |
| S | 174 | 16 | 32.066 | | | |
| C | 2805 | | | 109±8 | TGS-LA-Cs | 4 |
| S | 185 | | | | | |
| C | 2704 | | | 70.±4 | TGS-LA-Cs | 3 |
| S | 277 | | | | | |
| C | 3079 | | | 114±8 | TGS-LA-Cs | 2 |
| S | 194 | | | | | |
| C | 2685 | | | 104±8 | TGS-LA-Cs | 1 |
| S | 185 | | | | | |
| C | 2685 | | 12 | 2.36±0.06 | TGS-LA-Cs | 1 |
| S | 1555 | | 14 | | | |
| C | 2592 | | | 2.36±0.06 | TGS-LA-Cs | 5 |
| S | 1498 | | | | | |
| C | 2805 | | | 2.23±0.05 | TGS-LA-Cs | 4 |
| N | 1721 | | | | | |
| C | 2704 | | | 2.38±0.06 | TGS-LA-Cs | 3 |
| N | 1555 | | | | | |
| C | 3079 | | | 2.46±0.06 | TGS-LA-Cs | 2 |
| N | 1713 | | | | | |
| | | | | | | |

| | HOi | Zi | Mi | $N_1/N_2$ | |
|---|---|---|---|---|---|
| S | 225 | 16 | 32.066 | 12.4±1.8 | TGS-LA-Cs |
| Fe | 48 | 26 | 55.847 | | |
| N | 1241 | 7 | 14 | 300.±51 | TGS-Fe-Cs |
| Fe | 48 | 26 | 55.847 | | |
| C | 1630 | 6 | 12. | 646.±93 | TGS-Fe-Cs |
| Fe | 48 | 26 | 55.847 | | |
| C | 1630 | 6 | 12 | 1.79±0.05 | TGS-Fe-Cs |
| N | 1241 | 7 | 14 | | |
| S | 225 | 16 | 32.066 | 106.5±21 | TGS-Fe-Cs |
| Cs | 25 | 55 | 132.905 | | |
| N | 1241 | 7 | 14 | 3095±619 | TGS-Fe-Cs |
| Cs | 25 | 55 | 132.905 | | |
| | | | | | |

Hoi - Yield
Zi - Atomic No
Mi - Atomic Mass
$N_1/N_2$ - Atomic Ratio

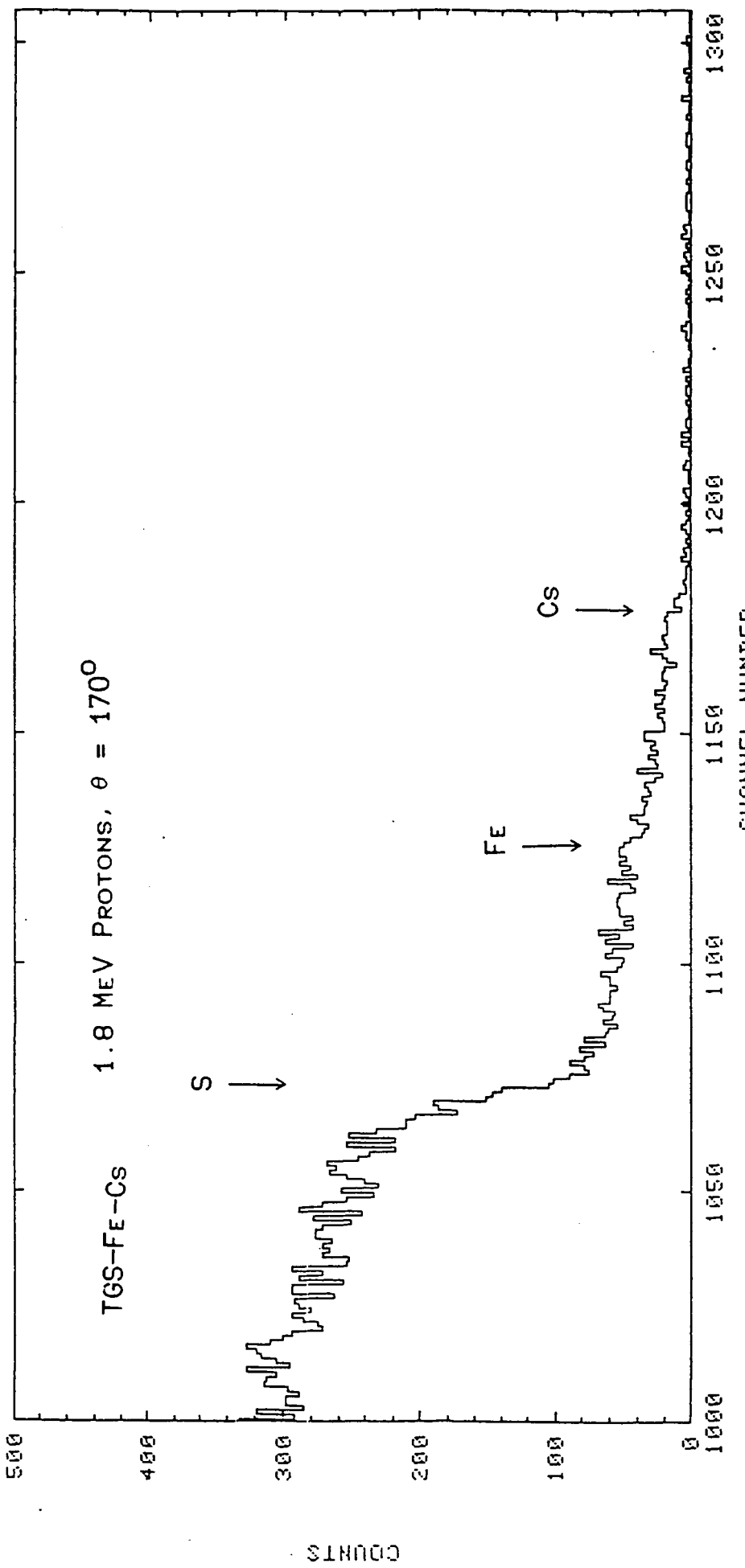
TGS-Fe-Cs
1.8 MeV Protons, θ = 170°
S
Fe
Cs
COUNTS
CHANNEL NUMBER
0
100
200
300
400
500
1000
1050
1100
1150
1200
1250
1300

FILE: TGSCE

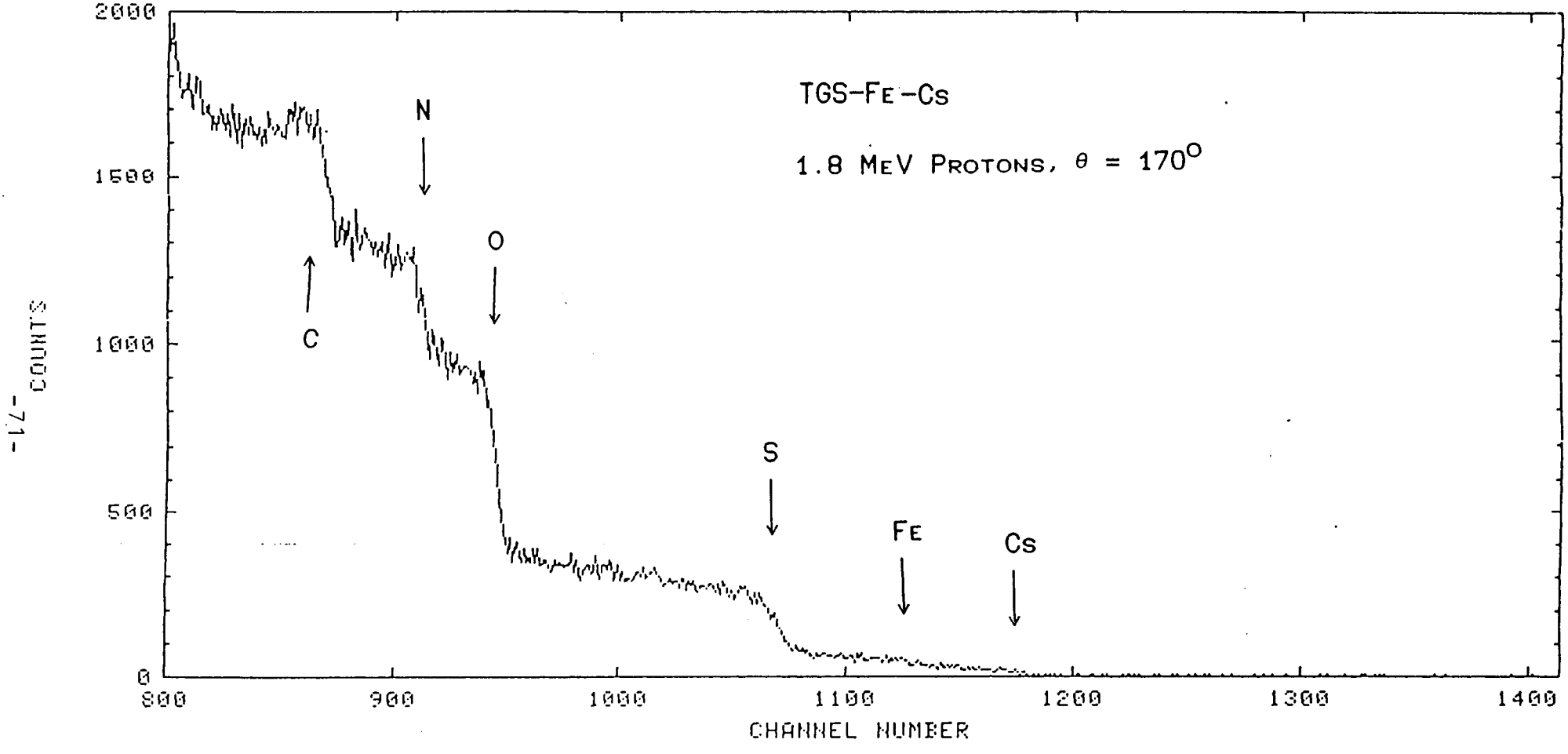
TGS-FE-CS
1.8 MEV PROTONS, θ = 170°
C
N
O
S
FE
CS
COUNTS
CHANNEL NUMBER
2000
1500
1000
500
0
800
900
1000
1100
1200
1300
1400

FILE: TGSCE

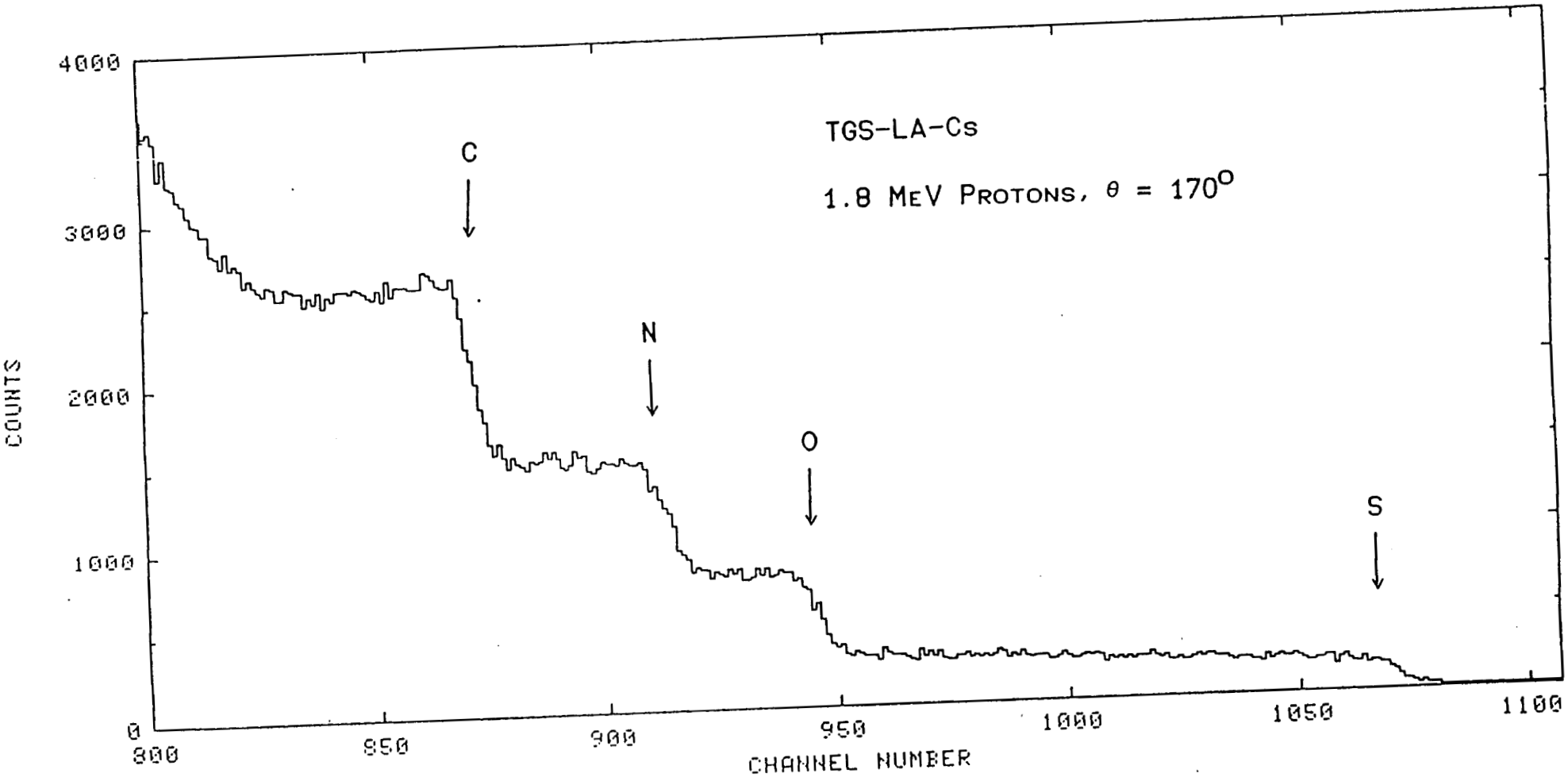
TGS-LA-Cs
1.8 MeV Protons, θ = 170°
C
N
O
S
4000
3000
2000
1000
0
COUNTS
800
850
900
950
1000
1050
1100
CHANNEL NUMBER

FILE: TGSLC7

# GROWTH OF L-ARGININE PHOSPHATE MONOHYDRATE CRYSTALS (LAP) FOR SECOND HARMONIC GENERATION (SHG)

R.B. LAL (AAMU), T. MOOKHERJI (TBE),
R.A. ADHAV (QTI), SDL, JIM TROLINGER (METRO LASER)

- **LONG TERM GOALS AND OBJECTIVES:**
  1. TO SEARCH FOR NEW NON-LINEAR MATERIALS IN ORDER TO FIND ALTERNATE SOURCES OF ENERGY AT VARIOUS WAVELENGTHS IN THE ELECTROMAGNETIC SPECTRUM.
  2. COMPARE LAP WITH OTHER POSSIBLE MATERIALS
  3. FABRICATE DEVICES
  4. PLAN FLIGHT EXPERIMENTS



- **SHORT TERM GOALS AND OBJECTIVES:**
  1. TO FORM THE COMPOUND LAP FROM L-ARGININE AND PHOSPHORIC ACID.
  2. TO MEASURE THE BASIC PHYSICAL PROPERTIES OF LAP (SOLUBILITY, REFRACTIVE INDEX. DENSITY, ETC.)
  3. TO ANALYZE THE FORMED COMPOUND BY X-RAY TECHNIQUES.
  4. TO GROW CRYSTALS OF LAP AND STUDY GROWTH KINETICS.
  5. TO STUDY GROWTH AS A FUNCTION OF pH OF LAP SOLUTION.
  6. TO CHARACTERIZE GROWN CRYSTALS.
  7. PLAN AND DESIGN "GAS" CAN EXPERIMENT, IN COLLABORATION WITH TBE, EDO/BED, AND METRO LASER.
  8. INVESTIGATE A SIMPLER VERSION OF SOLUTION GROWTH FACILITY.

# GROWTH OF NEW NONLINEAR OPTICAL CRYSTAL L-ARGININE PHOSPHATE [LAP] ($C_6H_{14}N_4O_2.H_3PO_4.H_2O$).

## IMPORTANCE

- OPTICAL QUALITY LAP CRYSTALS CAN BE GROWN FROM AQUEOUS SOLUTIONS.
- PHASE MATACHABLE, WITH CONVERSION EFFICIENCY THREE TIMES THAT OF KDP.
- DAMAGE THRESHOLD ABOUT TWICE THAT OF KDP.
- WIDE TRANSMISSION RANGE (IR TO UV).
- CHEMICALLY INERT AND MOISTURE FREE.

## REASONS FOR UNDERTAKING THIS STUDY

1. L-ARGININE PHOSPHATE IS A RELATIVELY NEW MATERIAL. PRACTICALLY NO RESEARCH LITERATURE IS AVAILABLE TO SUGGEST THE OPTIMUM CONDITIONS UNDER WHICH OPTICAL QUALITY LAP CRYSTALS CAN BE GROWN FROM AQUEOUS SOLUTIONS.

2. LAP HAS BEEN PROPOSED AS A REPLACEMENT FOR POTASSIUM DI HYDROGEN PHOSPHATE (KDP), THE MATERIAL MOST COMMONLY USED FOR FREQUENCY CONVERSION OF INFRA RED LASERS AT LLNS, CALIFORNIA.

# OBJECTIVES OF THIS RESEARCH

1. TO DETERMINE THE SOLUBILITY CURVE FOR LAP.

2. TO DETERMINE THE REFRACTIVE INDEX OF THE LAP SOLUTION AS A FUNCTION OF TEMPERATURE AND CONCENTRATION.

3. TO STUDY THE GROWTH OF LAP CRYSTALS AS A FUNCION OF pH OF SOLUTION AND STIRRING RATE, AND FROM THE OPTIMUM pH AND FORCED CONVECTION TO GROW TRANSPARENT CRYSTALS.

4. TO DETERMINE THE OPTIC AXIS OF THE LAP CRYSTALS GROWN BY USING He-Ne LASER.

5. TO VISUALLY ASSESS THE MORPHOLOGY OF LAP CRYSTALS AS A FUNCTION OF pH OF THE SOLUTION.

6. TO DETERMINE THE SECOND HARMONIC CONVERSION EFFICIENCY OF LAP AND TO COMPARE IT WITH THAT OF KDP.

7. TO DETERMINE THE FWHM AND WAVE LENGTH OF THE SECOND HARMONIC OF Nd:YAG LASER, GENERATED BY THE LAP CRYSTAL.

# SYNTHESIS OF LAP COMPOUND

1. COMPOUND L-ARGININE PHOSPHATE IS NOT AVAILABLE AS SUCH. IT THEREFORE HAS TO BE SYNTHESIZED IN THE LABORATORY.

2. L-ARGININE [$C_6H_{14}N_4O_2$] AND PHOSPHERIC ACID [$H_3PO_4$] ARE MIXED IN THE STOICHIOMETRIC RATIO AND DISSOLVED IN DEIONIZED WATER AS SHOWN BELOW:

$$C_6H_{14}N_4O_2 + H_3PO_4 \xrightarrow[H_2O]{50^\circ C} C_6H_{16}N_4O_3.H_3PO_4$$

250 gm OF L-ARGININE.
114 gm OF PHOSPHERIC ACID.
662 gm OF DEIONIZED WATER.

3. CRYSTALLITES OF LAP ARE FORMED AFTER ALLOWING THE SOLVENT TO EVAPORATE AT ROOM TEMPERATURE.

# CONFIRMATORY TEST OF FORMATION OF LAP COMPOUND

POWDER SAMPLE OF LAP CRYSTALS WAS PACKED BETWEEN TWO GLASS SLIDES TO FORM A CELL OF APPROXIMATELY 3mm THICKNESS AND IRRADIATED WITH Nd:YAG LASER [1064 nm] 10ns PULSE.

A GREEN COLORED GLOW WAS OBSERVED IN THE SAMPLE, WHICH WAS THE SECOND HARMONIC OUTPUT [532nm] CORRESPONDING TO THE 1064nm INFRARED INPUT.

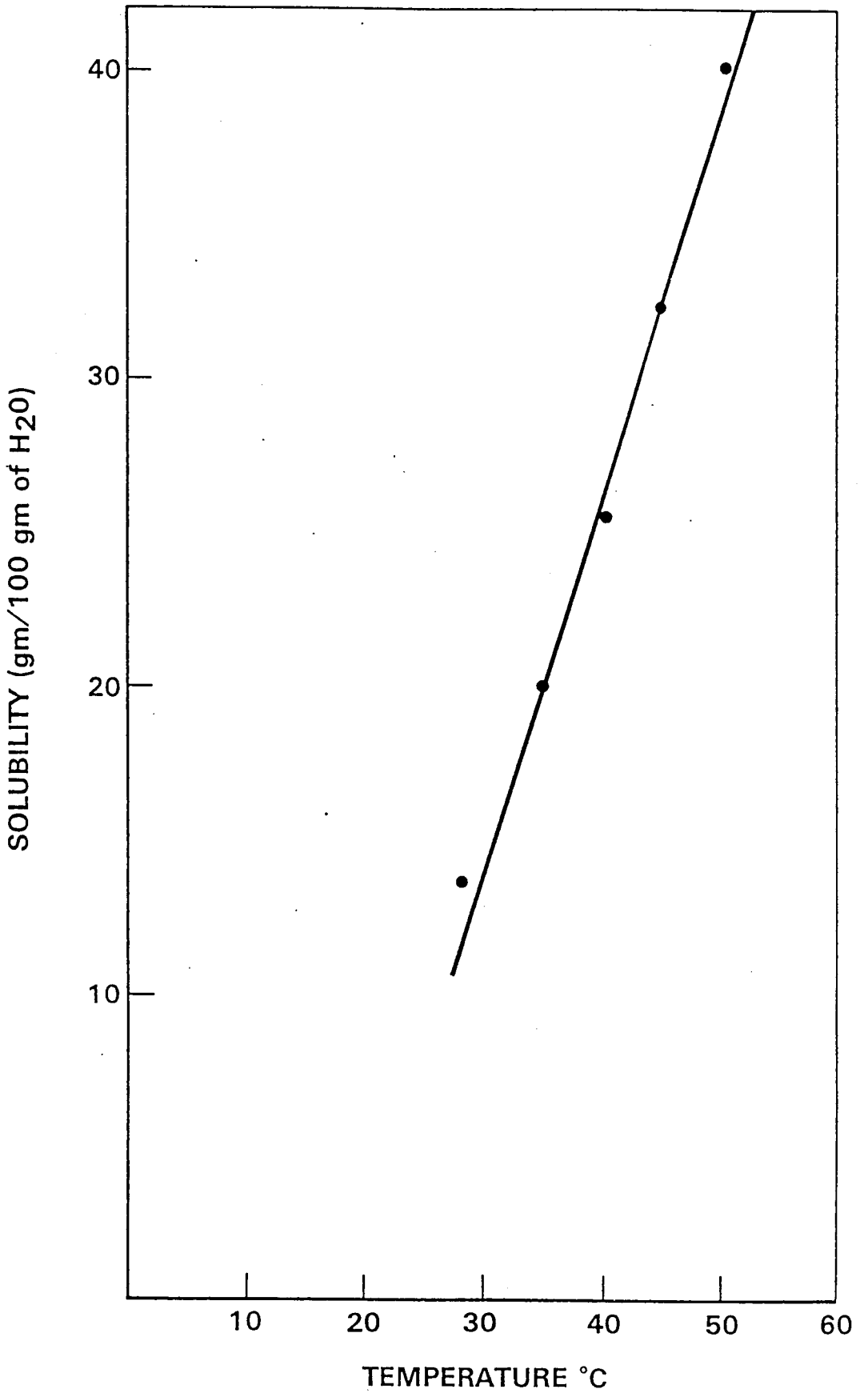


Figure 4.1 Solubility Curve for Lap.

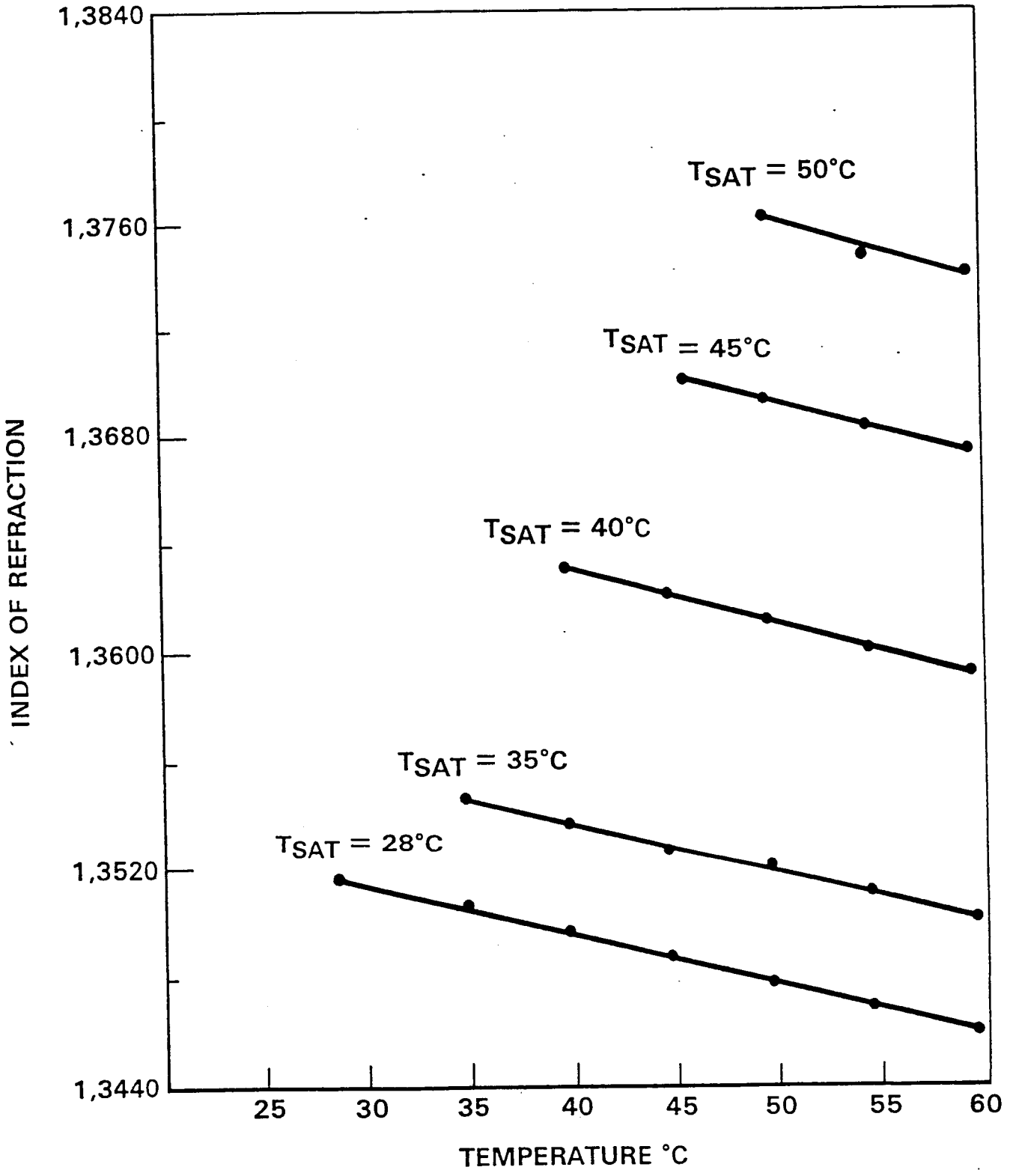


Figure 4.2 Index of Refraction Versus Temperature for Lap Solution.

# GROWTH CHARACTERESTICS OF LAP CRYSTALS

| Sr. NO. | pH Of Solution | Temp Range (°C) | Time Of Growth (Hrs) | Growth Yield (gm/Hr/°C) X $10^{-3}$ | Remarks |
|---|---|---|---|---|---|
| 1. | 4.19 | 1.33 | 264 | 22.0 | Not optical quality crystals |
| 2. | 4.27 | 3.19 | 312 | 8.42 | Not optical quality crystals |
| 3. | 5.61 | 2.39 | 696 | 0.82 | Very clear optical quality crystals |
| 4. | 5.77 | 6.41 | 960 | 0.158 | Clear smaller size crystals |

## GROWTH KINETICS OF LAP CRYSTALS

1. THE GROWTH RATE WAS HIGH AT A pH OF4.18 OF THE LAP SOLUTION. HOWEVER, THE QUALITY OF CRYSTALS GROWN WAS NOT GOOD.

2. ON VARYING THE pH FROM 4.19 TO 5.77, BY ADDING DIFFERENT QUANTITIES OF L-ARGININE TO THE SATURATED LAP SOLUTION, GROWTH RATES AND MORPHOLOGY OF THE CRYSTALS CHANGED APPRECIABLY.

3. AT LOWER VALUES OF pH, THE CRYSTALS WERE ROUNDED, MULTI-FACETED, HAD MANY INCLUSIONS, AND HENCE OF POOR OPTICAL QUALITY.

4. OPTIMUM pH FOR GROWING OPTICAL QUALITY, MEDIUM SIZE, SHARP FACETED CRYSTALS WAS FOUND TO BE 5.61.

# XRD MEASUREMENTS FOR LAP CRYSTAL

- REFINED PARAMETERS FOR FOUR DIFFERENT SCANS
- TWO SEPARATE SCANS (#1 AND #2) MADE ON DIFFERENT REGIONS OF ONE XRD SAMPLE.
- TWO ADDITIONAL SCANS (#3 AND #4) MADE ON SAME REGION OF SECOND XRD SAMPLE.
- LAP CRYSTALS WERE GROUND WITH ALUMINA MORTAR AND PESTLE TO A - 325 MESH WHITE POWDER.
- LAP POWDER WAS MIXED WITH 25 PERCENT SILICON POWDER (NBS) SRM 640a)
- DIFFRACTOMETRER WAS SCINTAG PAD V THETA-2-THETA UNIT USING CuK$\alpha$ RADIATION.
- CORRECTED 2-THETA DATA REDUCED TO CELL PARAMERS WITH LEAST SQUARES UNIT CELL REFINEMENT CODE.
- WORK PERFORMED AT LOS ALAMOS NATIONAL LABORATORY.

# RESULTS FOR LEAST SQUARES UNIT CELL REFINEMENT OF XRD MEASUREMENTS

The cell parameters are given for each scan with the estimated error in parenthesis taken from the refinement code.

| | a (Å) | b (Å) | c (Å) | beta | volume (Å$^3$) |
|---|---|---|---|---|---|
| Fact Sheet | 10.85 | 7.91 | 7.32 | 98.0° | (622.1) |
| Scan #1 | 10.8869 (18) | 7.9258 (9) | 7.3409 (8) | 97.963° (10) | 627.31 (18) |
| Scan #2 | 10.9000 (27) | 7.9253 (12) | 7.3519 (12) | 97.980° (10) | 628.95 (25) |
| Scan #3 | 10.8973 (27) | 7.9291 (10) | 7.3423 (11) | 97.947° (10) | 628.33 (25) |
| Scan #4 | 10.9005 (29) | 7.9294 (14) | 7.3458 (11) | 97.945° (12) | 628.84 (28) |
| Average | 10.8962 | 7.9274 | 7.3452 | 97.959° | |
| Std. Dev. | 0.0063 | 0.0021 | 0.0049 | 0.016 | |
| Range (Max-Min) | 0.0136 | 0.0041 | 0.0110 | 0.035 | |

# EFFECT OF pH ON THE QUALITY OF LAP CRYSTALS

1. L-ARGININE PHOSPHATE IS FORMED FROM THE STRONGLY BASIC AMINO-ACID AND PHOSPHERIC ACID.

2. THE ARGININE MOLECULE EXISTS AS A ZWITTERION IN A NEUTRAL SOLUTION.

3. IN AQUEOUS SOLUTION, AN EQUILIBRIUM EXISTS BETWEEN THE ANIONIC AND CATIONIC FORMS OF AN AMINO-ACID.

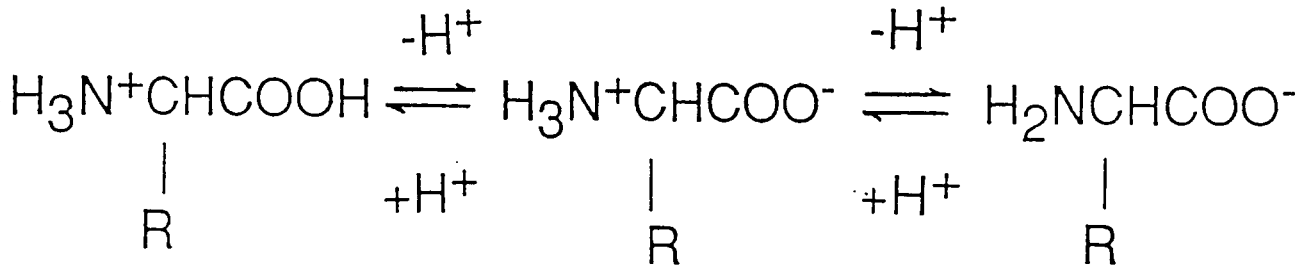

4. IN STRONGLY ACIDIC SOLUTIONS, ALL AMINO ACIDS ARE PRESENT AS CATIONS AND IN BASIC SOLUTIONS THEY ARE PRESENT AS ANIONS.

5. AT AN INTERMEDIATE pH, CALLED THE ISOELECTRIC POINT, THE CONCENTRATION OF ANIONS AND CATIONS ARE EQUAL AND THE ARGININE MOLECULE EXISTS AS A ZWITTERION.

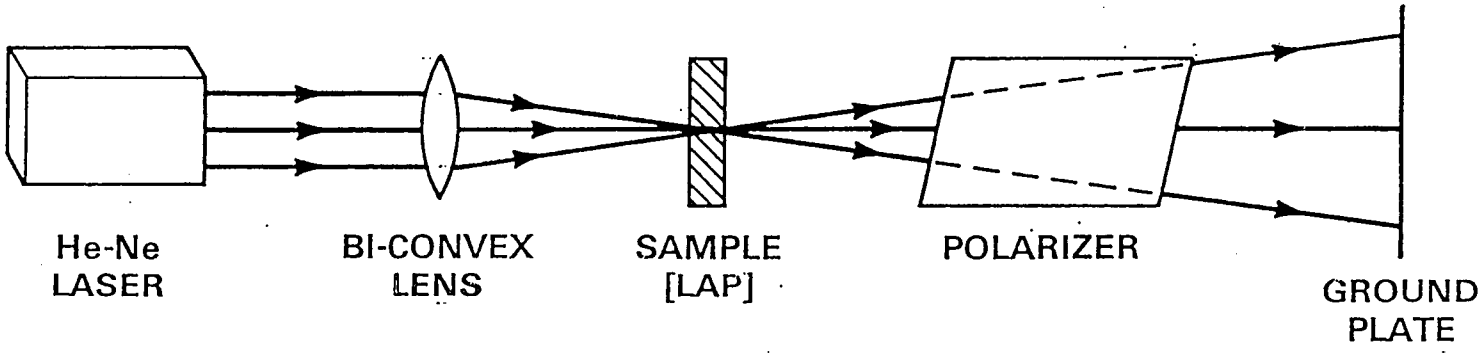


Figure 3.6 Schematic Layout of the Apparatus for Determination of Optic Axis of Lap Crystal.

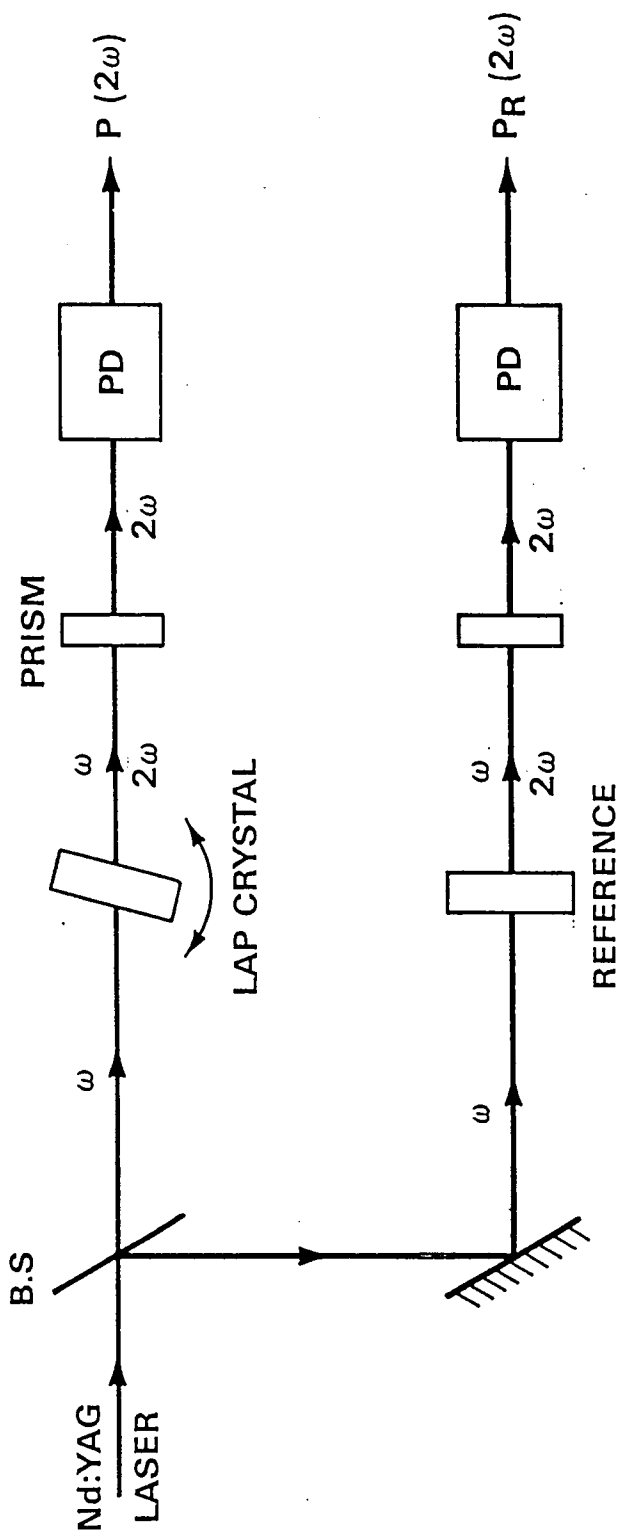


Figure 3.7 Experimental Arrangement for Measurement of the Second Harmonic Conversion Efficiency of Lap Crystal.

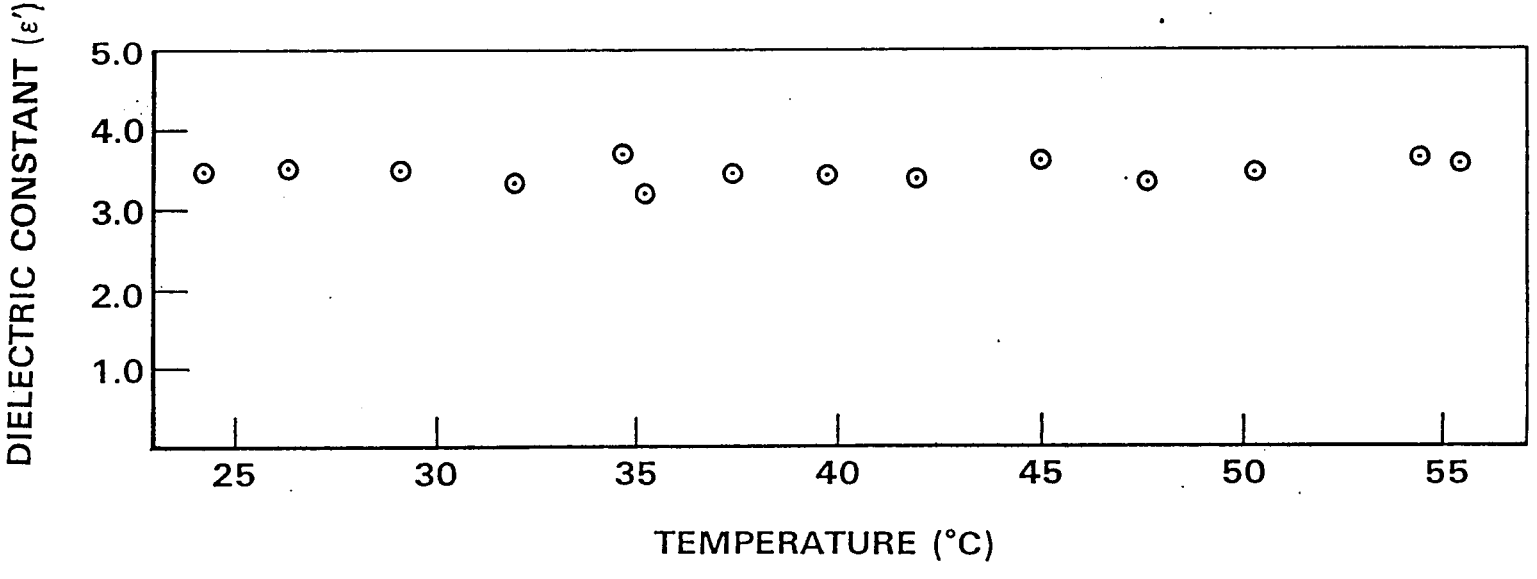


Figure 4.3 Dielectric Constant Versus Temperature for Lap Crystal.

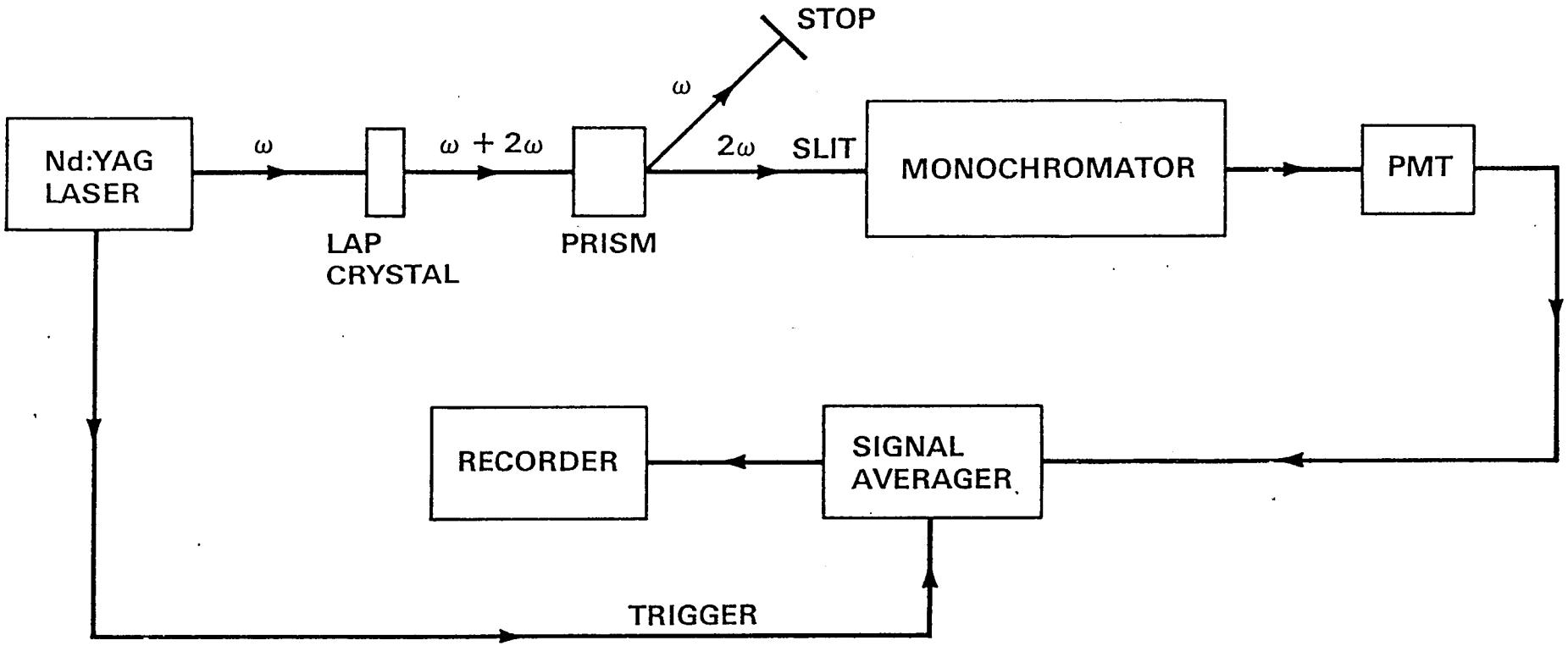


Figure 4.4 Schematic Layout for Determining the Wavelength of Second Harmonic Generated by Lap Crystal.

# WAVELENGTH Vs INTENSITY PLOT FOR THE SECOND HARMONIC OF Nd:YAG LASER GENERATED BY LAP CRYSTAL

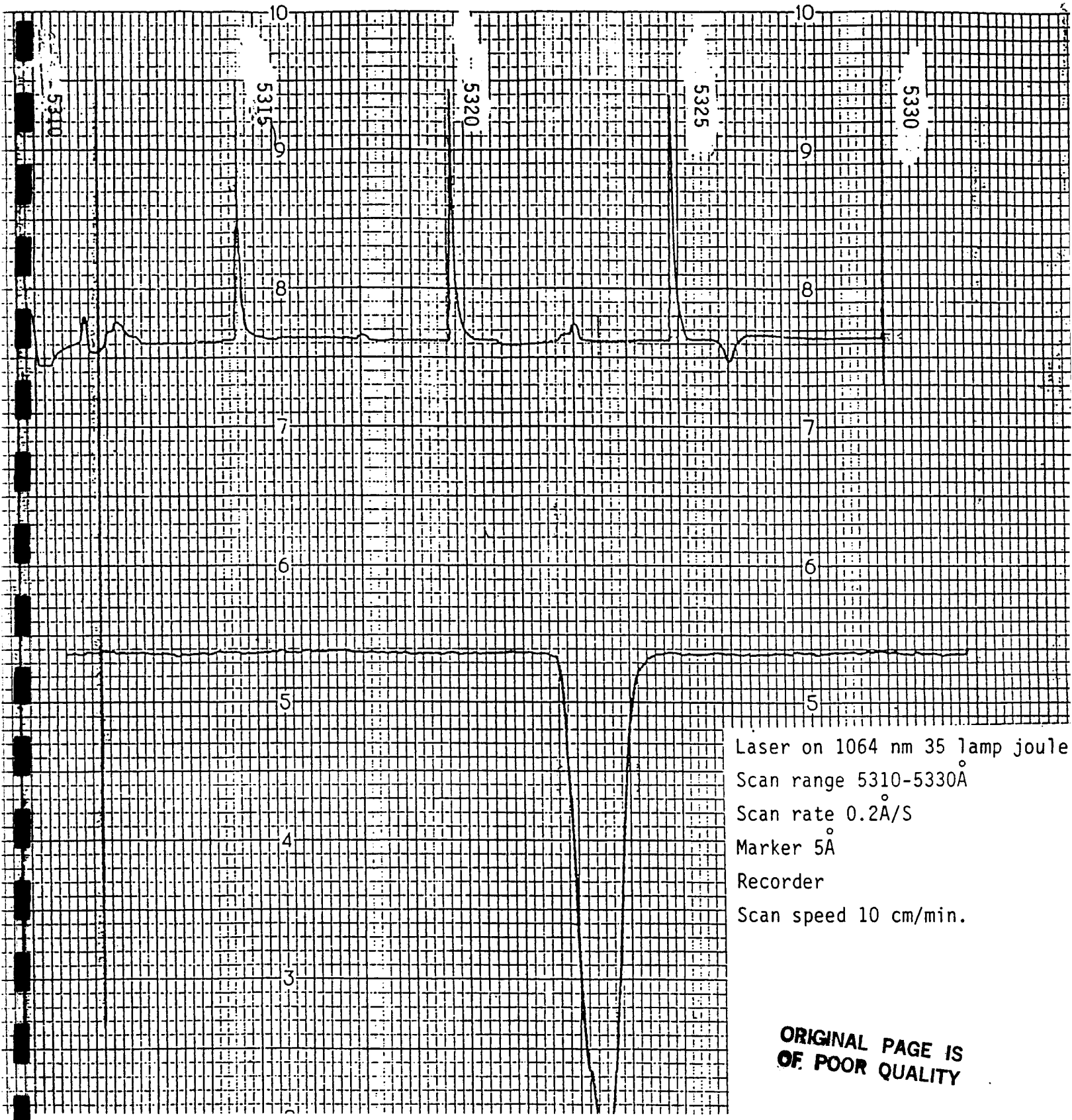


Laser on 1064 nm 35 lamp joule

Scan range 5310-5330Å

Scan rate 0.2Å/S

Marker 5Å

Recorder

Scan speed 10 cm/min.

# RATIONALE FOR COMMERCIAL SOLUTION GROWTH FACILITY

- CURRENT FES (FLUID EXPERIMENT SYSTEM) REQUIRES ONE DOUBLE RACK
- FES CAN ONLY BE ACCOMODATED IN SPACELAB
- FES DESIGNED FOR CRYSTALLIZATION/FLUID PHYSICS STUDY
- FES GROWTH CELL VOLUME IS LIMITED (1 LITER)
- FLIGHT OPPORTUNITY OF FES/VCGS IS LIMITED
- COMMERCIAL CRYSTAL GROWTH EXPERIMENT NEEDS ARE SIMPLER

# PLANNING OF GET AWAY SPECIAL (GAS) EXPERIMENT FOR SOLUTION CRYSTAL GROWTH (NASA-CCDS)

- MEETING WITH TRIPTY MOOKHERJI OF TELEDYNE BROWN ENGINEERING (TBE)
- TELECON WITH TBE AND EDO/BED ON AUG 31,1988
- DISCUSSIONS WITH JIM TROLINGER (METRO LASER) FOR OPTICAL SYSTEM
- A TWO CHAMBER GROWTH SYSTEM WITH SEEDED GROWTH
- TARGET CRYSTAL: LAP AND DOPED-TGS (GROWN FROM AQUEOUS SOLUTION)
- CRYSTAL GROWTH CELL: TOTALLY ENCLOSED WITH PROVISION TO MOUNT SEED CRYSTAL (CHAMBER B)
- SOLUTION RESERVOIR WITH BUBBLE ELIMINATION SYSTEM AND STIRRER
- HEATING AND COOLING CAPABILITY FOR BOTH CHAMBERS: PELTIER ELEMENTS ALONG WITH RESISTANCE HEATING (20 C - 100 C)
- ATLEAST FOUR TEMPERATURE MEASURING UNITS (+0.01)
- TEMPERATURE CONTROL ACCURACY (+0.1 C FOR TWO CHAMBERS AND +0.01 C FOR CRYSTAL)
- DESIRABLE OPTICAL DEVICE WITH ILLUMINATION AND OBSERVATION CAMERA
- IMAGE RECORDING (VTRs)
- DATA RECORDER
- POWER REQUIREMENTS (POSSIBLY LEAD ACID BATTERIES)
- DESIGN DIMENSIONS( 50 cm X 70 cm)
- WEIGHT: 90 kgs.

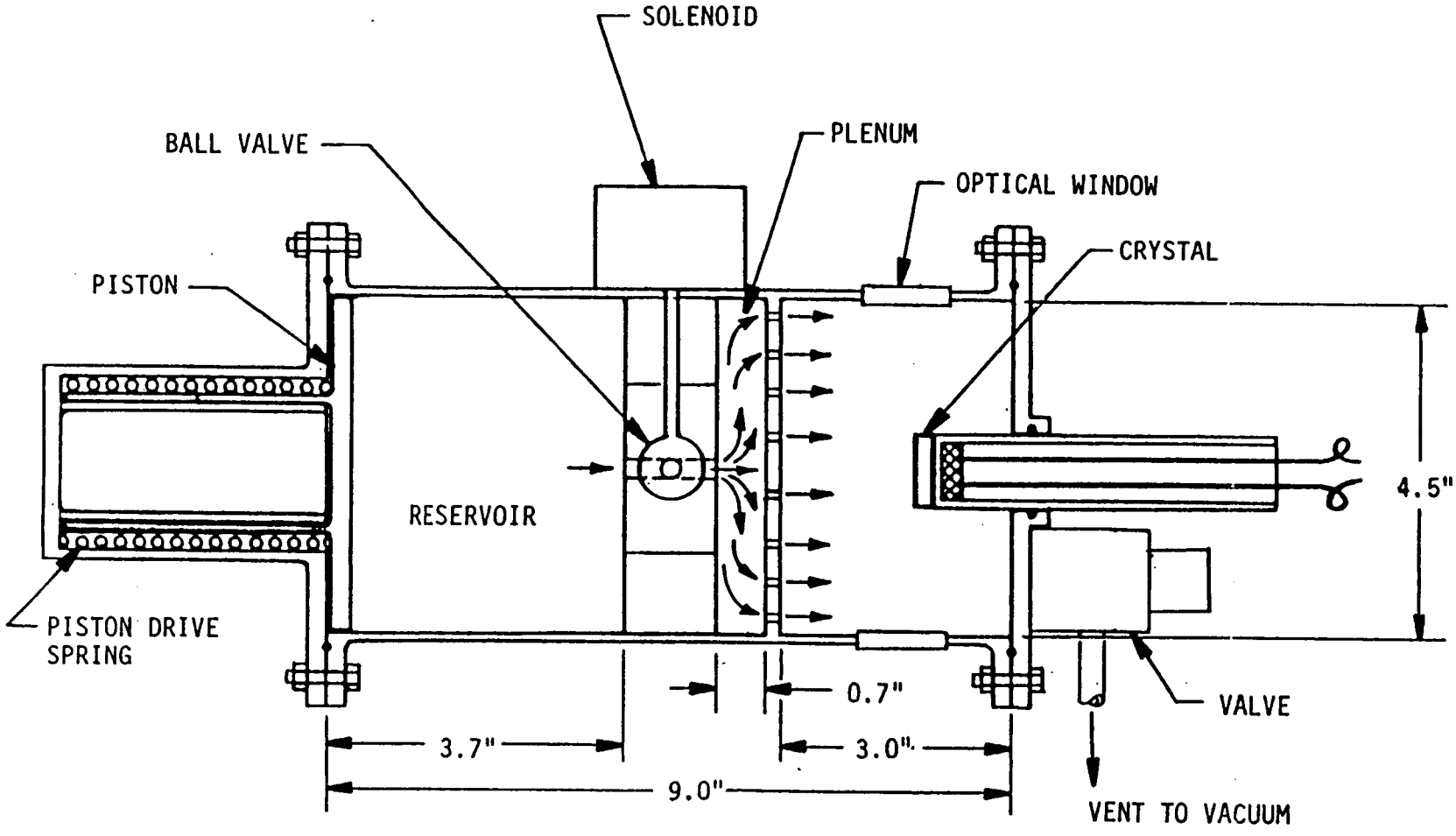


GROWTH CELL CONCEPT FOR GAS CAN EXPERIMENT

# CRYSTAL GROWTH MONITOR #1

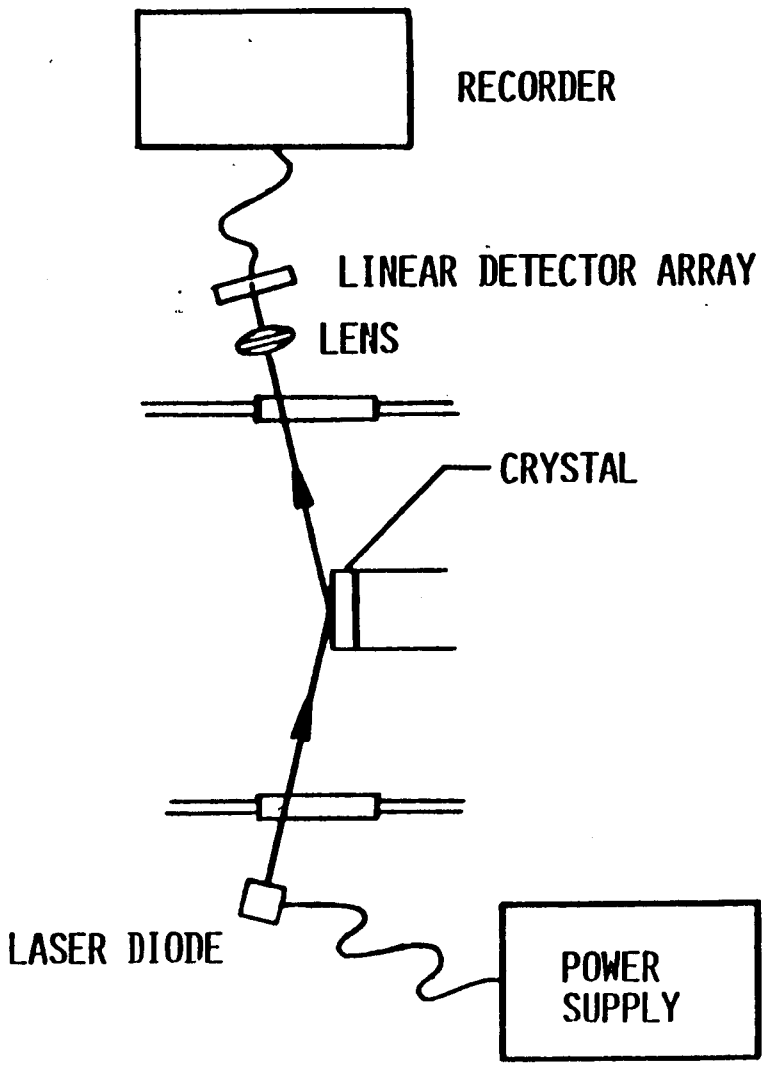

# CRYSTAL GROWTH MONITOR #2

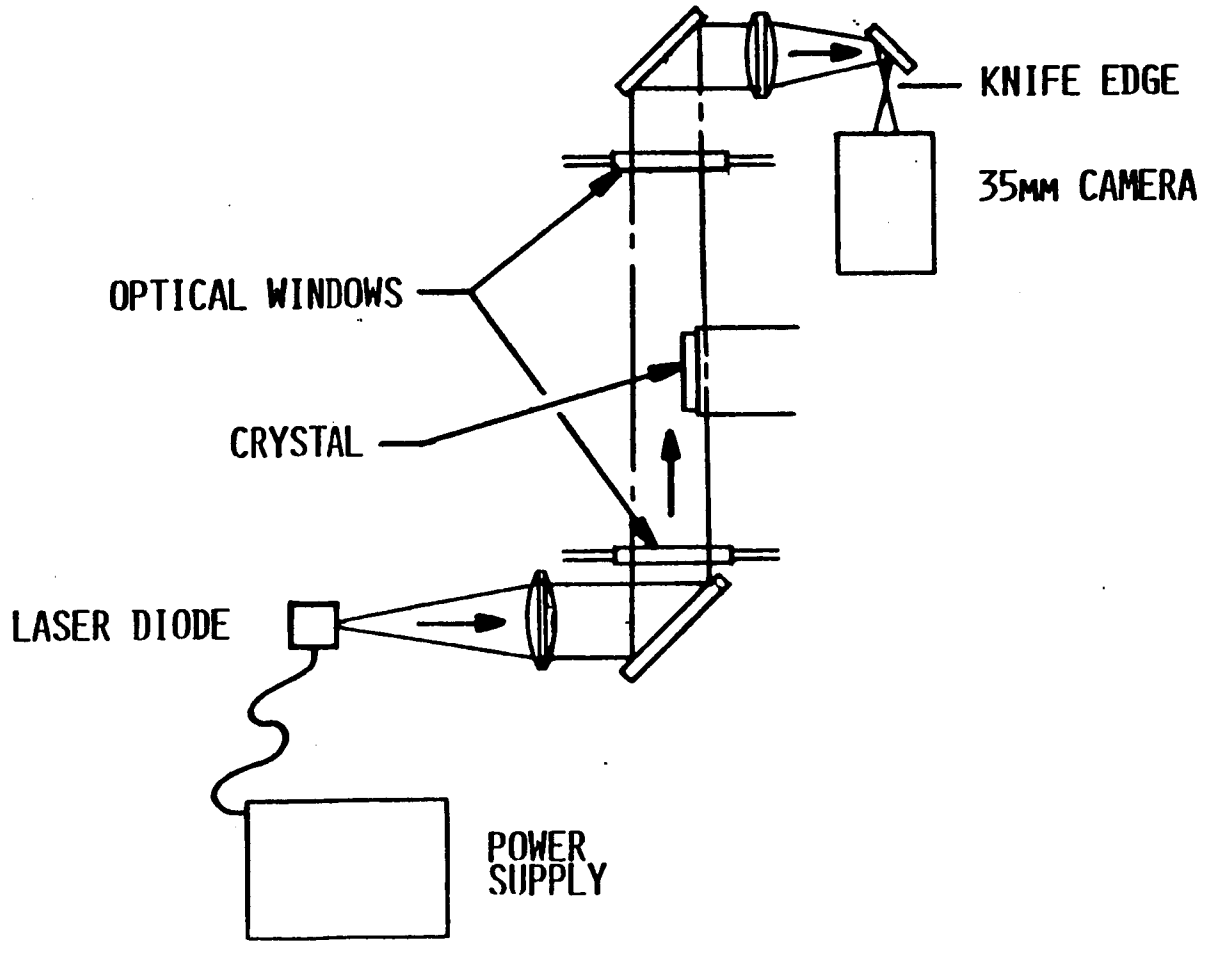

# ADVANTAGES OF THE PROPOSED FACILITY

- SUITABLE FOR BOTH TGS AND LAP
- LOW COST DESIGN
- DESIGN ADAPTABLE TO MIDDECK, GAS CAN AND MSL
- EASIER TO MANIFEST
- INCREASES FLIGHT OPPORTUNITY

# ANTICIPATED HARDWARE DEVELOPMENT SUPPORT

- DESIGN STUDY ( THERMAL AND STRUCTURAL ) TBE AND EDO/BED
- OPTICAL DESIGN SUPPORT METRO LASER
- PRELIMINARY DESIGN TBE, EDO/BED, AND METRO LASER
- HARDWARE DEVELOPMENT CCDS/NASA

# FLIGHT ACTIVITY

- EXPERIMENT INTEGRATION
- GROUND TESTING
- INTEGRATION TO SHUTTLE
- OPERATION/FLIGHT SUPPORT
- DATA ANALYSIS
- CRYSTAL CHARACTERIZATION
- DEVICE FABRICATION

# INSTRUMENT CHARACTERISTICS

- TOTAL VOLUME OF THE SOLUTION 2.5 LITERS
- TOTAL MASS 50-60 Kg
- AVERAGE POWER 60-100 WATTS
- VIDEO IMAGING
- TEMPERATURE HISTORY

# 7. CADMIUM TELLURIDE SOLIDIFICATION

W.R. Wilcox, R. Balasubramanian, H.R. Shetty, R. Derebail, V. White,
D. Aidun, G. Rosen, A. Nagras, F. Carlson, W. Rosch, J. Sheu, and C. Wen

**CLARKSON UNIVERSITY**
Potsdam, New York 13676

## CADMIUM TELLURIDE SOLIDIFICATION

**Clarkson University**

The research at Clarkson University is aimed at directional solidification of cadmium telluride, and possibly also gallium arsenide. Cadmium telluride crystals are currently widely used as substrates for growth of films of mercury cadmium telluride. These are fabricated into focal plane array infrared detectors, enabling very sensitive night vision in real time.

Commercial cadmium telluride suffers from polycrystallinity with uncontrolled variations in orientation, low angle grain boundaries, twins, precipitates, a high dislocation content, and excessive impurity levels. When an isoelectronic impurity is added to harden the material, the impurity concentration varies both macroscopically and microscopically. There are good reasons to believe that many of these problems can be overcome by crystal growth in space. However many aspects of the growth of cadmium telluride on earth are not understood. Thus it is uncertain how advantageous growth in space is likely to be, and it is uncertain what the optimal methods are to grow it in space. Our research is aimed at gaining the fundamental knowledge required for an optimal growth apparatus and optimal growth techniques.

The intrinsic properties of cadmium telluride lead one to believe that there are several potential applications in addition to serving as a substrate for mercury cadmium telluride films. However the impurity content and defect content of present crystals are too high for these applications. It is hoped that growth in space will provide crystals of the necessary purity and perfection.

## 7.A. DIRECTIONAL SOLIDIFICATION OF CADMIUM TELLURIDE

D. Aidun, V. White, G. Rosen and A. Nagras


### SUMMARY

The objective of this project is to determine experimentally the effects on the perfection of CdTe of solid-liquid interface shape, sticking of the crystal to the surface of the ampoule, weight of the melt, vibration, convection in the melt, and growth rate fluctuations.

The vertical Bridgman - Stockbarger technique is being used for the growth experiments. One apparatus was constructed using a purchased multizone furnace and the large Czochralski unit donated by Kayex a year ago. This apparatus includes provision for vibrating and rotating the ampoule. An additional apparatus was designed and purchased. It is currently being installed.

Difficulties were encountered with our ampoule sealing apparatus. Insufficient vacuum could be reached, so that air remained in the ampoules. This residual air caused destruction of the ampoules during growth experiments. Consequently a new vacuum sealing apparatus was designed and ordered (using University funds).

We performed model experiments using water to observe mixing caused by vibration. The mixing pattern and intensity depended on the aspect ratio of the column of water and on the frequency and amplitude of the vibrations.

An apparatus is being designed for measuring the stress at which solidified cadmium telluride breaks free from the surface of the ampoule.


### INTRODUCTION

Extensive experience has shown that crystal growth in space produces results quite different from growth on the ground. Some of these results were expected while others were a surprise. Only some of the surprising results have been explained; others remain a mystery. For example, often material solidified in space had a smaller diameter than its ampoule, with an irregular or wavy surface. While many mechanisms have been proposed, the cause will remain uncertain until the melt is directly observed during solidification in space.

The microgravity environment of space is expected to influence the growth of cadmium telluride in many ways:

> Convection will be reduced, resulting in a more uniform freezing rate, a more uniform impurity distribution, less contamination by the crucible wall, an altered interface shape for the same thermal conditions, etc. It is not known whether or not in growth of cadmium telluride a fluctuating freezing rate influences formation and selection of grain boundaries, twin formation, and precipitate formation. This needs to be determined.
>
> The weight of the melt and the crystal will be greatly reduced. Anecdotal evidence from crystal growers suggest that cadmium telluride is sufficiently soft at high temperature that the weight of the melt and the weight of the crystal are often sufficient to cause plastic deformation, i.e. "self-deformation." This needs to be verified by careful experiments.

The crystal will probably have reduced contact with the ampoule, reducing the effects of differential thermal expansion, altering the temperature distribution and thermal stress in the crystal, altering the interface shape, etc. Prior experience has shown that improved crystals result from growth under such conditions, so we intend to design ampoules to maximize the effect.

While the average acceleration level in an orbiting laboratory is about one millionth of that on earth, much larger fluctuations occur. In the Space Shuttle the "g jitter" level is about one thousandth of earth's gravity with a maximum at about 17 Hz, apparently the resonance frequency of the Shuttle. The g jitter may cause a variety of problems, including inducing convection, stressing the crystal to cause plastic deformation, causing a fluctuating freezing rate, etc. We would like to be able to know in advance whether this is a serious concern or not. It it is important, we must aim at performing experiments in un-manned spacecraft where the g jitter levels are lower.

Crystal growers generally ignore the fact that the coefficient of thermal expansion for nearly all materials is greater than the silica ampoules in which they are solidified. This is true for cadmium telluride. During directional solidification the material slowly cools from the melting point. On earth the crystal starts out with the same diameter as the ampoule. As it cools, differential thermal contraction causes the crystal to try to pull away from the ampoule wall. Because of adhesion between the crystal and the wall, some critical stress is required before this happens. Before pullaway the stress may be large enough to cause plastic deformation. After pullaway the temperature distribution in the crystal will be altered because the gap between the crystal and the ampoule wall will cause a significant increase in the resistance to heat transfer there. Furthermore the pullaway is not likely to be steady. In solidification of organic compounds pullaway occurs at infrequent intervals, over an appreciable distance along the crystal surface. Pullaway should produce a fluctuation in the freezing rate, and possibly even cause meltback. When pullaway reaches to the solid-liquid interface in organic compounds, melt has been observed to flow a short distance into the gap produced.

We plan to measure the stress at which solidified cadmium telluride pulls away from fused silica. We will determine the dependence of pullaway behavior on surface treatment, ambient gas, temperature, melt composition, etc. These results are needed for optimal ampoule design and for correct modelling of the heat transfer and stresses during directional solidification.

## RESEARCH

A year ago Kayex in Rochester donated a new apparatus designed for the Czochralski growth of large silicon crystals. We decided that it would be ideal as a containment vessel for vertical Bridgman - Stockbarger growth of cadmium telluride, with facilities that could be used to translate and rotate the growth ampoule. (Stopping and starting rotation is known to generate vigorous convection near the bottom of a cylinder, which is where the solid-liquid interface is located.)

The furnace necessary for the directional solidification of CdTe was designed and custom built by the Mellen Co. It is a 4-zone furnace; a heater on the bottom followed by an adjustable insulated zone, a short booster heater, and another long heater. The booster heater permits an extra degree of control of the interface position, interface shape, and the axial temperature gradient. Recent work at Clarkson showed that buoyancy-driven convection can be negligible when the temperature increases with height, and is extremely vigorous when the temperature decreases with height.

We plan to place an electromagnet around the ampoule to quench convection in the melt. When used in conjuction with a temperature increasing with height, a very low level of convection should be achieved, comparable to what can be obtained in space.

A vibration unit was purchased and inserted between the ampoule lift mechanism and the ampoule. The vibration unit produces a maximum peak to peak displacement of 3 mm at a frequency of 1 Hz to 1 KHz.

With the booster heater, rotating mechanism, vibrator, and electromagnet we will have the ability to vary the convection, freezing rate fluctuations, and vibrations independently over a wide range. Diagrams of the completed apparatus are shown in Figures 1 and 2.

To try to understand the fluid flow caused by vibrations we performed experiments using water with licopodium powder suspended in it. We used an ampoule diameter of 11 mm with different water column heights and frequencies. Figure 3 shows a typical flow pattern. Most of the fluid motion occurred near the free surface. No motion could be observed near the interface. Figures 4 and 5 give the mixing height versus frequency, with the mixing height being defined as the height of the water column where the fluid motion was vigorous. For a water column height of 5 cm the peak mixing height was 2.25 cm and was at 30 Hz. For a water column height of 9 cm the peak mixing height was 5 cm at 70 Hz. The velocity of the fluid flow increased exponentially with increasing frequency. The effect of amplitude at constant frequency on the fluid flow pattern is shown in Figure 6; the mixing height decreased with increasing amplitude.

Fused silica (quartz) ampoules were used for growth experiments. The ampoules were degreased by soaking them in a detergent solution for 6 to 8 hours. They were rinsed with de-ionized water for 20 minutes and flushed with methanol. This was followed by a degreasing schedule to remove all polar and non-polar contaminants. The degreasing schedule consisted of rinsing the ampoules for 10 to 15 minutes with trichloroethane, acetone and methanol consecutively. The ampoules were then soaked in a solution of 1% hydrofluoric acid for 20 to 25 minutes, rinsed with de-ionized water and soaked in aqua regia for 1 hour. During these operations the ampoules were handled with clean gloves.

After the cleaning the ampoules were carbon coated. At high temperature, cadmium reacts with silica to form cadmium metasilicate, $CdSiO_3$. This reaction is more intense when traces of moisture or oxygen are present. Under such conditions the melt sticks to the wall of the quartz tube, which leads to breakage of the tube during directional solidification. It is thought to be important to avoid direct contact between the melt and the silica tube. It is reported that commercial CdTe crystal growers have found that carbon contamination is minimal and does not affect device performance.

In order to carbon coat the interior wall of the ampoule it was evacuated to $10^{-5}$ torr and heated to $1000^{0}$C for 1/2 hour. Methane gas was passed in at 470 torr for 2 minutes. Then the ampoule was again evacuated to $10^{-5}$ torr. The ampoule was cooled. This procedure has been shown to produce an uniform carbon coating. The ampoule was now ready to load the charge.

High purity (five nines) undoped CdTe was donated by II-VI Incorporated, a small business member of the NASA Center. The material was cleaned in an ultrasonic bath to remove particulates and any grease or oil. This material was chemically etched with a 2% bromine-methanol solution. The CdTe was then quickly transferred to another beaker containing methanol and finally sprayed with additional methanol. The next step was to remove the oxide layer in a strong solution of HCl. Finally, the chemically cleaned CdTe was rinsed thouroughly in de-ionized water and dried with air. The last two cleaning steps were performed just before placing the CdTe in the ampoule.

In the first experiment the above cleaning procedures were used but the ampoule was not coated with carbon. The ampoule burst during the experiment. For the second experiment the ampoule was prepared by Rockwell International Science Center, another industrial member of the NASA Center. This run produced a polycrystalline ingot, which is being characterized by Rockwell.

An additional vertical Bridgman - Stockbarger apparatus was purchased. This apparatus design, shown in Figures 7 through 9, has successfully produced
high quality gallium arsenide crystals. The furnace is capable of growing crystals up to 3 inches in

diameter. The temperature controllers are programmable and have ramp and soak options. These features allow for repeatable growth runs and *in-situ* annealing. The growth chamber is isolated from the surrounding room and vented through a HEPA filter. The electrician has finished wiring the furnace and the temperature controllers have been tuned. Temperature profiling will commence upon arrival of the crucible pedestal.

An apparatus was designed for measurement of the stress at which solidified cadmium telluride pops off of a substrate. Components for construction of the apparatus have been ordered. This apparatus can be grouped in three sections; the tension test mechanism, the ampoule, and the furnace.

The mechanism will consist of a linear motion feedthrough connected in series with a miniature load cell. As shown in Figure 10, the feedthrough will be bolted to a stainless steel 4-way cross. The cross will contain pressure fittings to allow the load cell wires and thermocouple to feed through the vacuum flanges. A braided graphite string will be utilized to connect the substrate material to the load cell.

The ampoule will be constructed from a stainless steel-to-Pyrex adapter. Since CdTe melts at 1092 C, the lower portion of the ampoule must withstand this temperature. Therefore it will be constructed of fused quartz. The hot wall/ excess cadmium technique will be utilized to prevent condensation on the ampoule wall. As shown in Figured 11, a cadmium reservoir will be located at the bottom of the ampoule. This will provide the cadmium overpressure required to prevent condensation. A quartz plug, with the graphite string passing through it, will be positioned above the reservoir. This will maintain the overpressure in the lower portion of the ampoule.

A gold film transparent tube furnace (donated by Trans-Temp) will be utilized to provide the hot wall for condensation control. The CdTe charge will be melted with a Kanthal wire resistance heater. The substrate will be lowered to contact the melt. The charge will be slowly solidified and brought down to the test temperature. At this point, the substrate will be pulled from the solidified charge using the linear motion feedthrough. The maximum force detected by the load cell will be recorded.

## PLANS

In the growth experiments the ampoule translation rate will be varied from 0.5 mm/hr to 2 mm/hr during a solidification run with constant convection conditions. The interface shape will be revealed by suddenly changing the growth rate during a solidification run. The ampoule translation rate will be held constant while convection conditions are varied by:

Vibrations.

Varying the ampoule rotation rate.

Buoyancy-driven convection, by varying the booster heater temperature.

Applying a magnetic field.

The ingots grown in these experiments will be examined by optical microscopy, scanning electron microscopy, energy-dispersive X-ray spectroscopy in the SEM, etching to reveal dislocations and striations, and transmission electron microscopy. Slices of better crystals will be sent to NIST for X-ray topographic studies using the synchrotron.

The stress required to pop solidified cadmium telluride off of fused silica will be measured at various temperatures, surface treatments and coatings on the silica, gas ambients, and melt compositions.

Figure 1. First cadmium telluride growth furnace and accessories.

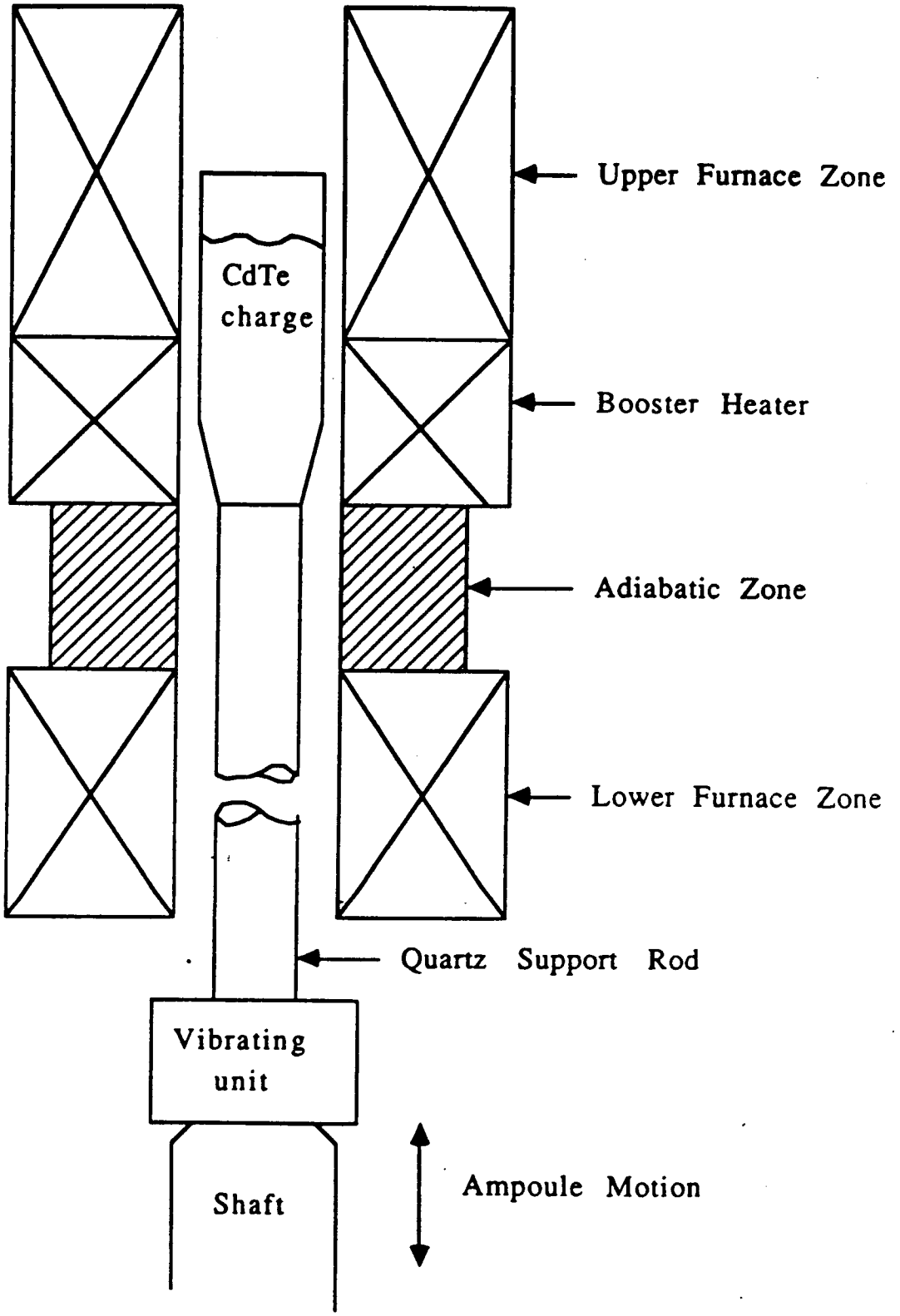

Figure 2. Assembled cadmium telluride growth apparatus.

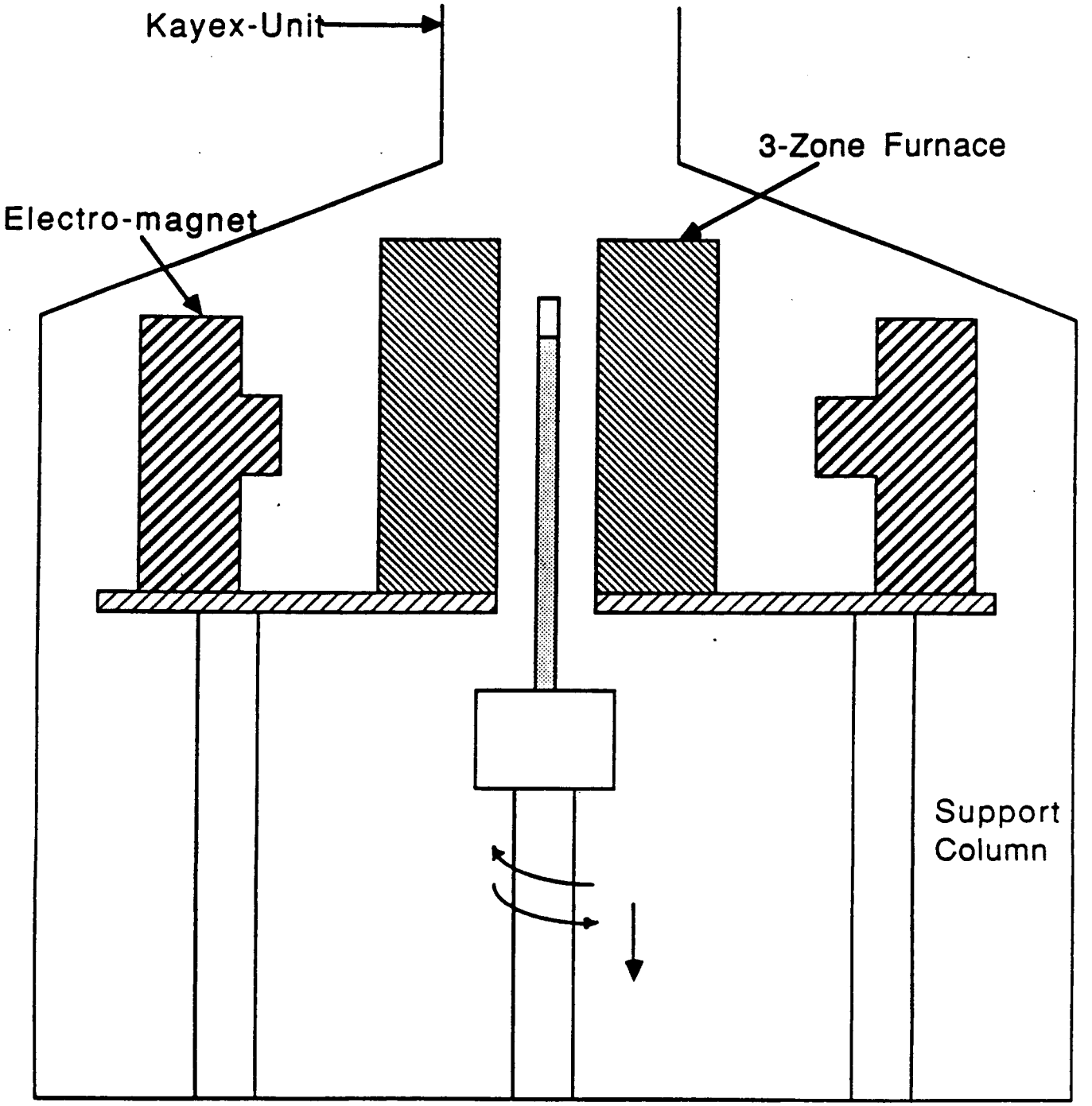

Figure 3. Typical flow pattern caused by vibrating column of water.

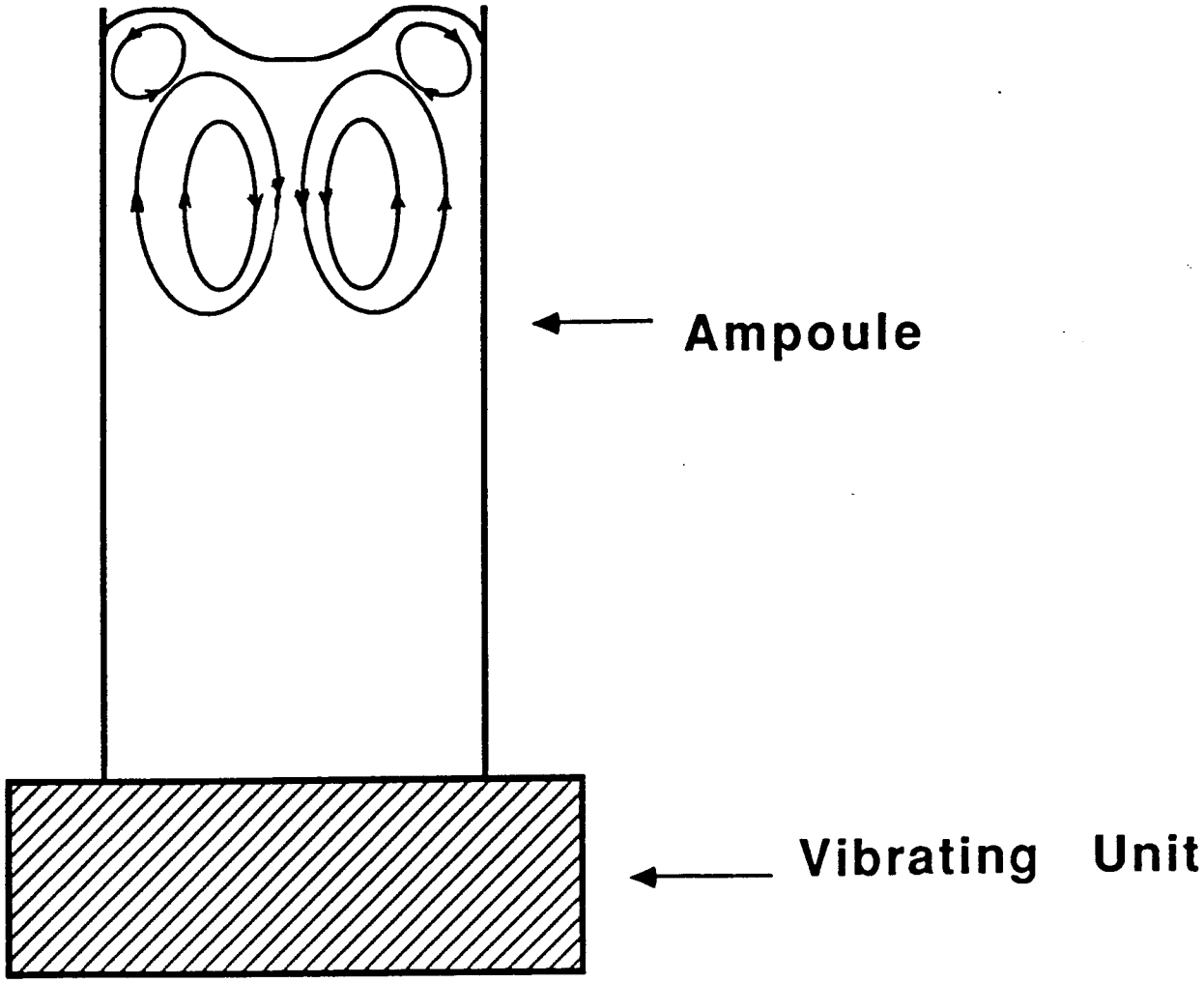

Figure 4. Mixing height vs. frequency for vibration of water column. Aspect ratio is 5 (height 5X diameter).

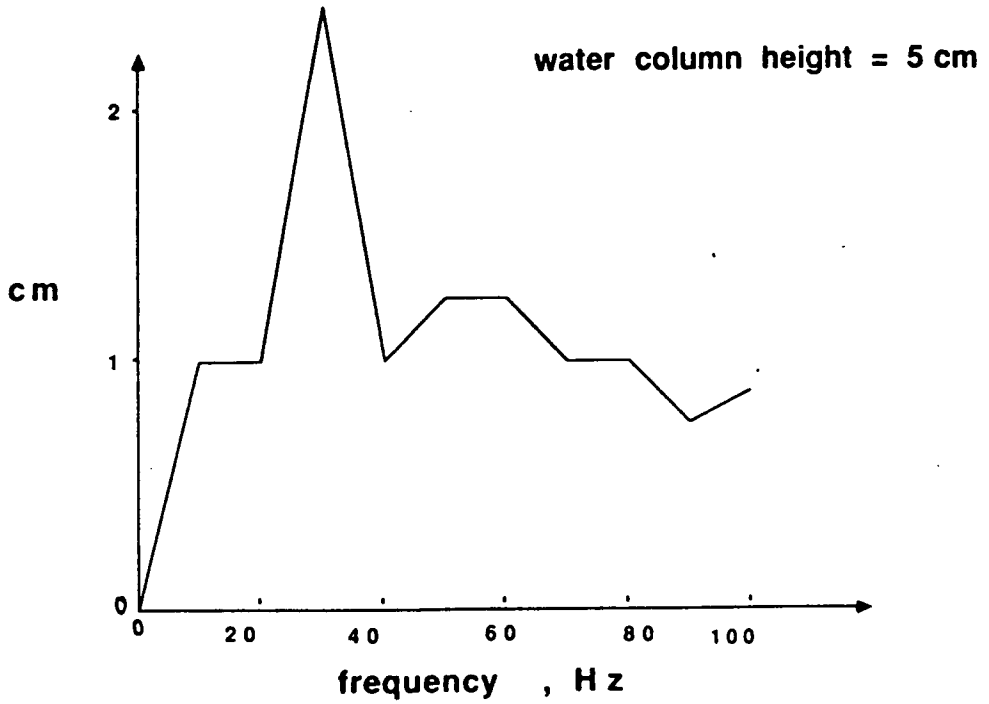


Figure 5. Mixing height vs. frequency for aspect ratio of 9.

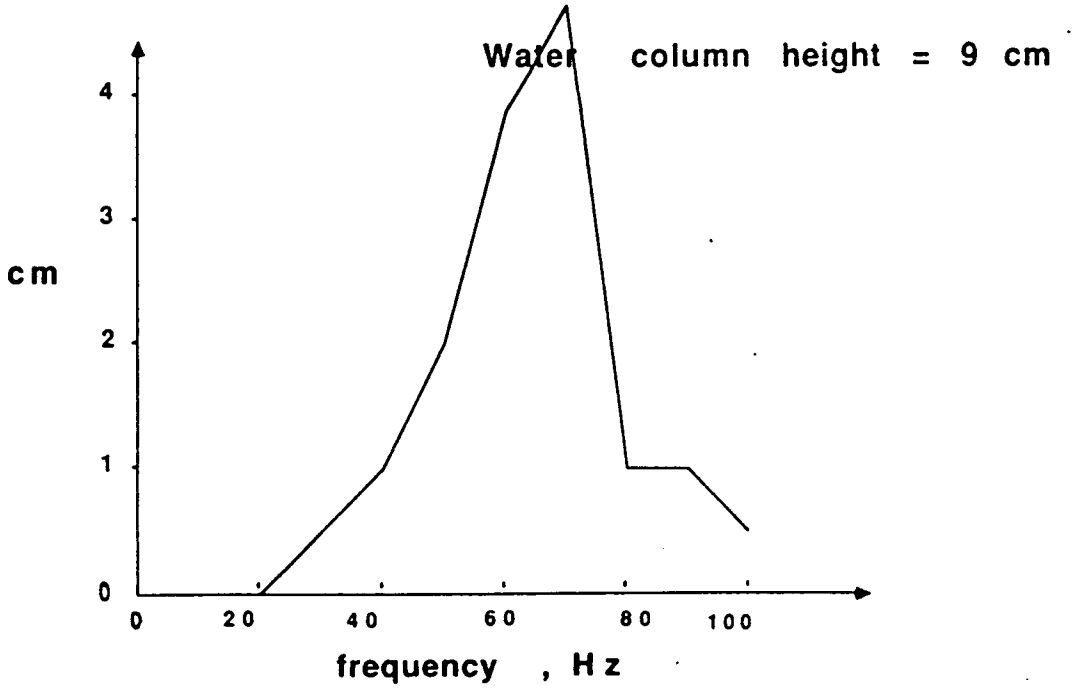

Figure 6. Schematic diagram of influence of vibration amplitude on flow pattern.

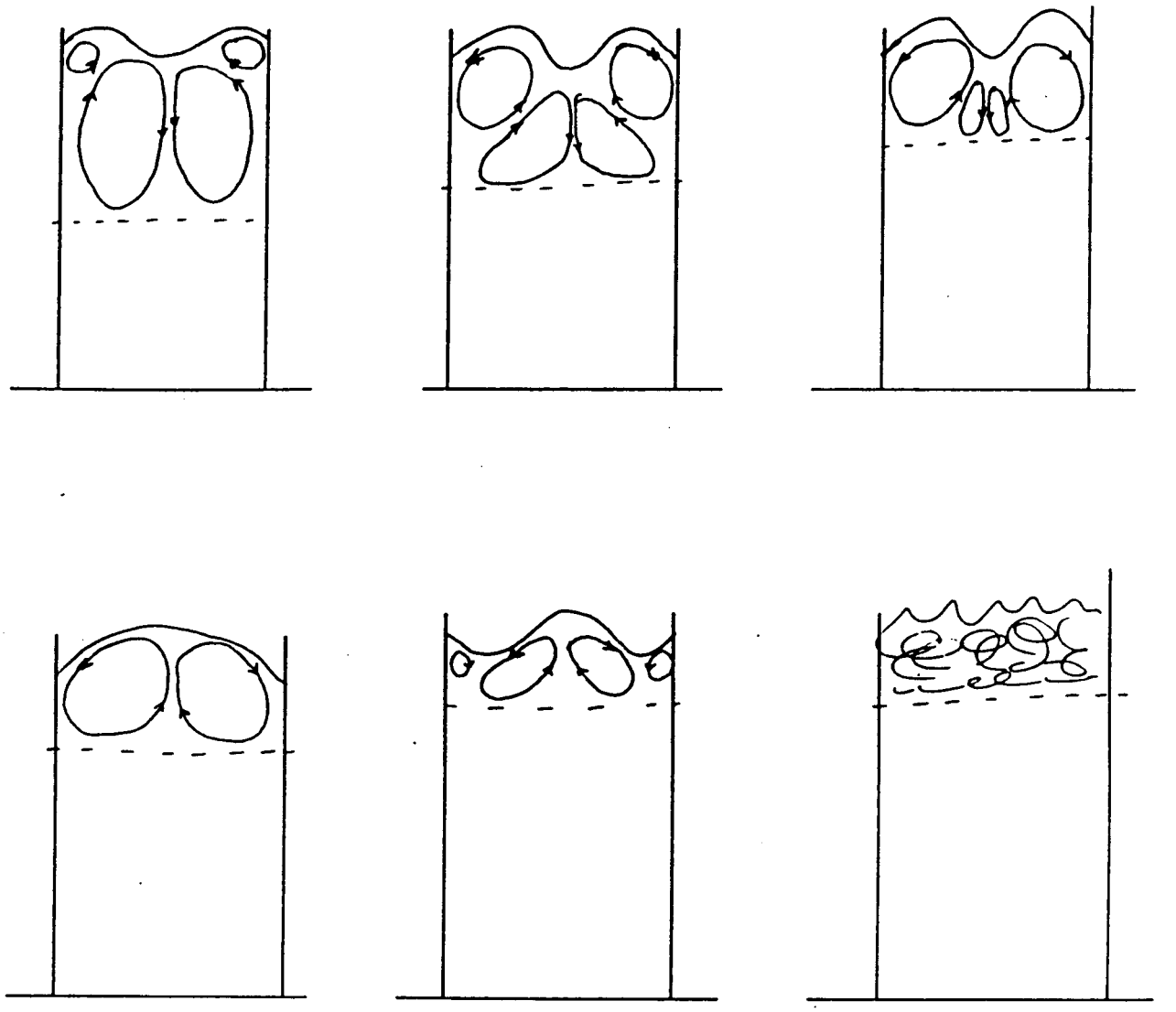

Figure 7. Heater for new vertical Bridgman-Stockbarger apparatus.

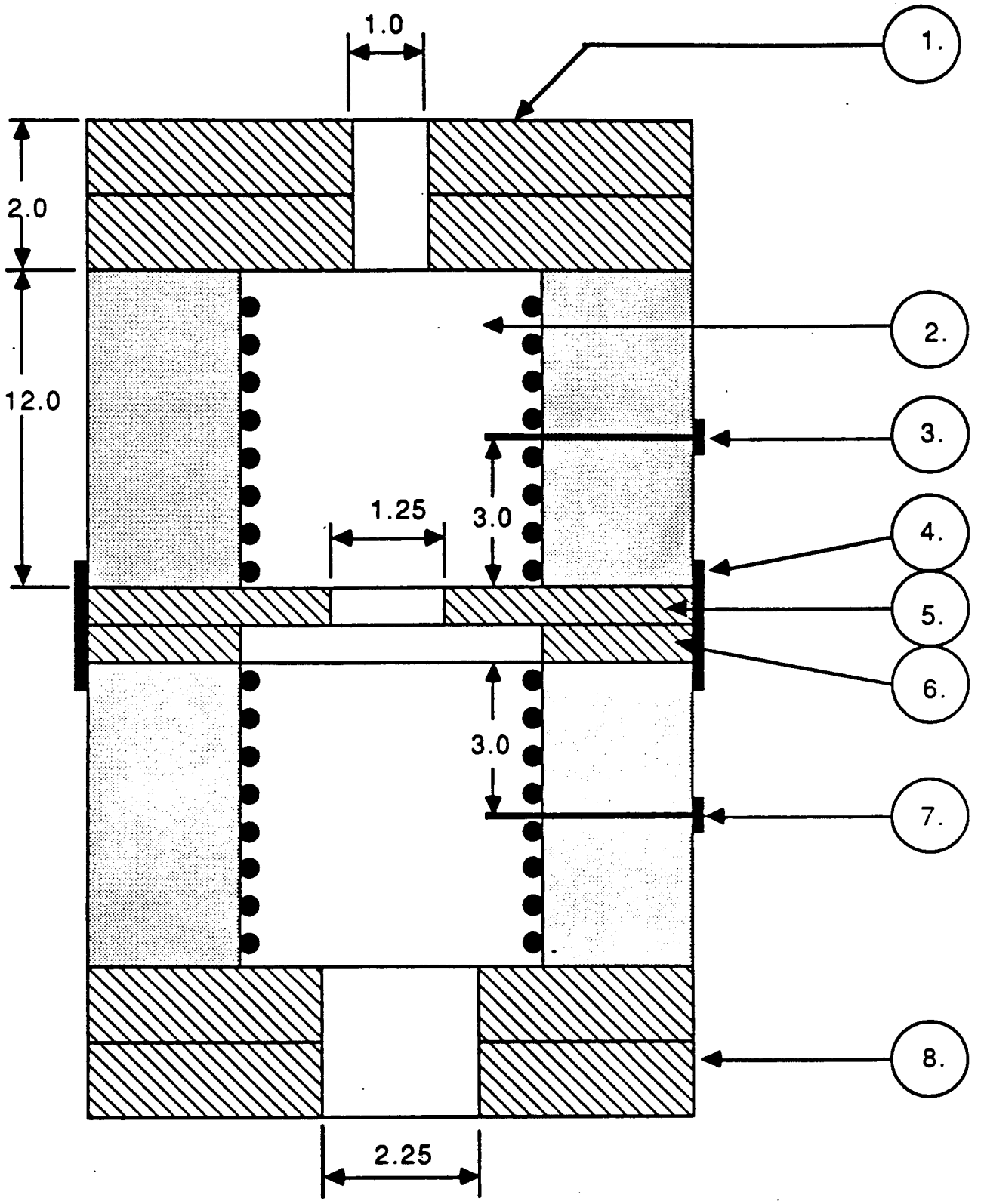

VERTICAL BRIDGMAN FURNACE
HEATER ASSEMBLY

1. TOP VESTIBULE 1.0 INCH I.D.X 2.0 INCH THICK.
2. HEATER ZONES TOP AND BOTTOM 12.0 INCHES LONG X 4.0 INCH I.D.
3. HOT ZONE CONTROL THERMOCOUPLE WITH MOUNTING CONNECTOR. TYPE R ,24 GAUGE WIRE,ALUMINA SHEATH .125 O.D. THE BEAD SHOULD POSITIONED 3.0 INCHES AWAY FROM BAFFLES AND 1.25 INCHES IN FROM THE COIL I.D.
4. LOCKING STRAP.
5. INTERCHANGEABLE BAFFLE 0.5 THICK X 1.25 I.D.
6. SAME AS ITEM 5. WITH 4.0 I.D.
7. COLD ZONE CONTROL THERMOCOUPLE SAME AS ITEM 3..
8. BOTTOM VESTIBLE SAME AS ITEM 1. WITH 2.25 I.D.

Figure 8. Ampoule in Bridgman-Stockbarger heater.

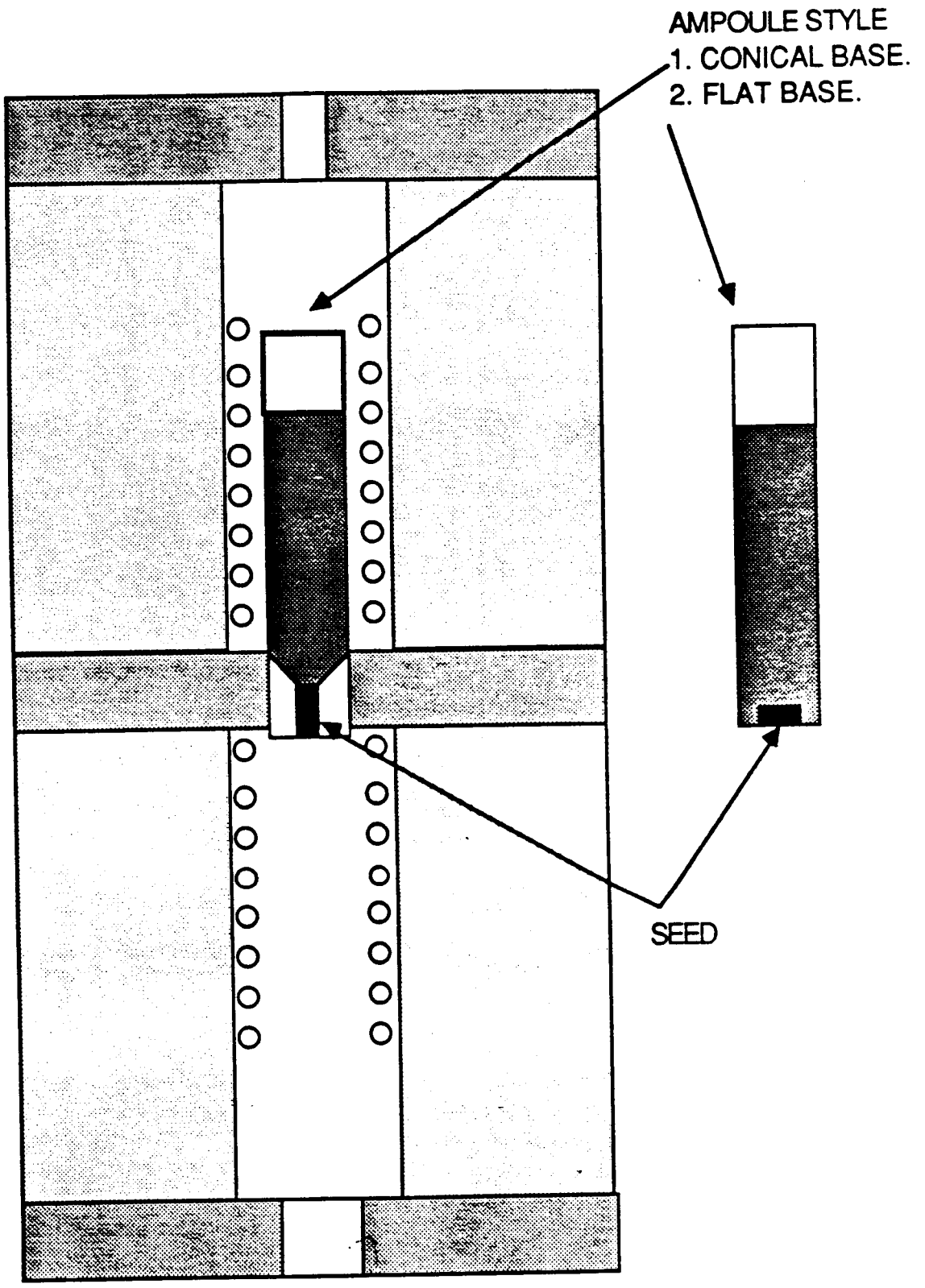

Figure 9. Assembled Bridgman-Stockbarger apparatus.

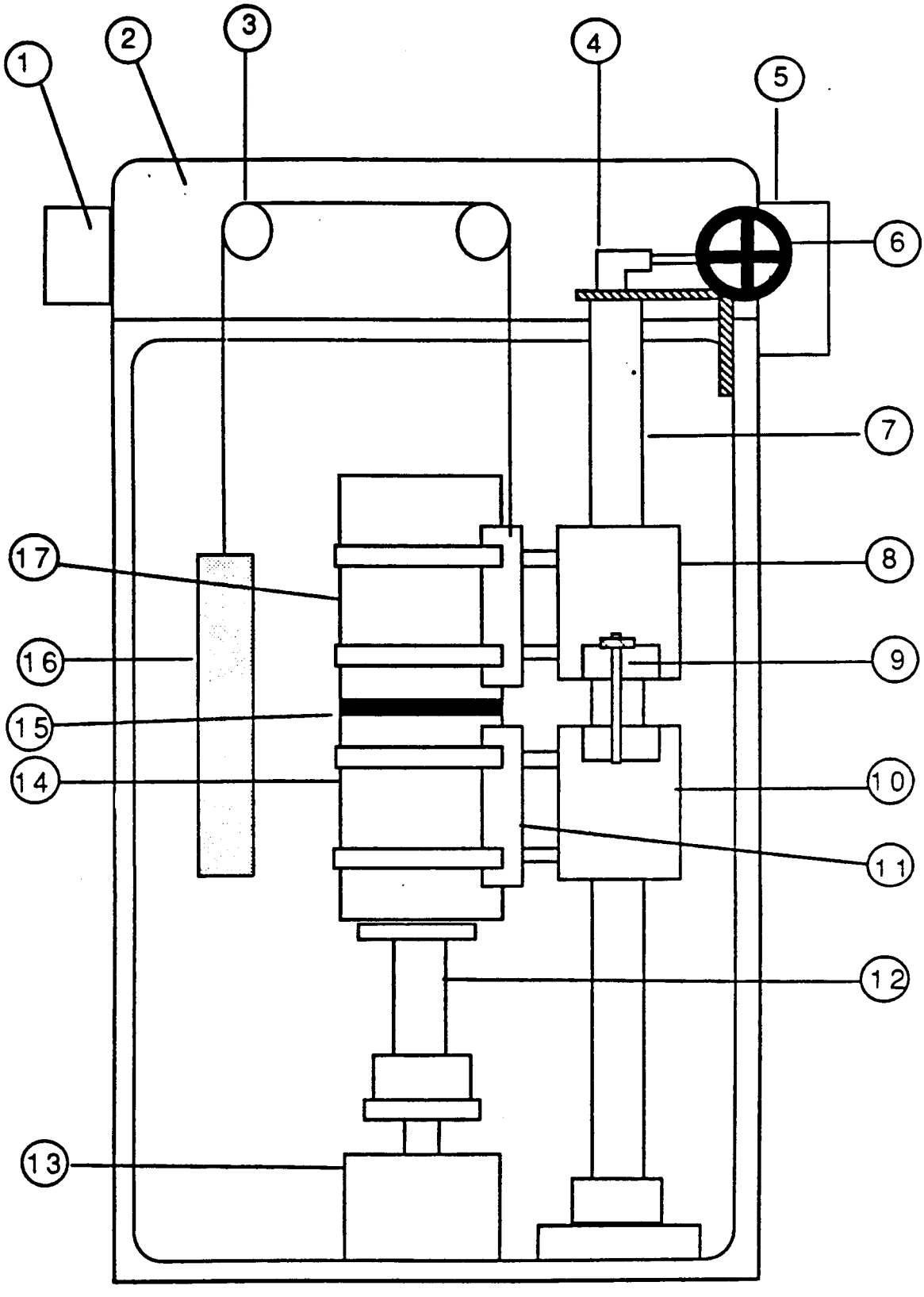

VERTICAL BRIDGMAN FURNACE

1. AIR EXHAUST VENT.
2. FURNACE ENCLOSURE.
3. COUNTER WEIGHT PULLEY ASSEMBLY.
4. ANGLE GEAR DRIVE FOR LIFT SCREW.
5. LIFT MOTOR AND CLUTCH ASSEMBLY.
6. MANUAL LIFT CRANK.
7. MAIN GUIDE AND FURNACE SUPPORT COLUMN.
8. HOT ZONE COLUMN SUPPORT BLOCK.
9. HOT/COLD ZONE LOCKING.
10. FURNACE SUPPORT AND DRIVE BLOCK .
11. HEATER CARRIER SUPPORT.
12. AMPOULE SUPPORT PEDESTAL.
13. SPIN MOTOR AND GEAR BOX ENCLOSURE.
14. COLD ZONE HEATER.
15. HOT/COLD ZONE THERMAL BAFFLE.
16. COUNTER WEIGHT.
17. HOT ZONE HEATER.

Figure 10. Apparatus for measurement of popoff stress.

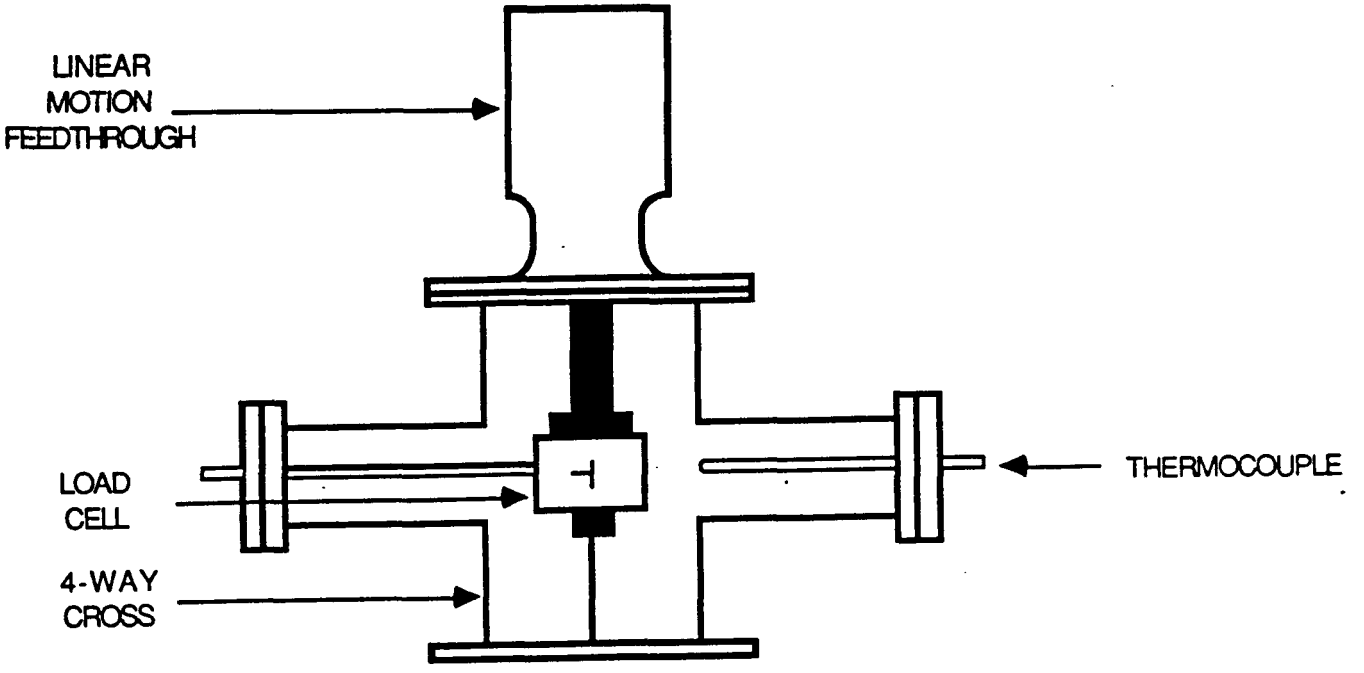

Figure 11. Ampoule for popoff experiments.

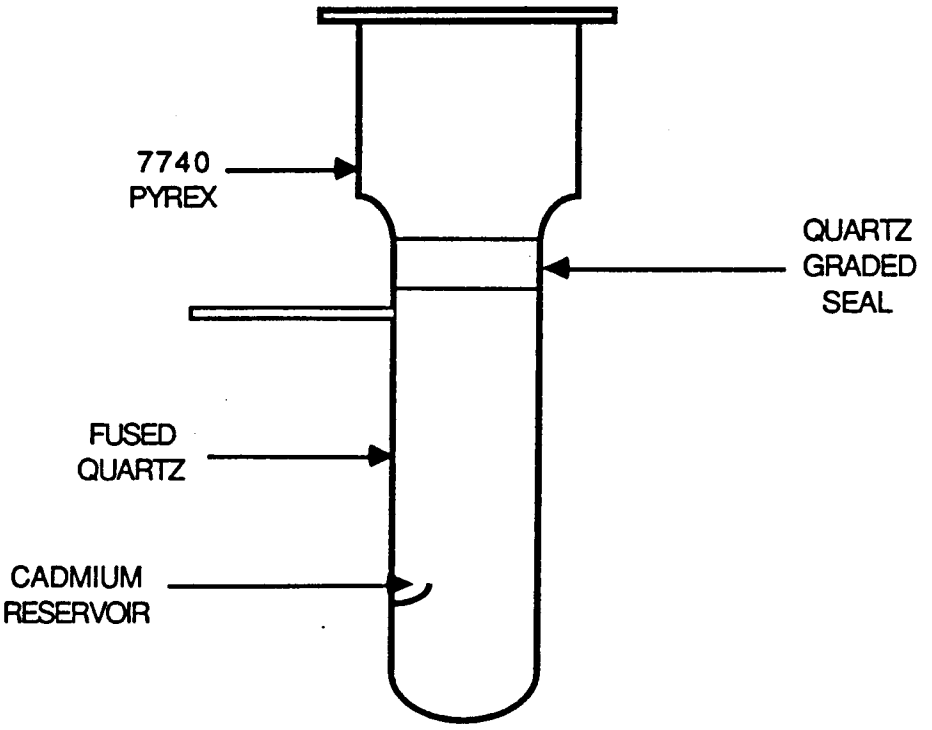

# 7.B. Computer Model for Optimization of Design of Flight Hardware

F. Carlson, W. Rosch, J. Sheu, and C. Wen

## SUMMARY

Our long term research goal is to develop a reliable computer simulation of the Bridgman process which will predict the interface shape, compositional homogeneity, and the thermal stress distribution in a crystal at any time during the growth process. This tool will then be used to design a furnace-ampoule system and a control policy which will result in growing a crystal with improved properties.

This year's objective has been to improve the capabilities of our model by including more physics and experimentally verifying the calculations. Our emphasis has been to develop a stress model and improve our existing heat transfer model by adding radiation heat transport. Both of these projects are well advanced and completion is expected before 1989. Partial model verification was achieved for the thermal model.

Future work will integrate the thermal, fluid, and stress models into a production code.

## INTRODUCTION

Progress made during this reporting period is part of an ongoing process to develop a tool which will enable us to design flight hardware. The tool, a computer simulation which models the transport process, is fairly well developed. It is currently capable of solving the thermal field [1] including the calculation of the solid-liquid interface in a growing

[1] without radiation

solid. Interface shape profoundly influences the melt flow field. Melt flow is a major part of the species transport process which determines the compositional homogeneity of the crystal. To control the growth process, it is imperative to understand the behavior of this surface during solidification.

Existing evidence suggests that the shape of the solid-liquid interface affects the stress field in the crystal. Another surface, a solid-solid interface between the crystal and ampoule wall, also affects the stress level in the crystal and hence the defect level. Knowledge of both of these surfaces is necessary to minimize defects and compositional variations in the final crystal.

## STRESS MODELING

On a macroscopic scale, materials have a critical value called the yield stress that determines how they will behave under an applied load. As long as the applied load is below the yield stress, the material will resume its original shape when unloaded. A material will plastically deform, that is permanently change shape, after the yield stress has been exceeded.

On the atomic scale, the same types of reactions can be seen. A crystal can be pictured as a system of boxes that are neatly stacked and glued together. When the system is stressed, all the little boxes stretch or elongate until they find the most comfortable position. However, as the applied load is increased, the system of boxes can no longer stay intact. At some critical value, some of the boxes will permanently move to reduce the stress of the system. This movement is analogous to dislocation formation. Crystals are more vulnerable to dislocations in certain directions because of the way atoms fit together. That is, a crystal will have slip systems in which it will dislocate first. Therefore when predicting dislocation formation, the applied stress must be resolved into these slip systems. The value of the resolved stress when dislocations just start to occur is known as the critical resolved shear stress, or CRSS. The CRSS is basically analogous to the yield stress.

Since crystals with fewer dislocations are wanted, it is desirable to reduce the stress level to below the CRSS at all times. If this is impossible, then this excess stress should be made as low as possible because it has been shown that the dislocation density is roughly proportional to the stress.

During the vertical Bridgman growth process, the newly formed crystal passes through a large temperature gradient. This gradient will create thermal strains due to the shrinkage that occurs. To use the box analogy, each of the boxes will shrink as they get cooler. If all the boxes are at the same temperature, they will shrink the same amount and fit together perfectly. Likewise, if the temperature gradient is constant then the boxes will also fit

together nicely. Both of these cases represent zero thermal stress states. However, if the boxes do not shrink in either of these fashions, they will stress each other, and produce thermal stress in the system.

Since the crystal grows in a container made from a different material, it will shrink at a different rate. If the container shrinks more than the crystal, it will apply a compressive stress to it. If on the other hand, it shrinks less than the crystal does, the crystal will try to pull away from the surface of the wall. If it adheres tightly and is not able to pull away, the container will apply a tensile stress to the crystal. Finally, if the crystal does pull away from the surface of the wall, it forces the weight of the crystal to be supported by some other area. It is conceivable that the entire weight of the crystal could be supported by the section near the interface which has just solidified, is at the highest temperature, and so is the weakest part.

A finite element model is presently being developed to find the steady state stress field during the Bridgman growth process. The program uses the principle of energy minimization to determine the displacements of each of the nodes. If a body is initially in equilibrium and then is disturbed, it will assume a new equilibrium state corresponding to the lowest energy level it can attain. By solving for this minimum energy in terms of displacements, the new equilibrium position can be determined.

Once the displacements are known, the strains can be calculated by taking the derivatives of the displacements. The stress components are calculated by multiplying the strain components by the elasticity matrix. Since the program calculates the derivative of displacement, the finite element mesh is made up of quadratic isoparametric elements. This allows the derivatives of displacement, stress and strain, to vary linearly across the element. By using quadratic isoparametric elements, the program is also able to handle problems with curved boundaries.

Once they are calculated, the stress components are resolved onto the crystal slip systems so they can be compared to the CRSS. Also, if the tensile stress at the container-crystal boundary is too large for the crystal to remain attached, provision has been made to release the charge at a predetermined stress level.

Instead of writing the whole program at once, it is being constructed from a large number of chunks. This allows the program to be checked at each intermediate step to be sure that it is functioning properly. At this time, the stress model will solve a limited set of problems. These correspond to plane stress, plane strain, and axisymmetric problems. In addition, since the input is presently being generated by hand, the problems are limited to a small number of elements. This will be automated in the final version.

The program is correctly calculating the components of stress for problems involving crys-

tal weight, temperature effects, and known displacements. This shows that the backbone of the program and the knowledge base are working satisfactorily.

Future versions of the program will have greatly increased input and output capabilities. In addition, the number of nodes and elements will not be limited except by practicality. The mesh will be able to deform to take into account the crystal-wall cohesion properties. Finally, this program will be linked with other programs to solve the stress field during the crystal growth process. Possible future enhancements could be full three-dimensional problem solving, and using anisotropic elastic properties.

## RADIATION HEAT TRANSFER

The current thermal transport model has the capability of simulating one dimensional radiation heat transfer between the ampoule and the furnace wall. Since the growth process is at such elevated temperatures, radiation is important. Currently we can not simulate radiation from the ends of the ampoule or across a large gap between the furnace and the ampoule because the transport is then multidimensional. We intend to eliminate this deficiency. Upon completion, this radiation transport model will be incorporated into the combined simulation.

Solution of the radiation heat transfer problem can be separated into two steps. In the first step, radiation between the inner surface of the furnace and the outer surface of the ampoule is considered. The second step is an extension of previous work, which includes heat transfer between the inner surface of the furnace and the inner surface of the ampoule or the charge itself. The reason for separating the problem is that the materials of the ampoule and the charge may become partially transparent at high temperatures. This makes the problem very complex.

Although heat transfer in directional solidification is time dependent, the rate of change is low so that the thermal radiation can be considered as steady during each time step. When solving the first part of the problem further assumptions are made:

1. All surfaces are gray.
2. The air between the surface is completely transparent, and conductive and convective heat transfer are negligible.
3. Axisymmetric configurations.

The surfaces are divided into axisymmetric elements and the temperature of each element is constant during a given time step. The absorption factor method is used to calculate

the net radiant loss from each element. In this method the net radiant loss from an element is determined by:

$$q_j = W_j A_j - \sum_{i=1}^{n} B_{ij} W_i A_i. \tag{1}$$

where $q_j$ is the net rate of radiant loss from $j^{th}$ element surface;
$A_j$ is the area of $j^{th}$ element surface;
$W_j$ is the rate of emissive power per unit area of surface $j$;
$W_j = \epsilon_j \sigma T_j^4$, where $\sigma = 5.669 \times 10^{-8}\ W/m^2K^4$, $\epsilon$ is the emissivity of the surface, and $T$ is the absolute temperature of the surface, which is a known value obtained from other parts of the code;
$B_{ij}$ is the absorption factor, which can be calculated from the following linear system:

$$\begin{bmatrix} (K_{11}-1) & K_{12} & K_{13} & \cdots & K_{1n} \\ K_{21} & (K_{22}-1) & K_{23} & \cdots & K_{2n} \\ K_{31} & K_{32} & (K_{33}-1) & \cdots & K_{3n} \\ \cdot & & & & \\ \cdot & & & & \\ \cdot & & & & \\ K_{n1} & K_{n2} & K_{n3} & \cdots & (K_{nn}-1) \end{bmatrix} \begin{bmatrix} B_{1j} \\ B_{2j} \\ B_{3j} \\ \cdot \\ \cdot \\ \cdot \\ B_{nj} \end{bmatrix} = \begin{bmatrix} -\epsilon_j F_{1j} \\ -\epsilon_j F_{2j} \\ -\epsilon_j F_{3j} \\ \cdot \\ \cdot \\ \cdot \\ -\epsilon_j F_{nj} \end{bmatrix}$$

where $K_{rs} = F_{rs}\rho_s$;
$\rho_s$ is the reflectivity of surface $s$;
$F_{rs}$ is the view factor from surface $r$ to $s$.

After $q_j$ calculated, it is introduced into the combined simulation as a source term in the energy equation.

The programming for calculating $q_j$ is almost complete. All of the view factors which are necessary for the general case have not yet been calculated. They will be generated by a combination of closed form algebraic solutions, numerical integrations, and view factor algebra.

The materials of the ampoule and the charge may partially transparent at high temperature. The next step will account for this by modifying the absorption factor method. It is assumed that an interface exists between the transparent and nontransparent material. The transparent medium is not reflectable at all, i.e., $\alpha_m + \tau_m = 1$. Otherwise, $\alpha + \rho = 1$ for the nontransparent material.

The factor K in the linear system above can be defined by: $K_{ij} = F_{ij}\rho_j\tau_m^2$, and $\epsilon_j F_{ij}\tau_m$ is used instead of $\epsilon_j F_{ij}$, where $\tau_m$ is the transmissivity of the medium. Then the mod-

ified absorption factors can be calculated for determining the net radiant loss from the interface.

One of the difficulties in this method is to determine $\tau_m$. There are several methods for calculating $\tau_m$. The most promising is:

$$\tau_m = \int_0^\infty \tau_{m_\lambda} d\lambda$$

where $\tau_{m_\lambda}$ is the spectral transmissivity,

$$\tau_{m_\lambda}(s) = \frac{I_\lambda(s)}{I_\lambda(0)}$$

$s$ is the path in the medium, $I_\lambda(s)$ is the spectral intensity which can be determined by:

$$I_\lambda(s) = I_\lambda(0)e^{K_\lambda s} + (1 - e^{K\lambda s})I_{b\lambda}(T)$$

where $K_\lambda$ is the spectral absorption coefficient.

## MODEL VERIFICATION

A set of three experiments were planned in an effort to verify the conduction, advection, and limited radiation components of the heat transfer code. In the conduction-radiation experiments a 12 inch long 3.1 inch diameter ceramic cylinder encased in a 0.1 inch thick silica ampoule was instrumented and placed in a 4 inch diameter furnace at the Rockwell International Science Center. Temperatures ranged between 60°C and 520°C at the bottom of the ampoule and between 480°C and 1080°C at the top. The furnace wall temperature ranged from 80°C to 1120°C. Tests were conducted with and without the silica ampoule in order to evaluate the radiation and conduction portions of the code, respectively.

The results were quantitatively lacking because of an undetected hole in the top of the furnace which caused a chimney effect. In spite of this problem, qualitative information was produced as follows:

1. With the silica ampoule in place and the furnace controller set, temperatures in the ceramic were hotter by as much as 70°C and the furnace cooler by 20 - 40°C than without the silica. This indicates the importance of radiation effects and the semitransparency of the silica.

2. When the furnace controller was set and the ampoule translated upward farther into the furnace, the maximum furnace temperature increased in magnitude and was at a higher axial location, always above the ampoule. This happened whether or not the silica was in place and at any particular controller setting. This indicates the strong coupling between the furnace and the ampoule-charge, and the need for modelers to include the furnace in their simulations.

3. The simulation qualitatively followed the experimental results of 1 above, but was inconclusive because there was no way to account for the chimney effect. As expected, even with the unwanted furnace advection, the heat transfer was dominated by radiation.

The advection experiment did not work because the temperature controllers did not a low enough setting for the charge material. This experiment will be repeated at Clarkson University in the future.

## 7.C. PROPERTIES OF CADMIUM TELLURIDE

W.R. Wilcox, R. Balasubramanian, H.R. Shetty, R. Derebail and V. White

SUMMARY

The longterm goal of this research is to develop the optimal ampoule design for crystal growth in space, but taking advantage of the increased importance of surface phenomena in comparison to gravitational phenomena. The specific objectives are to:

1. Determine the contact angle and surface tension of CdTe and GaAs melts vs. temperature, surface type and treatment, melt composition, and gas composition.

2. Determine other properties required in the theoretical model just described.

3. Using X-ray topograph observe in real time the formation and alteration of defects in CdTe vs. stress, temperature, time, etc.

4. Observe directional solidification in low gravity using a melt - ampoule system with a high contact angle (non-wetting).

INTRODUCTION

The Soviets claim that significantly higher perfection is obtained when crystals are solidified in space so that they are somewhat smaller in diameter than the ampoule, and that this happens when the level of accelerational disturbances (g jitter) is low. In American Shuttle missions it does not seem possible to control the g jitter. Since g jitter is caused largely by human activities, the Soviets believe it will be necessary to grow crystals in un-manned space stations. We believe, however, that proper choice of ampoule materials and geometry can lead to reduced interaction of melt and solid with the ampoule, resulting in high perfection crystals.

While the mechanism for reduced crystal diameter is not known, it is believed that it involves poor wetting of the ampoule wall by the melt, i.e. a high contact angle. The surface tension of the melt and the interaction between the melt and processes at the freezing interface may also play a role. Contact angle is known to depend on the nature of the surface, which in turn is a function of the composition of the bulk material, prior treatment of the surface, and coatings which may be applied. Contact angle and surface tension depend on the composition of the melt and the composition of the gas phase. Therefore we are measuring contact angle and surface tension of cadmium telluride melts on various surfaces vs. temperature, melt composition, and gas composition.

It would help immensely to know the mechanism for reduced crystal diameter resulting from directional solidification in space. Direct observation is needed, but has not been possible thus far because only closed opaque furnaces have been used thus far in space. NASA's Marshall Space Flight Center has had a transparent furnace (the "polymer furnace") fabricated for use on aircraft. Parabolic maneuvers of suitable aircraft provide low gravity periods of about 20 to 30 seconds. This may be long enough to provide meaningful observations of solidification. Furthermore it should be possible to use the furnace on the Shuttle for longer duration experiments.

While cadmium telluride produced on earth has too many defects, it is not known to what extent these defects are incorporated at the solid-liquid interface as compared to formation in the crystal as it

slowly cools from the melting point to room temperature. Without this knowledge it is unclear how advantageous growth in space will be and how best to go about it. We are working on direct observation of defect formation and behavior using real time X-ray topography on the National Synchrotron Light Source at Brookhaven National Laboratory.

## RESEARCH

### Contact angle and surface tension measurements

A sessile drop technique was developed to use in determining the surface tension and contact angle of cadmium telluride melts on various surfaces. A weighed and cleaned piece of cadmium telluride is placed on a plate of the desired surface and sealed in a quartz ampoule. Each ampoule is cylindrical, two inches long and one inch in diameter. It is sealed at its ends by optical quartz discs. A small weighed amount of cadmium is added to suppress the evaporation of molten CdTe. A diagram of the sessile drop cell is shown in Figure 1.

In a sessile drop experiment the ampoule is placed in a tube furnace and rotated until the substrate is horizontal. The furnace temperature is raised to the melting point of CdTe to form a sessile drop. A light source is placed at one end of the furnace tube and a camera with suitable lens at the other end. When all components are properly adjusted, photographs can be taken with high contrast between the drop and the background. Example photographs are given in Figure 2. Two or three photographs of the drop are taken at every $5^{o}$ F increment starting from the melting point until a controller setting of $2200^{o}$ F is reached. The temperature is then slowly reduced and photographs again taken. After each temperature change, one hour or more is allowed for equilibration before a photograph is taken.

Coordinates are obtained at intervals along the drop surface using a Sigma-scan digitizer tablet on a photograph. These coordinates are then converted to surface tension using a suitable computer program, which basically compares the actual shape of the drop with computed shapes. In our early work we developed our own computer program, which required separate input of the contact angle measured directly from the photograph. This process produced reasonable data for contact angle, but excessive scatter for surface tension. Currently we are using software developed at the University of Toronto, "Axisymmetric Drop Shape Analysis," or ADSA. This computer program uses measured coordinates along the surface of an axisymmetric sessile drop to find the best values for surface tension and contact angle. (Our thanks to Professor Wilhelm Neumann at Toronto for providing this software at no charge.) Use of this software has reduced the scatter in surface tension values.

We have performed experiments with "pure" cadmium telluride in an atmosphere of cadmium, hydrogen and argon on the following surfaces:

Quartz (fused silica) microscope slides
Polished quartz optical flats
Quartz coated with boron nitride powder, fired in air
Sandblasted quartz
Quartz coated with silicone oil
Pyrolytic boron nitride

Figures 3 to 5 show contact angles measured directly from photographs in our early experiments. In recent experiments analzed with the Toronto software we obtained a contact angle on HF-etched quartz of about $90^{o}$ at the melting point of cadmium telluride. This value is appreciably higher than the contact angle obtained earlier on unetched quartz surfaces (Figures 3 and 4). However more excess cadmium was used in the runs on HF-etched quartz surfaces. We have not yet determined the dependence of contact angle on the cadmium content of the melt. The contact angle on sandblasted quartz was about $100^{o}$ at the melting point. On pyrolytic boron nitride it was about $125^{o}$. Thus is the least

wetting of the surfaces studied thus far. Contact angles, in general, decreased with inreasing temperature.

Figures 6 and 7 show early results for surface tension computed using our software from measured contact angles and drop profiles. In recent experiments using the Toronto software we obtained 195 dynes/cm for the surface tension of CdTe at its melting point. This value is somewhat higher than the values of 162 dynes/cm on quartz and 185 dynes/cm on boron nitride coated quartz from the earlier experiments. The higher values might be due to the slightly larger amounts of Cd used in these experiments.

The siliconized quartz surface did not yield a sessile drop, probably because of decomposition of silicone oil at higher temperatures to yield a surface wet well by the cadmium telluride.

Solidification in transparent furnace

The "polymer furnace" developed for NASA's Marshall Space Flight Center allows the solidification ampoule to be viewed and photographed between two heaters. The maximum temperature is a few hundred degrees Celsius. Thus we are searching for a system with a melting point within this range that exhibits a large contact angle.

Contact angle measurements of various substances are being carried out on glass slides made of Pyrex. Thus far we have tested phenyl salicylate (salol), benzoic acid, anthracene, naphthalene, stilbene, benzophenone and other organic compounds. None of these substances are non-wetting on untreated Pyrex.

Direct observation of defect formation and behavior

Mr. Balasubramanian is at the National Institute of Standards and Technology in Gaithersburg working with NIST personnel on developing techniques for direct observation of defect formation and behavior in cadmium telluride crystals. This first step in accomplishing this was to gain a working knowledge of X-ray diffraction. Laue diffraction patterns were obtained for eleven gallium arsenide wafers. Topographs of some of the planes were also obtained.

An experimental apparatus was designed to observe defects while a tensile stress is applied. As a preliminary test the apparatus was tested on a (100) silicon wafer using a copper X-ray source. Laue pictures were taken and the deflection of the wafer measured. Neither epoxying the edge of the wafer nor the cleaving along the [110] planes produced strain fields that would affect image analysis during actual tension/compression experiments as observed from the asymmetric diffractions obtained.

For cadmium telluride it was decided to begin at room temperature and gradually proceed to higher temperatures. A suitable apparatus was designed. This apparatus has to meet requirements for mechanical rigidity, conformance with the X-ray conditions at the National Sychrotron Light Source, etc. It must also weigh no more than 10 lb in order to be placed on the stage at the NBS beam line. Since the smallest commercial load testing machine weighs at least 400 lb, we decided to design and construct our own apparatus. The load testing machine will consist of an air cylinder (Bellofram Industries) with capability to change to a hydraulic cylinder, double cushion ball bearing linear motion units (Thompson Industries) for rigidity and smooth motion, a subminiature load cell (Sensotec or other) and an aluminum frame. When completed this unit will be capable of applying loads up to 46 lb, apply a maximum strain of 0.7 inch, and will weigh approximately 11 lb.

Graphite notched plate heaters are being considered.

PLANNED RESEARCH

We will determine the influence of melt composition and gas composition on contact angle and surface tension. In particular we will perform sessile drop experiments with different amounts of excess cadmium in the ampoule. Experiments will be performed on quartz coated with carbon. We will attempt to automate the analysis of our photographs using electronic video digitization of the drop profiles. We will reanalyze the photographs taken during our early sessile drop experiments using our improved techniques. Similar sessile drop experiments will be performed on gallium arsenide when the cadmium telluride work is complete.

In our search for low-melting non-wetting systems we will try organic compounds on plastics and on glass coated with silicone oil, polytetrafluoroethylene, fluorosilanes, etc. Low melting metals like tin and indium will be tried. Indium antimonide is another possibility, although its melting point may be too high for the polymer furnace. Once a suitable system is found, we will design and fabricate the ampoule. Experiments will be flown in cooperation with Marshall Space Flight Center on the KC-135 aircraft.

We will construct and operate the apparatus for stressing cadmium telluride in the synchrotron X-ray beam. We will design an apparatus for *in-situ* observation of crystal growth.

Figure 1. Quartz ampoule for sessile drop experiments on CdTe.

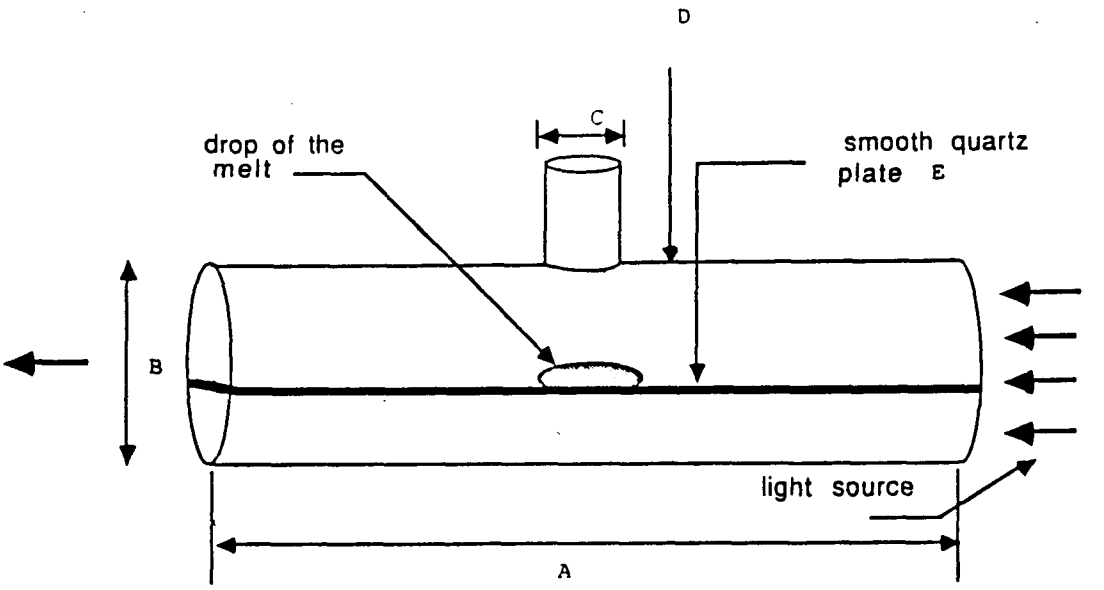

Figure 2. Photographs of sessile drops taken in apparatus of Figure 1.

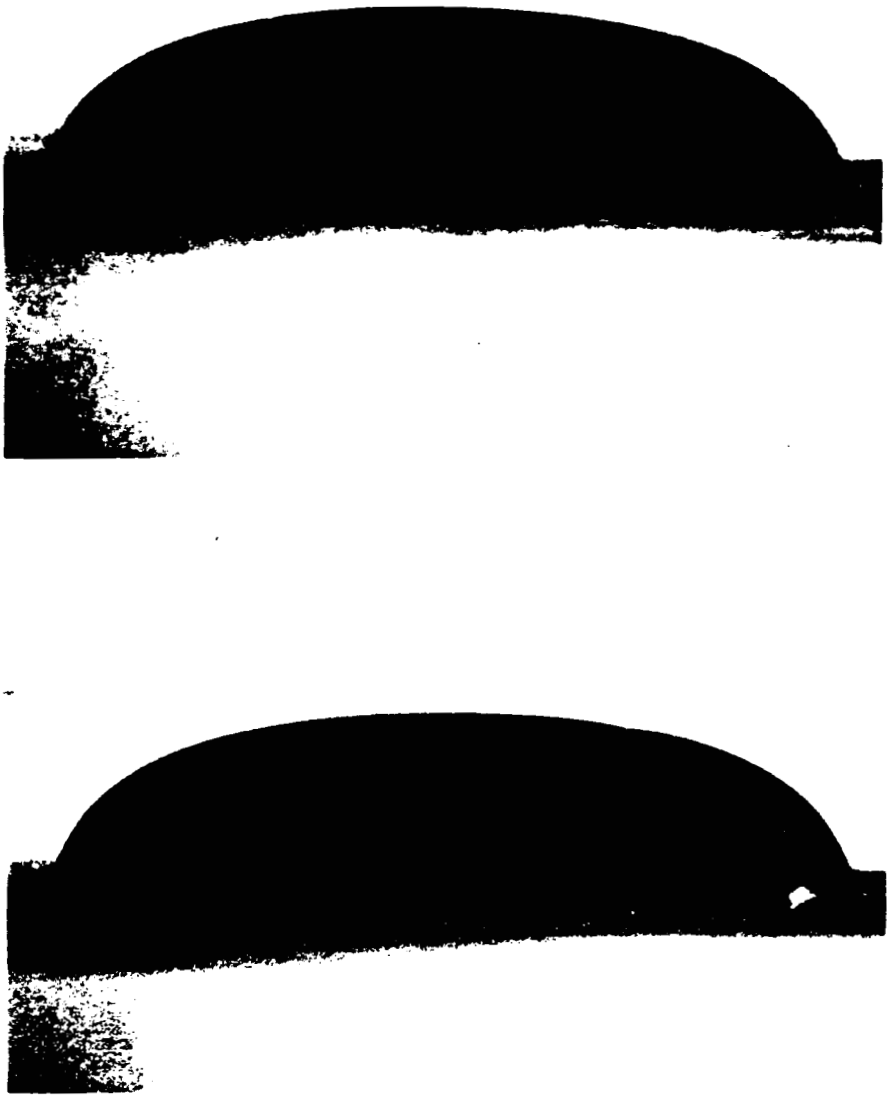

Figure 3. Contact angle of CdTe on quartz microscope slides.

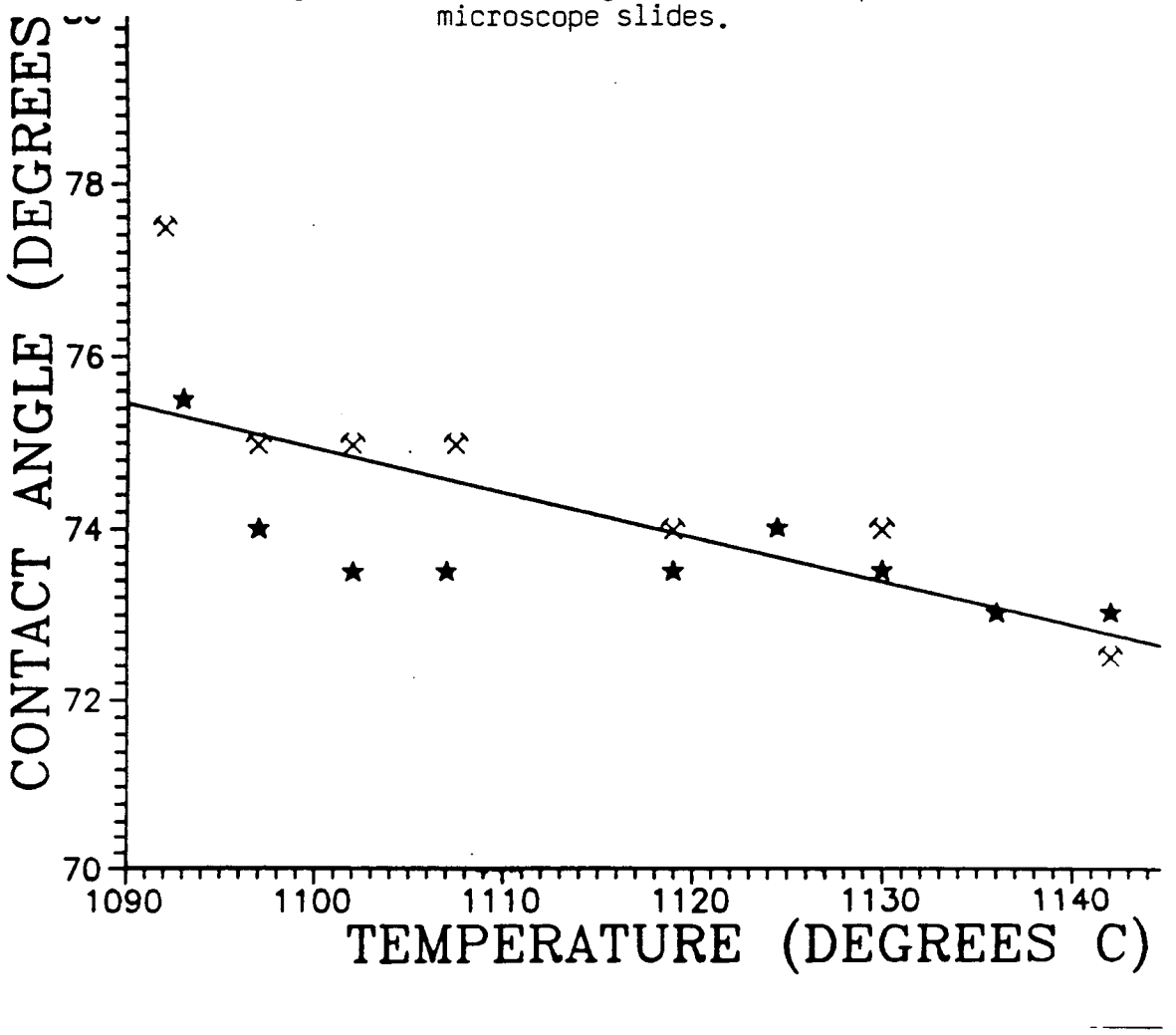

Figure 4. Contact angle of CdTe on quartz optical flats.

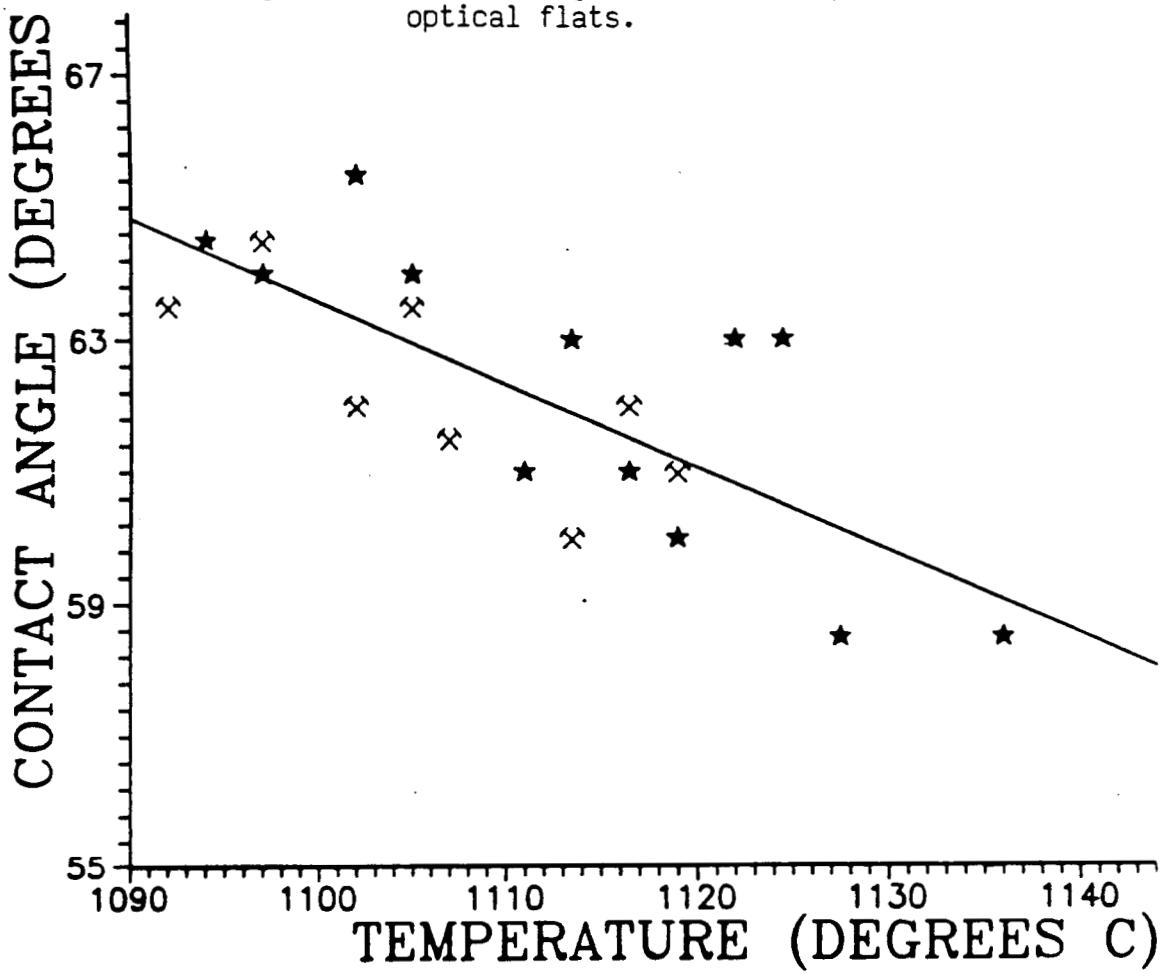

Figure 5. Contact angle of CdTe on quartz coated with boron mitride powder and heated in air.

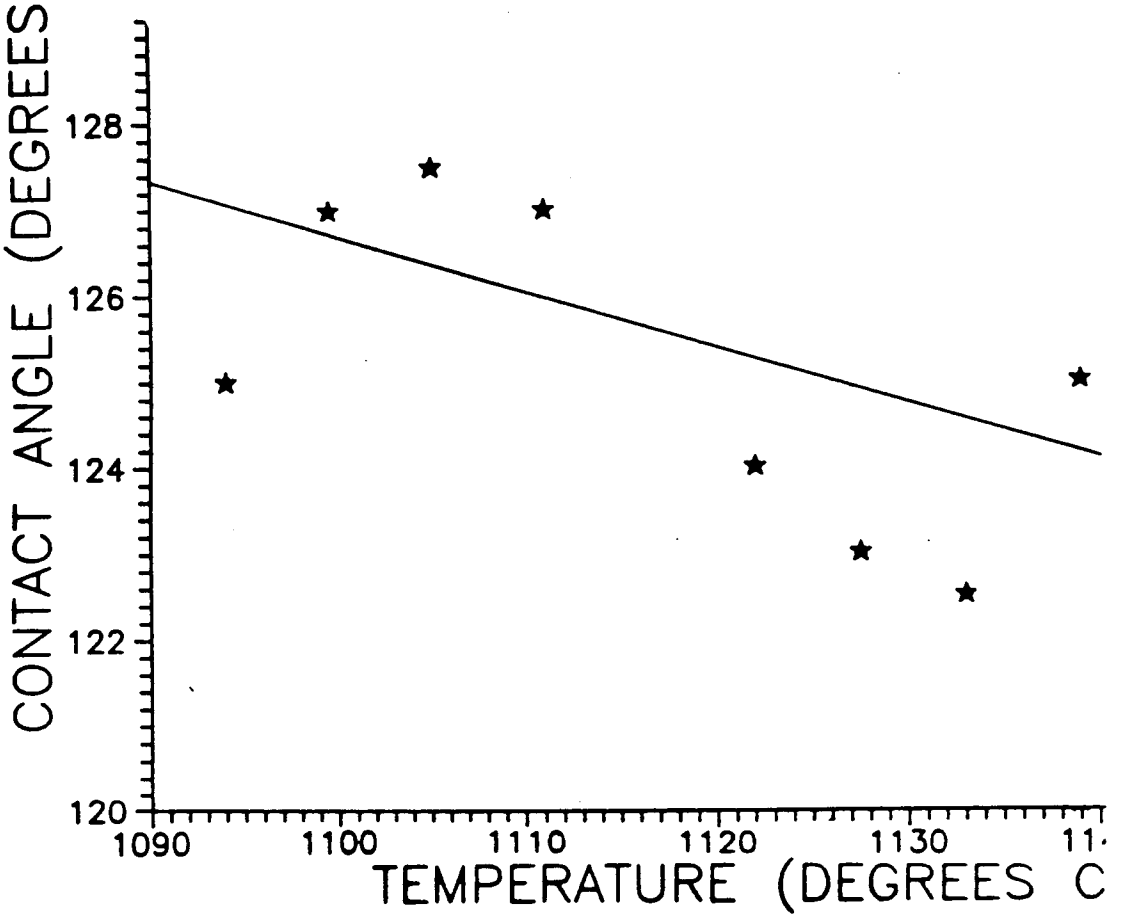

Figure 6. Surface tension of CdTe from shape of sessile drops on quartz.

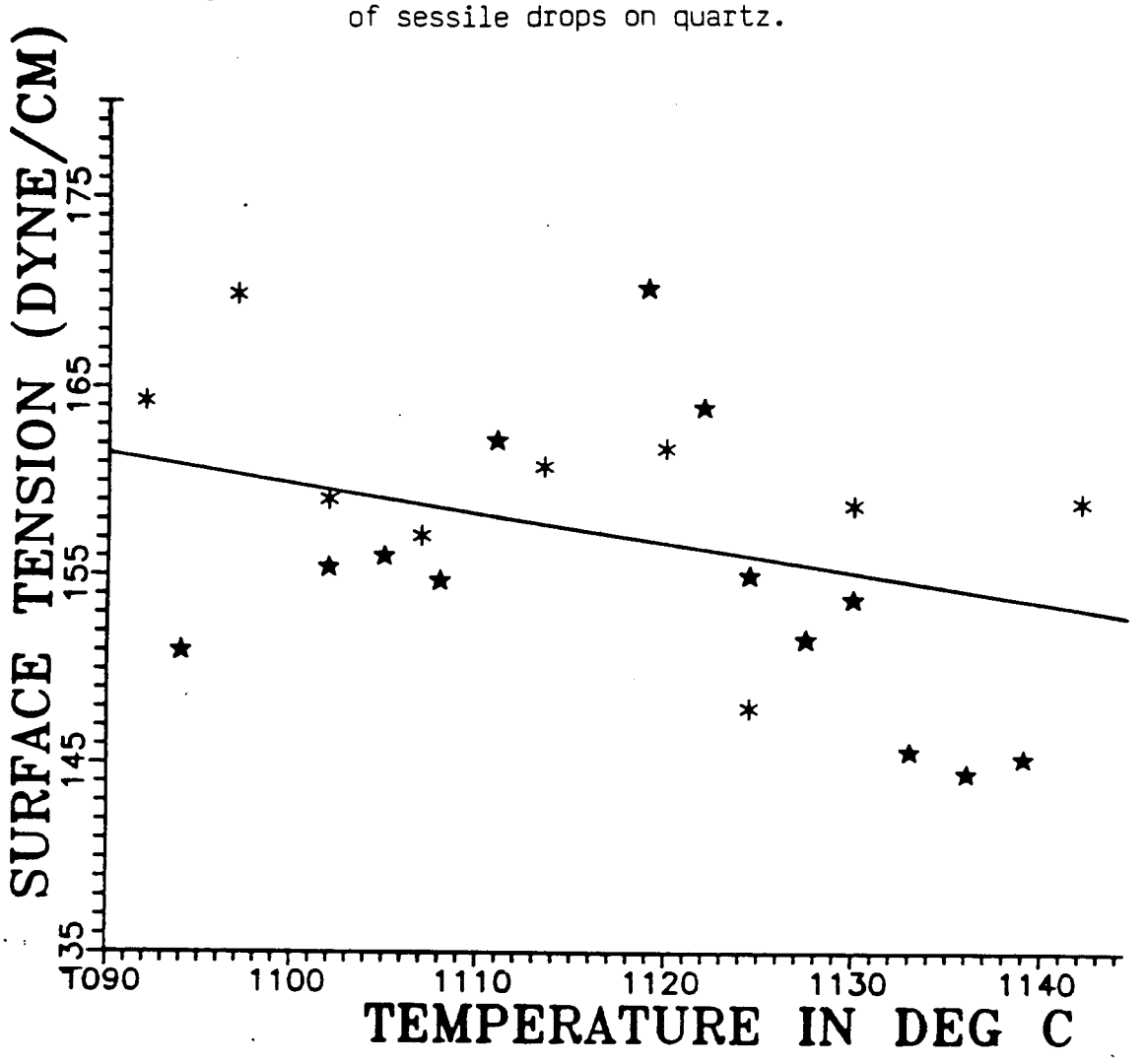

Figure 7. Surface tension of CdTe from shape of sessile drops on quartz coated with boron nitride powder.

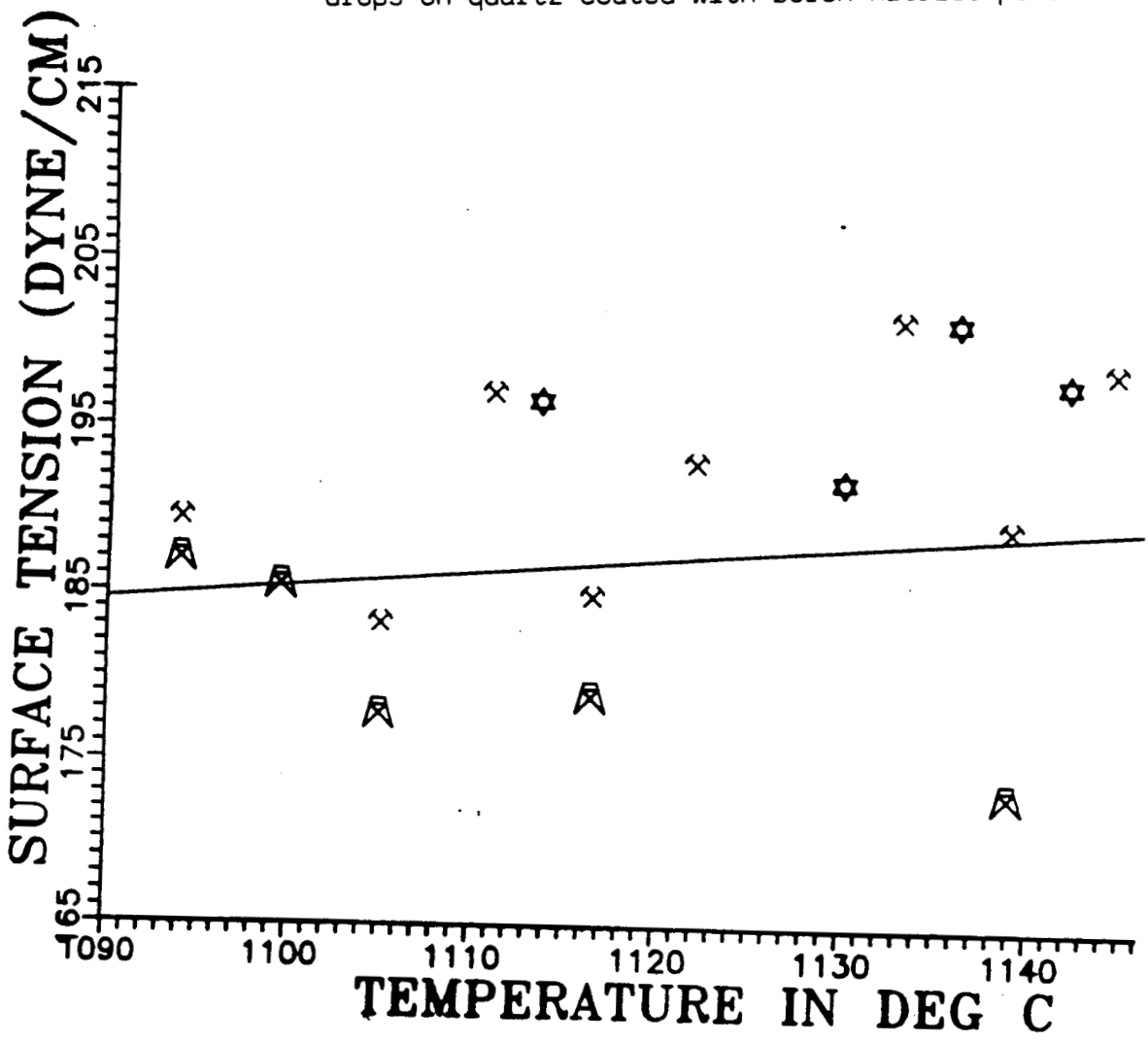

# 8. CRYSTAL GROWTH OF CdTe IN SPACE AND THERMAL FIELD EFFECTS ON MASS FLUX AND MORPHOLOGY

H. Wiedemeier

**RENSSELAER POLYTECHNIC INSTITUTE**
Troy, New York 12180

# CRYSTAL GROWTH OF CdTe IN SPACE AND THERMAL FIELD EFFECTS ON MASS FLUX AND MORPHOLOGY

H. Wiedemeier
Rensselaer Polytechnic Institute, Troy, New York 12180-3590

November 1988

## SUMMARY

Our research and development efforts in vapor phase crystal growth of CdTe during the past year were focused on the following individual tasks.

1. During this period of effort, emphasis was on the further elucidation of the effects of source material stoichiometry and of extrinsic process variables on the physical vapor transport properties of CdTe. Significant progress has been achieved in the CdTe synthesis and pretreatment procedures. Complete control of source material stoichiometry is essential for the reproducible growth of CdTe single crystals. Because of the interrelation between stoichiometry, mass flux, and crystal morphology, the detailed understanding of these relationships is of critical importance for a meaningful analysis of gravity-driven convection effects on mass flux and crystal growth of CdTe. The combined results to date demonstrate that the degree of stoichiometry control achieved in this program is greater than reported before in the literature.

2. The development and refinement of a theoretical model for the prediction of diffusion limited mass transport rates of CdTe has been continued. The reliable prediction of mass fluxes under vertical, stabilizing conditions is of great importance for the comparison to experimental data and the observation of the effects of residual convection on mass flux. As discussed in this report, most recent experimental transport rates are in close agreement with theoretically predicted data.

3. Crystal growth experiments performed under the above conditions yielded promising results. A CdTe crystal boule of about 15 mm length, 12 mm maximum diameter, and a weight of about 6 g was grown. Optical microscopy and X-ray diffraction studies revealed that the boule contained several large sized crystal grains of a high degree of single crystallinity. Further characterization studies of the CdTe crystal are in progress. In view of the reported difficulties in the growth of CdTe single crystals, the crystal growth experiment performed as part of this effort may be considered as rather successful.

4. The reaction chamber, furnace dimensions, and ampoule location of the dynamic microbalance system were modified in order to minimize radiation effects on the balance performance. Operational testing and sensitivity measurements for the modified balance facility were performed.

## INTRODUCTION

The primary objectives of this project are the development of vapor phase crystal growth experiments of electronic materials, and the growth of single crystals of such materials in space. The microgravity environment provides a significant reduction in the average magnitude of the gravitational force, but most other experimental parameters are the same as on earth. It is, thus, of critical importance to distinguish gravity-related from gravity-unrelated effects on crystal growth, in order for commercial crystal growth in space to become a reality. In addition, all ground-based processing parameters must be optimized in order to observe genuine microgravity effects on crystal morphology and properties. The major parameters affecting crystal growth and quality in a normal gravity environment are the mass flow and temperature conditions. Very little experimental information is available concerning the effects of temperature perturbations on mass flux and crystal growth. It is, therefore, difficult to determine "a priori" the relative impact of the above parameters on crystal morphology under normal and reduced gravity conditions. For closed-tube vapor transport systems, we have demonstrated a relationship between transport mode and boundary layer thickness [1]. In addition, we have shown previously that even under vertical, stabilizing conditions the vapor phase of transport systems is thermally not stable [2]. The interrelation between temperature perturbations, fluid flow, and crystal morphology indicates the complexity of reactive solid-vapor transport systems. For the design of meaningful crystal growth experiments in space it is of great importance to understand as much as possible the interrelation between crystallographic, thermodynamic, and fluid dynamic parameters and their relative impact on crystal morphology and properties. Under these conditions, it is possible to fully exploit the benefits of a microgravity environment for crystal growth.

## SCIENTIFIC AND TECHNICAL BASIS

The development of crystal growth experiments in space and the growth of electronic materials of improved properties in microgravity environment are the dominant aspects of this program. Based on an extensive literature evaluation of electronic materials, cadmium telluride appears to be one of the most valuable semiconducting materials presently available. Its useful properties for nuclear radiation and infrared detection, for high energy laser windows, for solar cells, and as substrates for HgCdTe crystals are well-known and have been exhaustively discussed in the literature. Frequently, CdTe single crystals are grown from the condensed phase (melt or solution) [3]. Although these techniques produce crystals with high growth rates, the main problems encountered include poor grain size, lack of control of orientation of grains, and a variety of other crystalline defects [3,4]. The growth of CdTe from the vapor phase offers a possibility of producing crystals of high compositional uniformity, high resistivity, and low density of imperfections [5,6]. A closer analysis of these and other recent literature concerning the vapor transport of CdTe reveals inconsistencies and discrepancies in transport and growth rates of CdTe. Experimental evidence produced in our laboratory for this system strongly suggests that the above discrepancies are caused

by stoichiometry problems of the source material. Practically no systematic studies of stoichiometry effects on mass transport and crystal growth of CdTe in closed ampoules are available in the literature. A similar situation exists for the correlation of crystalline quality and growth parameters for closed ampoule CdTe growth. To achieve better control of the transport and growth process of CdTe, a thorough understanding of the mass transport - growth mechanism and its dependence on the overall stoichiometry of the system is required. This is also of importance because of the relation between stoichiometry, mass flux, growth rate and properties of the grown crystal. These intrinsic, gravity-independent parameters of a system must be controlled in order to unambiguously determine the effects of gravity-dependent parameters on crystal growth.

For the analysis of the average and momentary mass flux of the vapor growth system, dynamic microbalance techniques will be employed. For this purpose, a vacuum microbalance facility has been assembled. From the observed mass flux and thermochemical data of the system, the dominant transport mode can be deduced. In addition, the effects of induced and inherent temperature oscillations on the mass transport rates are of particular interest with respect to variations in mass flux and flow pattern. The dynamic microbalance technique offers the potential to observe changes of transport phenomena in-situ under actual transport conditions. Independent measurements of the vacancy formation in $Hg_{0.8}Cd_{0.2}Te$ [7] have demonstrated the suitability of this technique for transport studies in closed ampoules.

In-situ measurements of transport phenomena are of basic scientific and technological value. In the context of this program, their primary function is to support the crystal growth effort. In order to distinguish between the effects of the above discussed different parameters on crystal growth, the stability of experimental parameters must be well established. We have demonstrated that even minute fluid dynamic disturbances in the vapor phase have a significant effect on the uniformity and crystallographic perfection of $Hg_{0.8}Cd_{0.2}Te$ single crystals [8]. To minimize such disturbances on ground is important for the interpretation and optimal use of microgravity effects in space. In addition, reduced convectional instabilities in space offer the possibility to grow CdTe crystals of larger diameters than available on ground for comparable levels of perfection. However, the interrelation of the above indicated stoichiometry and of convectional effects on mass transport and growth of CdTe must be experimentally analyzed and understood in order to develop flight conditions. The systematic investigation of this problem is the immediate goal of our CdTe effort.

## PROGRESS ACCOMPLISHED

### Crystal Growth of Cadmium Telluride

Development of Theoretical Transport Model for CdTe

In order to compare experimental data with expected mass fluxes for "ideal" conditions, a transport model for the physical vapor transport of CdTe was developed as part of this effort. This requires the computation of partial pressures from thermochemical data, and of diffusion

coefficients based on physical constants of the vapor species. Individual mass fluxes were computed based on the assumption of 1-dimensional diffusive-advective flow. The presence of residual gas in the ampoule was considered. The computations were performed for increasing deviations from stoichiometry of the overall solid-vapor phase composition. The program developed applies iterative procedures for a given set of experimental parameters (temperatures of the source and deposition product, partial pressures of vapor species, and source to deposit distance).

A basic theoretical model for the physical vapor transport of CdTe and a temperature difference of 850° → 830°C was developed and reported earlier [9] by us. A comparison of predicted and experimental mass flux data [9] revealed good agreement with respect to the overall trend of the mass fluxes as a function of stoichiometry of the system. However, there were considerable differences in the magnitude of the predicted and observed mass fluxes, the latter being lower than the former, particularly in the vicinity of the stoichiometric composition of the solid-vapor transport system [9]. These differences could be related to the actual homogeneity range of CdTe.

In connection with on-going mass transport rate experiments of CdTe, to be discussed below, it appears desirable to employ higher source temperatures than used previously [9] for the crystal growth of CdTe. Higher source temperatures would not only increase the mass flux, but a corresponding increase of the growth temperature would also increase the surface mobility of Cd and Te atoms on the growing surface of the crystal. Both changes are expected to increase the growth rate and crystalline quality of CdTe. Therefore, in order to compare experimental transport rates with predicted data, the theoretical transport model for CdTe was modified and adjusted to a temperature differences of 900° → 880°C. In addition, two different residual pressures of CO have been considered, namely 0.03 and 0.006 atm. A source to deposit distance of $\Delta \ell$ = 10 cm was assumed for these computations. The theoretical flux curves are graphically represented in Fig. 1. The abszissa shows the excess Cd and Te in mg per $cm^3$ free ampoule volume relative to the stoichiometric (Cd:Te = 1:1) composition. The overall shapes of the theoretical flux curves are very similar to that reported earlier [9], but the magnitudes of the predicted data are different from those of the earlier computations. The theoretial curves predict a significant decrease in mass flux for even minute deviations of the solid-vapor system from stoichiometry.

## Mass Transport Experiments of CdTe

CdTe source materials employed for mass flux experiments were synthesized from stoichiometric (1:1) ratios of elemental Cd (99.9999%) and Te (99.9999%), which were further purified by sublimation prior to the synthesis of CdTe. The elemental mixture was annealed in evacuated, sealed fused silica ampoules at about 850°C for several days. Debye-Scherrer X-ray diffraction patterns of the annealing product confirmed the chemical and structural identity of CdTe. The fused silica ampoules employed for the synthesis of CdTe and for the transport experiments were cleaned and pretreated as discussed before [8]. Several different types of mass flux experiments were performed with the above

Figure 1

Mass transport rates (moles·cm$^{-2}$·s$^{-1}$) of CdTe as a function of deviation of the source material from stoichiometry (excess Cd or Te, mg/cm$^3$). Solid lines are theoretically predicted mass fluxes for the temperature difference 900° → 880°C, for (1) residual CO pressure of 0.03 atm and (2) for residual CO pressure of 0.006 atm. Experimental data: (O) open circles, earlier data [9] for 850° → 830°C and elements purified before CdTe synthesis; (▲) closed triangles, present data for 900° → 880°C and elements purified before CdTe synthesis, (□) open squares, present data for 900° → 880°C and elements purified before synthesis of CdTe and source material annealed (500°C, 5 h) prior to sealing.

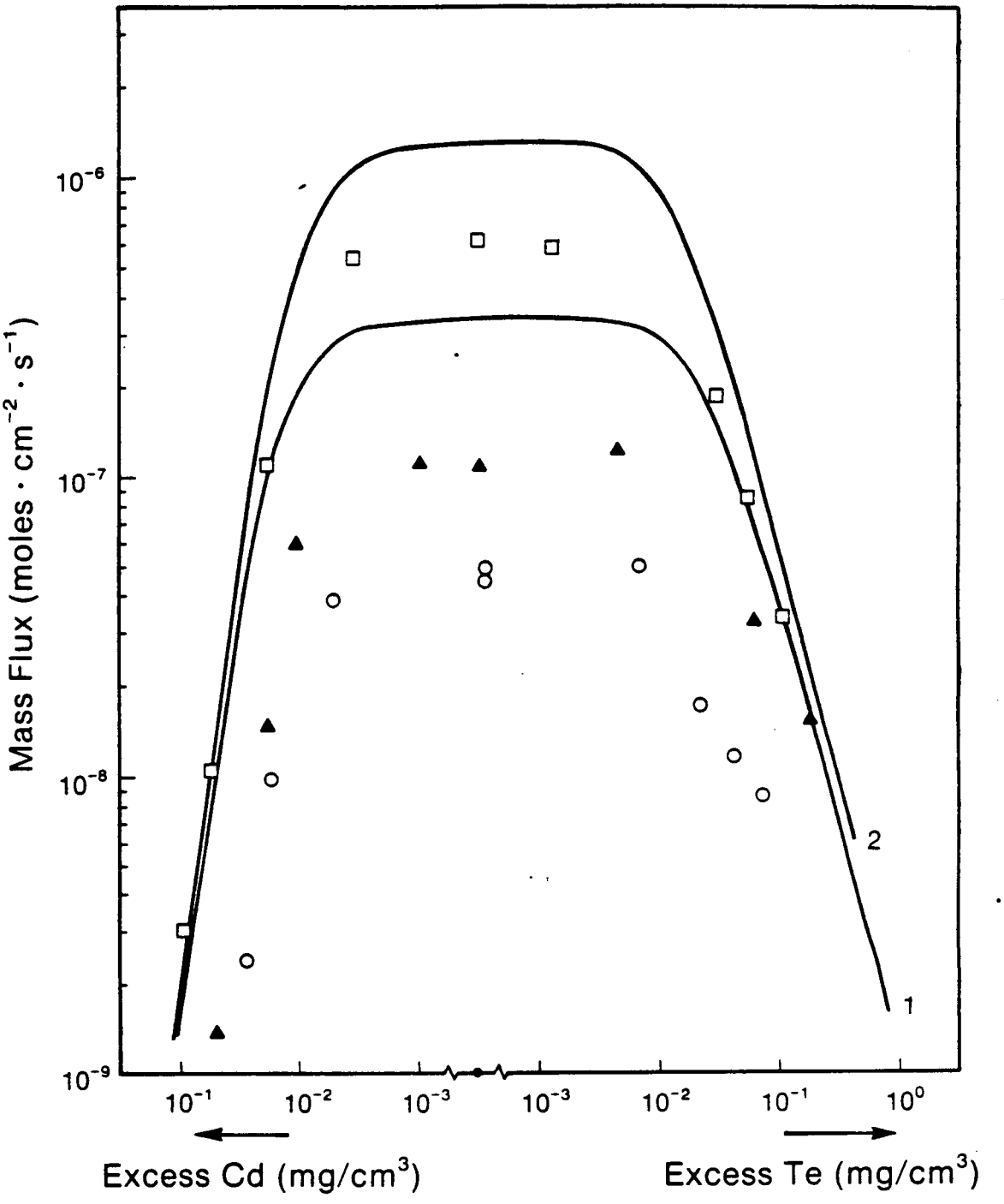
Mass Flux (moles · cm$^{-2}$ · s$^{-1}$)
$10^{-6}$
$10^{-7}$
$10^{-8}$
$10^{-9}$
$10^{-1}$
$10^{-2}$
$10^{-3}$
$10^{-3}$
$10^{-2}$
$10^{-1}$
$10^{0}$
1
2
Excess Cd (mg/cm$^3$)
Excess Te (mg/cm$^3$)

source material. Any additional treatment of this source material prior to use is discussed in connection with the particular experiments.

We have observed and reported previously [9] that annealing of the source material under dynamic vacuum conditions and at elevated temperatures prior to sealing of the transport ampoule has a significant effect on the mass flux. With increasing annealing temperature the mass flux increases [9]. In order to standardize the pretreatment procedures employed for the present experiments, the synthesized source material was transferred from the synthesis ampoule to the transport ampoule and attached to the vacuum system. Prior to sealing, the ampoules containing the source material were continuously evacuated and annealed for 5 hours at about 500°C. After sealing, the ampoule was used for the particular experiment.

In order to determine the dependence of the mass flux on the source temperature, a series of experiments was performed in which amounts of 1 g of source material, synthesized and pretreated as discussed above, were transported at different source temperatures. For this purpose, the temperature difference between the source and condensation region was fixed at $\Delta T = 20°C$ and the source to deposit distance was $\Delta \ell = 10$ cm. The transport experiments were performed under vertical, stabilizing conditions. The results to date in terms of mass flux as a function of source temperature are graphically represented in Fig. 2. The data indicate a relatively steeper increase in mass flux in the temperature range of 825° to 900°C than at source temperatures above about 900°C. With temperatures greater than 900°C, the mass flux appears to level off. The latter observation (above 900°C) is not consistent with theoretical considerations which suggest that the mass flux should continuously increase with source temperature, at least within the temperature range investigated. The slight deviation of experimental data from theoretical expectations indicates that residual deviations from "stoichiometry" of the preannealed source material become more effective at higher temperatures and reduce the mass flux. This is also indicated by the "reproducibility" of the mass fluxes at a source temperature of 900°C. The source materials used for the experiments at 900°C were pretreated as discussed above, but come from different batches of elements and/or synthesized CdTe. The combined observations suggest that at least part of the residual deviations from stoichiometry could be trace impurities of the source material.

In order to further investigate the stoichiometry problems, special purification procedures of CdTe are being developed in our laboratory. Emphasis in these procedures is on the minimization of exposure of the source material to regular and even controlled atmospheres. The procedures include repeated sublimation of the synthesized source material in a multi-compartment reaction tube at elevated temperatures followed by annealing at 500°C for about 5 hours under dynamic vacuum conditions. Because the above development is still in progress and consists of several individual steps, a standardized procedure and detailed results will be reported at a later time. Some results to date for the latter material are included in Fig. 2. The mass fluxes observed are consistently greater than those obtained with the other source materials, and the dependence of the mass flux on source temperature is similar to that of the other

Figure 2

Mass transport rates (moles·cm$^{-2}$·s$^{-1}$) of CdTe as a function of source temperature. Closed circles (●) and triangles (▲) are based on source materals synthesized from purified elements and annealed (500°C, 5 h) prior to sealing. Open circles (○) based on source materials subjected to special purification procedures. Other data at 900°C based on source materials (purified elements; annealed at 500°C, 5 h) from different batches.

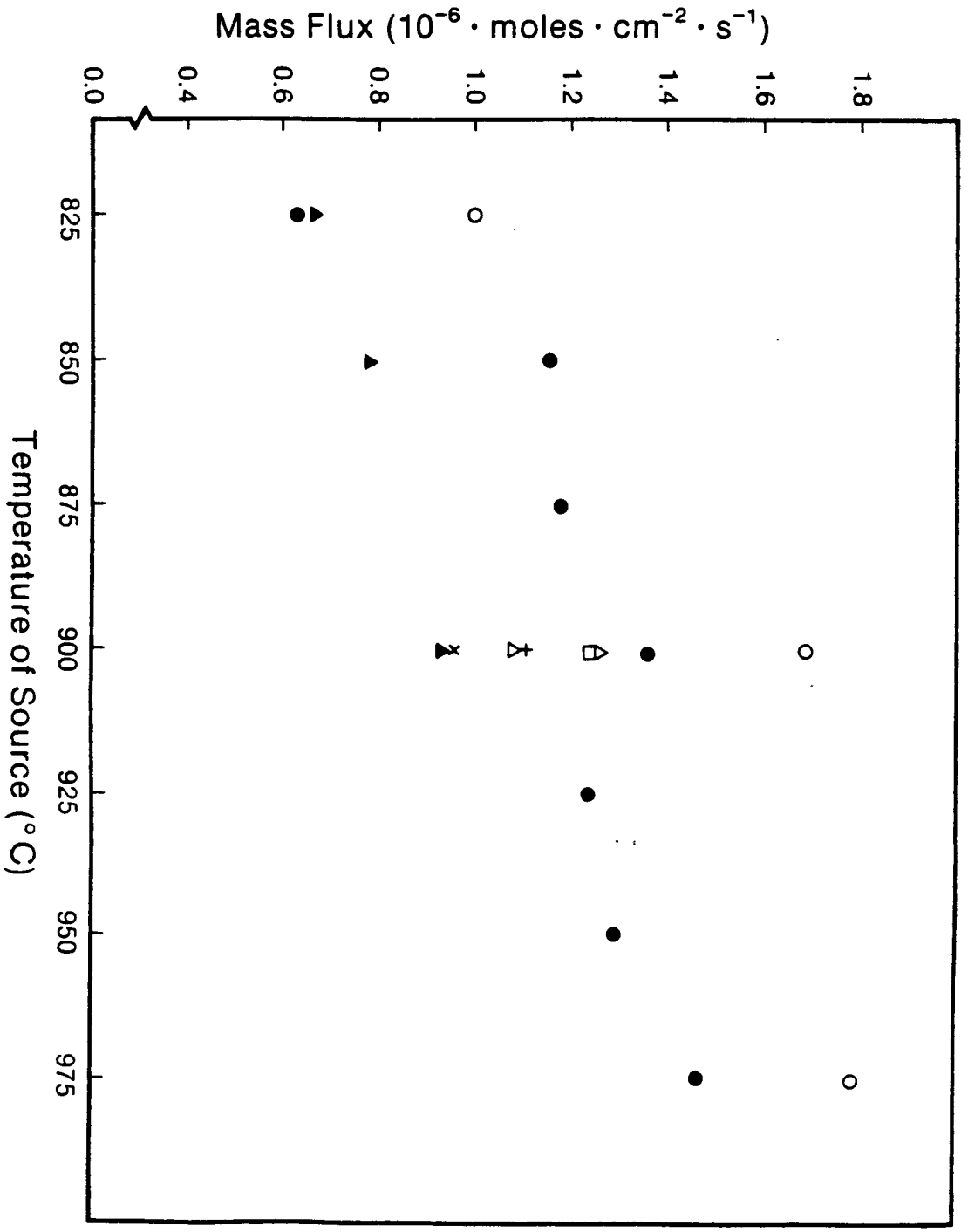
Mass Flux ($10^{-6}$ · moles · $cm^{-2}$ · $s^{-1}$)
0.0
0.4
0.6
0.8
1.0
1.2
1.4
1.6
1.8
Temperature of Source (°C)
825
850
875
900
925
950
975

source materials. A further interpretation of the limited results obtained with the specially treated source material is presently not justified.

For crystal growth in space to be commercially viable, large crystals of high quality have to be produced. That requires the use of large amounts of source material. We have observed and reported previously [9] that the mass flux of synthesized source materials, annealed at 400°C for 3.5 hours, decreases considerably with increasing amount of source material. These earlier data, obtained for a temperature difference of 863° → 848°C, are included for comparison in Fig. 3. Based on the results of Fig. 2, a source temperature of 900°C was chosen for analogous measurements of the dependence of mass flux on the amount of source material. For this purpose, a fixed temperature difference of 900° → 880°C and a source to deposit distance of $\Delta\ell$ = 10 cm were employed. The synthesized source materials were annealed at 500°C for a period of 5 hours prior to sealing. The results of these experiments in terms of mass flux as a function of amount of source material are shown in Fig. 3. The magnitudes of the mass fluxes are greater than those reported earlier [9], because of the higher source temperature of the present experiments. The overall trend of the mass fluxes with source material amount is very similar to that observed earlier (Fig. 3). The source materials employed for the experiments using 1 g amounts were pretreated the same way, but come from different batches of elements or CdTe. The combined observations strongly support the above discussed effects of small deviations from stoichiometry on the mass flux. Even for minute deviations, such effects are magnified for large amounts of source material, as demonstrated by the data in Fig. 3. In order to further support the critical importance of stoichiometry control of the source material, some preliminary mass flux data of specially treated source materials are included in Fig. 3. For the same temperature difference (900° → 880°C), the mass fluxes of the specially treated sources are about five to six times greater than those of the other sources for large amounts of source material. In addition, the mass fluxes of the "high purity" sources are apparently independent of the amount of source material. The latter results indicate that a higher degree of stoichiometry control than ever before has been achieved for these experiments. Because of the technological implications with respect to growth rate and crystal quality, the development effort and investigation of the stoichiometry effects are being continued.

The systematic investigation of the effects of deliberate deviations from stoichiometry of CdTe source material on mass flux has been continued. Earlier experiments for the temperature difference 850° → 830°C have been reported previously [9] and are included for comparison in Fig. 1. The present experiments are performed for a temperature difference of 900° → 880°C and a source to deposit distance of $\Delta\ell$ = 10 cm. The first set of transport experiments is based on synthesized CdTe, as discussed above, but without annealing at 500°C prior to sealing. For the second series of experiments, CdTe source materials synthesized (as discussed above) and annealed at 500°C for about 5 hours prior to sealing were used for the transport experiments. For both series, 1 g amounts of source material were employed. It should be noted that, except for the stoichiometric composition (zero excess of Cd or Te), the loaded ampoule after annealing at 500°C and prior to sealing had to be briefly

Figure 3

Mass transport rates (moles·cm$^{-1}$·s$^{-1}$) of CdTe as a function of amount of source material for the temperature difference 900° → 880°C. Open circles ( O ), earlier data [9] for 863° → 848°C and based on source materials synthesized from purified elements and annealed (400°C, 3.5 h) prior to sealing. Closed circles ( ● ), present data based on source materials synthesized from purified elements and annealed (500°C, 5 h) prior to sealing. Open squares ( □ ), present data based on source materials subjected to special purification procedures. Other data at 1 g based on source materials (purified elements; annealed 500°C, 5 h) from different batches.

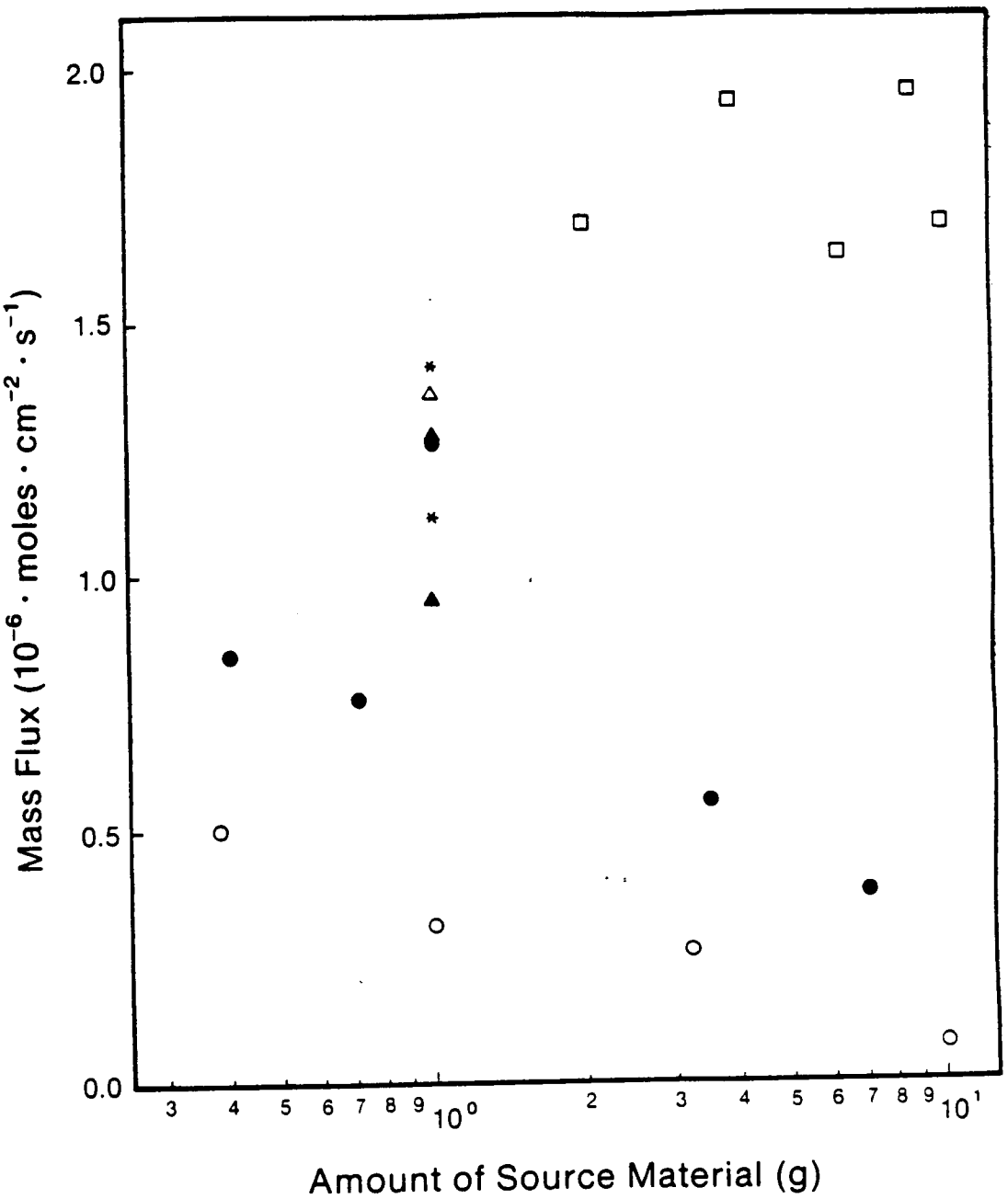
2.0
1.5
1.0
0.5
0.0
Mass Flux ($10^{-6}$ · moles · $cm^{-2}$ · $s^{-1}$)
3 4 5 6 7 8 9 $10^0$ 2 3 4 5 6 7 8 9 $10^1$
Amount of Source Material (g)

removed from the vacuum system to add the desired excess of elemental Cd or Te. After this addition, the ampoule was evacuated again and sealed. The results to date of these experiments in terms of mass flux versus excess Cd or Te (relative to the stoichiometric composition) in the source material are shown in Fig. 1. Both sets of data for the temperature difference 900° → 880°C are in very close agreement with the functional trend of mass flux versus stoichiometry predicted by the theoretical curves. The differences in magnitude between the two theoretical curves is a result of different residual CO pressures employed for the theoretical computations. The magnitude differences between the two series of experiments clearly reflect the influence of the source treatment, namely annealing at 500°C prior to sealing, which was employed for one series of experiments. This annealing procedure apparently improved the stoichiometry of the source material to such an extent, that the mass fluxes increased by about a factor of five to six relative to the untreated source material and for same excess amounts of Cd or Te. Higher transport rates yield increased growth rates and shorter growth times which are of immediate practical importance for space experiments. The magnitude differences in mass fluxes between the present data (900° → 880°C) and earlier results (850° → 830°C, [9]) reflect the different transport temperatures for the same pretreatment procedures.

The combined experimental results of Figs. 1-3 are internally consistent and demonstrate considerable progress in the better understanding of the mass transport behavior of CdTe. The effect of source temperature on the mass flux has been established. The previously observed dependence of the mass flux on the amount of source material [9] has been further investigated, and preliminary results to date indicate that the mass fluxes of "properly" treated source materials are independent of the amount of source material. The magnitude of the mass fluxes has been considerably improved, and the agreement of experimental results (for source materials annealed at 500°C) with theoretical predictions is rather close. The data in Fig. 1 also indicate that the homogeneity range of CdTe is very narrow. The quantitative determination of the homogeneity range of CdTe, the effects of stoichiometric deviations of the source material on the growth rate and on crystal properties are of primary importance for this program. The interrelations of these effects with those of convective contributions to the mass transport and growth processes are rather complex.

## Growth of CdTe Crystal Boule

In order to investigate the correlation of present results on the mass transport properties with the actual growth of CdTe single crystals, growth experiments have been initiated during this period of effort. As mentioned earlier, the primary emphasis of crystal growth experiments is on the development of crystal growth parameters for microgravity conditions. This, in turn, requires a thorough understanding of gravity related and unrelated effects on the growth properties. For the design of meaningful space experiments it is necessary to differentiate the effects of intrinsic parameters, such as stoichiometry and purity, from extrinsic variables, such as convective disturbances or ampoule geometry, on crystal growth and quality. In accordance with this approach, growth experiments are planned in which controllable variables are changed

systematically in order to observe and measure corresponding changes in the crystal growth properties of CdTe.

The source material employed for the present growth experiment consisted of CdTe synthesized, as discussed above, from elemental Cd and Te, which were purified by sublimation prior to synthesis. No additional treatment was applied to the starting material. The growth ampoule of fused silica was of 15 mm inner diameter and 10 cm in length, rounded at the source region end and conically shaped in the growth region. The ampoule was pretreated as described earlier [8]. After loading the ampoule was evacuated and sealed at a pressure of $10^{-6}$ torr or less.

The furnace used had a nearly isothermal temperature profile of several cm length with a maximum temperature of about 900°C. The temperature difference between the source and condensation end was less than 10°C. The ampoule was positioned in the vertical furnace with the source material at about 900°C, and the ampoule was pulled at a slow rate to maintain the growth surface of the crystal at about the same temperature.

The crystal boule of CdTe obtained by this procedure is shown in Fig. 4a. The boule has the external shape of the conical part of the ampoule, and has a very shiny, metallic black appearance. The boule is about 15 mm long, has a maximum width of about 12 mm, and weighs about 6 g. About one-third from the tip of the boule, the crystal shows a macroscopic irregular boundary suggesting an interference with the growth process at this time leading to the formation of grains. The crystal surface is nearly flat, of high reflectivity, and displays several facets around the edge. These macroscopic observations indicate that the boule is at least partly single crystalline and contains several grains. The optical photomicrograph, using Nomarski differential interference contrast microscopy, of the native surface of the crystal boule in Fig. 4b confirms the mirror smooth surface morphology and the presence of grains.

The natural cleavage plane of the zinc blende type structure of CdTe is parallel to the (110) set of planes. Two typical large sized grains, obtained by cleaving the crystal boule, are shown in the optical photograph of Fig. 5a. The smooth (110) cleavage planes of metallic black luster are clearly visible in the photograph. It should be noted that the presence of smooth cleavage planes nearly always indicate a high degree of single crystallinity of the corresponding grains. This is confirmed by the Laue X-ray back reflection pattern in Fig. 5b of the cleavage plane of the CdTe grain (from Fig. 5a). The Laue pattern clearly reveals the two-fold symmetry of the (110) plane. The Laue spots are well-defined and indicate a considerable degree of single crystallinity of the large grains.

Further characterization studies of the CdTe crystal boule, employing chemical etching and other techniques, are in progress. Preliminary results indicate the occurrence of etch patterns, which may be related to the type and density of dislocations.

In view of the well-known difficulties encountered in the growth of CdTe single crystals, it is justified to consider the present growth

Figure 4

Optical photograph (Fig. 4a) of a CdTe crystal boule grown by physical vapor transport. Grid dimensions are 1 mm. Nomarski differential interference contrast photomicrograph (Fig. 4b; magnification 200 X) of the native, top surface of the CdTe crystal boule.

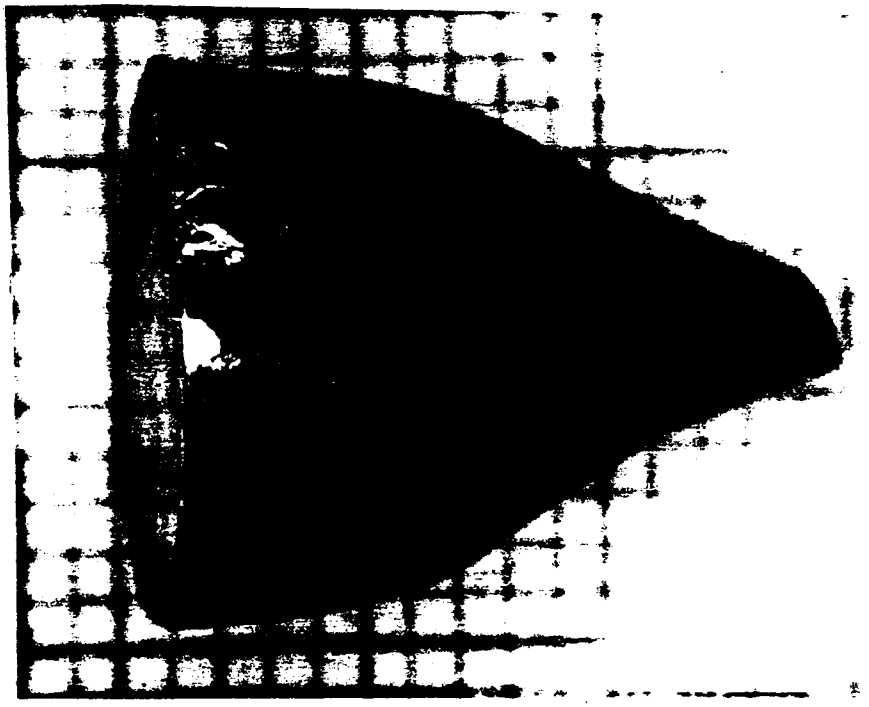

a

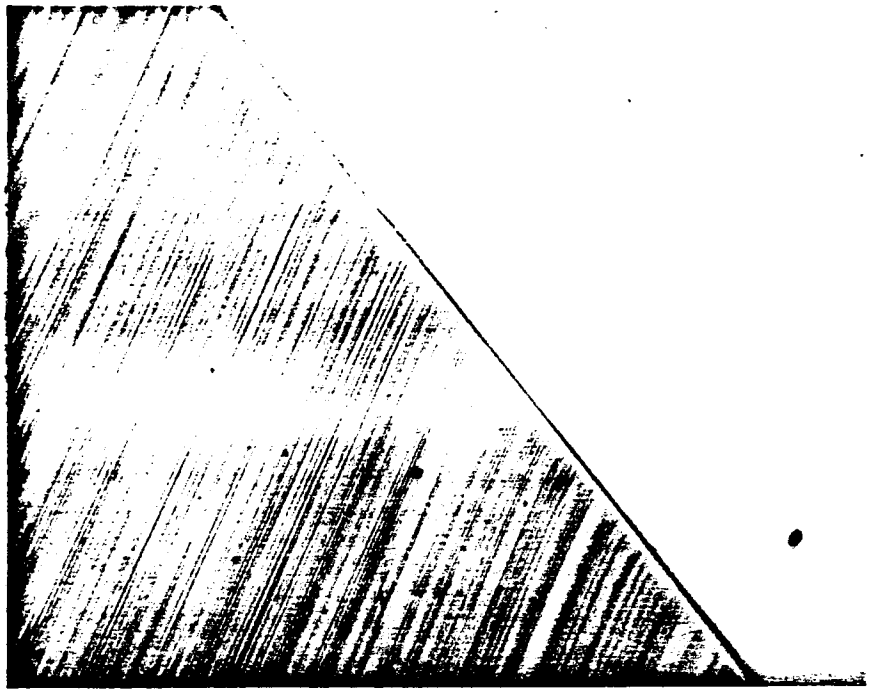

b

Figure 5

Optical photograph (Fig. 5a) of two typical CdTe grains of the CdTe boule from Fig. 4a. Grid dimensions are 1 mm. The large front face of the grains is a cleavage plane. Laue X-ray back reflection pattern (Fig. 5b) of the cleavage plane of one of the grains from Fig. 5a revealing the (110) orientation of the natural cleavage plane and a high degree of single crystallinity of the grain.

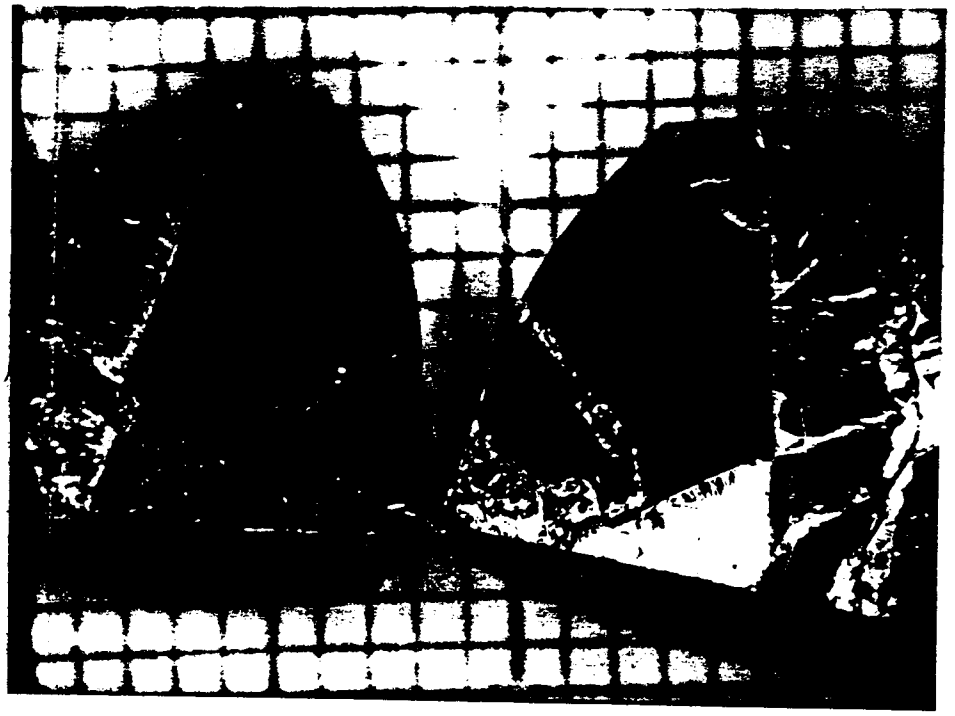

a

b

eriment rather successful. It should also be noted that this experiment was performed on the basis of systematic investigations of the mass transport properties of CdTe performed in our laboratory under the present contract.

## Mass Flux Phenomena Measurements

### Operational Testing of Microbalance System

After the dynamic microbalance facility had been assembled, operational testing procedures of the individual and of interfaced units were initiated during the previous period of effort [9]. These procedures have been continued as part of the present effort. Occasional vacuum problems as a result of heat conduction from the reaction chamber of the system to the vacuum connections required a modification of the furnace dimensions, heated zone lengths, and transport ampoule location relative to the balance system. Because of the complexity of the system with respect to heat losses from the furnace and sensitivity of the balance, the optimum relationship between these parameters cannot be accurately predetermined, but must be tested experimentally. The reaction chamber and furnace dimensions have been modified during the recent period of effort, and operational testing of the facility has been resumed.

As apparent from this report, primary emphasis during this period of effort has been placed on the further development of the CdTe crystal growth experiment and on the investigation of relevant mass transport properties of cadmium telluride. This is in line with the overall priorities of the program. Because of the rather limited man-power available for this particular project, the investigation of mass flux phenomena by microbalance techniques could only be continued at a minor level of effort.

## PRELIMINARY CONCLUSIONS

During the present period of investigation, the experimental and theoretical effort was primarily devoted to the further investigation of the mass transport and crystal growth properties of CdTe. Significant progress has been achieved in the better understanding of the interrelation between the stoichiometry of the source material and the transport behavior of CdTe. The computational model for the physical vapor transport of CdTe has been extended to higher temperature ranges. The dependence of the mass flux on the source temperature has been experimentally established. Most importantly, synthesis and source material treatment procedures are being developed to clarify the effects of stoichiometry on mass flux. Results to date show that source materials subjected to these special procedures yielded significantly greater mass transport rates than observed previously, and mass fluxes that are independent of the amount of source material. In addition, the most recently observed mass fluxes are in very close agreement with theoretical predictions of the mass transport rates of CdTe as a function of deviation f stoichiometry of the overall system. The combined results demon that a considerably improved stoichiometry control of the source r has been accomplished.

Based on the above investigations, a CdTe crystal growth experiment yielded a large crystal boule. Preliminary characterization of the boule by optical microscopy and Laue X-ray diffraction studies revealed a very smooth, native growth surface, the presence of crystal facets at the edge of the surface, and the existence of large crystal grains within the boule. The rather smooth cleavage plane and Laue patterns demonstrate the high degree of single crystallinity of the CdTe grains. These observations will be further supported by additional crystal characterization studies. In view of reported difficulties encountered with CdTe crystal growth, the results of this experiment are very promising.

Because of the limited man-power available for this project, a reduced effort was devoted to the modification and continued testing of the dynamic microbalance facility.

**FUTURE PLANS**

In accordance with the priorities of the center and of this project, future activities will be directed towards the further development of CdTe crystal growth in microgravity environment. This involves two major aspects for the immediate future. The further quantitative investigation and identification of the effects of stoichiometry on the mass flux and crystal growth properties of CdTe represent one important part of our approach. The second aspect is concerned with the differentiation of gravity unrelated effects from those of convective disturbances on crystal growth properties. The experimental approach will be supported by theoretical considerations. The results to date and to be obtained provide the scientific and technological basis for the definition of optimum experimental parameters for CdTe crystal growth in microgravity.

Within the limitations of available man-power, the above mass transport and crystal growth experiments will be supported by in-situ measurements of transport phenomena in closed ampoules. For this purpose, the dynamic microbalance facility will be employed. Emphasis will be on the observation of temperature oscillation effects on the transient behavior of vapor transport systems. The task for the immediate future is concerned with the determination of sensitivity limits of the balance with respect to temperature variation effects on the vapor phase.

## REFERENCES


1. H. Wiedemeier, D. Chandra, and F. C. Klaessig, J. Crystal Growth, 51, 345 (1981).
2. D. Chandra and H. Wiedemeier, J. Crystal Growth, 57, 159 (1982).
3. K. Zanio, in "Semiconductors and Semimetals", Vol. 13, Eds. R. K. Willardson and A. C. Beer, Academic Press, New York (1978).
4. S. B. Sudhir and H. Wiedemeier, J. Electrochem. Soc., 134(12), 3199 (1987).
5. P. Buck and R. Nitsche, J. Crystal Growth, 48, 29 (1980).
6. Y. Yellin, D. Eger, and S. Shachna, J. Crystal Growth, 60, 343 (1982).
7. H. Wiedemeier, S. B. Trivedi, R. C. Whiteside, and W. Palosz, J. Electrochem. Soc., 133(11), 2399 (1986).
8. H. Wiedemeier and D. Chandra, Z. Anorg. Allg. Chem., 488, 137 (1982).
9. H. Wiedemeier, Clarkson University CCDS Semiannual Report, January 1988.